DETERMINATION OF THE ARGON INTERMOLECULAR PAIR POTENTIAL

FROM DISTRIBUTION FUNCTIONS MEASURED BY X-RAY

DIFFRACTION FROM FLUID ARGON

Thesis by

Joseph Francis Karnicky

In Partial Fulfillment of the Requirements

for the Degree of

Doctor of Philosophy

California Institute of Technology

Pasadena, California

1974

(Submitted November 21, 1973)

To My Mother

ACKNOWLEDGEMENTS

and the National Science Foundation.

The assistance of Ray Schmidt was very helpful in the early stages of this project, as were conversations with George Wignall, Ernie Henninger, Ron Brown, Paul Morrison, and Mike Piliavin.

ABSTRACT

X-ray diffraction experiments were carried out on fluid argon at a temperature of -100°C and densities of .0824 g/cm^3, .1331 g/cm^3, .2087 g/cm^3, and .3111 g/cm^3. The measurements of the state at .2087 g/cm^3 were repeated to establish reproducibility. The methods used to obtain the experimental quantities and to subsequently analyze the data included significant improvements over previous investigations.

The data from each experiment at the three higher densities were analyzed to obtain a set of structure factors which were Fourier transformed to obtain sets of direct correlation functions and radial distribution functions. The Percus-Yevick equation was applied to these distribution functions to obtain the effective intermolecular potential from each experiment. These potentials were corrected for three-body effects to give four estimates of the argon pair potential, and a final estimate which is the precision weighted average of the four seperate estimates.

The characteristics of these potentials, with error limits determined by a perturbation analysis of the uncertainties in the experimental quantities, are:

state 1- n=.2087 g/cm^3, σ =3.401 $\pm$ .038 A°, ϵ = 143.2 $\pm$ 10.2 °K, r_{min}= 3.89 $\pm$ .09 A°.

<u>state 1R-</u> $n = .2087$ g/cm^3, $\sigma = 3.402 \pm .035$ A$^\circ$, $\epsilon = 149.9 \pm$ 10.2 $^\circ$K, $r_{min} = 3.87 \pm .07$ A$^\circ$.

<u>state 2-</u> $\mathbf{n} = .3111$ g/cm^3, $\sigma = 3.375 \pm .023$ A$^\circ$, $\epsilon = 146.6 \pm$ 6.8 $^\circ$K, $r_{min} = 3.87 \pm .05$ A$^\circ$.

<u>state 3-</u> $n = .1331$ g/cm^3, $\sigma = 3.379 \pm .050$ A$^\circ$, $\epsilon = 145.1 \pm$ 16.0 $^\circ$K, $r_{min} = 3.83 \pm .13$ A$^\circ$.

<u>average u(r)-</u> $\sigma = 3.389 \pm .015$ A$^\circ$, $\epsilon = 146.3 \pm 4.9$ $^\circ$K $r_{min} = 3.86 \pm .05$ A$^\circ$.

Physical quantities were calculated from the average potential and agreed with the experimental values for the second virial coefficient of argon and the vibrational transition energies of the argon dimer, as well as the theoretical long range dispersion potential.

The range of densities studied was not large enough to allow direct determination of three-body forces. Methods are suggested whereby information about non-additive forces could be derived from the combination of the results of these experiments with the results of previous x-ray experiments or with third virial coefficient data.

TABLE OF CONTENTS

INDEX FOR FIGURES

INDEX FOR FIGURES

x

INDEX FOR TABLES

INDEX FOR TABLES

INDEX FOR TABLES

NOMENCLATURE

$\underline{A^*}$ dimensionless factor to correct scattered x-ray intensity for absorption of the incident and diffracted beams by the cell and argon

   subscript notation: c and a denote scattering which originates in the cell or argon respectively, thus A_c^* is the factor which corrects scattering from the cell for absorption by the cell and argon. A_a^* corrects scattering from the argon for absorption by the cell and sample.

   subscripts (c) and (i) denote coherent and incoherent scatter. (e) denotes scatter from the empty cryostat, thus

   $A_{a(c)}^*$ corrects coherent argon scatter

   $A_{a(i)}^*$ corrects incoherent argon scatter

   $A_{c(c)}^*$ corrects coherent cell scatter

   $A_{c(i)}^*$ corrects incoherent cell scatter

   $A_{c(e)}^*$ corrects empty cryostat scatter

$A^*(2)$ corrects the twice-scattered x-ray intensity for absorption by the cell and argon.

$\underline{A}$ is the integral of A^* over the irradiated path length. A has dimensions of length. The subscript notation is the same as that for A^*

$\underline{A'}$ Integrated absorption factor to correct the scattered x-ray intensity for absorption by the cell alone. A' has dimensions of length. Subscript notation is the same as that for A^*.

$\underline{A^\circ}$ Angstrom unit

$\underline{b}$ arbitrary error which is a constant factor of $P_a(2\theta)$ over the range s=0 to s= 3.5 A°.

$\underline{B(T)}$ second virial coefficient

$\underline{c}$ speed of light in vacuum

$\underline{c(r)}$ direct correlation function

$\underline{C_6, C_8, C_{10}}$ coefficients of the r^{-6}, r^{-8}, r^{-10} dispersion terms in the pair potential

NOMENCLATURE

$\left\{ C_{jk}(2\theta) \right\}_i$ number of counts during a 30 second interval. j indicates the filter in position (j is alpha or beta). k indicates the counter (k=1 or 2) . i indicates the number of the scan (i = 1 to 12).

$d(2\theta)$ an arbitrary error which is a reproducible factor of $P_{a(c)}(2\theta)$

e charge on the electron

f atomic scattering factor

f_{exptl} experimentally measured f

f_{H-F} f calculated from Hartree-Foch wavefunctions

$f*$ the complex conjugate of f

$\Delta f'$ real relativistic correction to f

$\Delta f''$ imaginary relativistic correction to f

$f°$ non-relativistic atomic scattering factor

F a generalized function to be evaluated by Monte Carlo methods

$g(r)$ radial distribution function

g_i additive coefficient of n^i in the cluster integral expansion of g(r)

g_1^{NA} non-additive density coefficient in the cluster integral expansion of g(r)

$h(2\theta)$ an arbitrary error function modifying $P_a(2\theta)$

H_c height of a beryllium crystal peak measured in the scattering from the empty cell and corrected for absorption by the cell

H_{ca} height of a beryllium crystal peak measured in the scattering from the cell+argon and corrected for absorption by the cell and by argon

I intensity of radiation- units can be energy/area for energy flux counting or counts per second/area for quantum flux counting.

$I°$ intensity incident on the sample

$I(2)$ intensity of twice scattered radiation

I_{inc} incoherent argon scatter in electron units for

NOMENCLATURE

$\mathcal{J}_{inc}$ energy flux counting
incoherent argon scatter in electron units
for quantum flux counting

$\underline{In}$ double volume integral of the Monte Carlo calibration
function $1/r_{12}^2$

$\underline{i(s)}$ structure factor in reciprocal space

$\underline{J}$ scattering in electron units per atom. Subscript
notation is the same as that for A*. For example,
$J_{a(c)}$ is the coherent argon scattering.
$J_i(2\theta_i)$ (i= 1 or 2) refers to the first or second
scattering event in double scattering.

$\underline{k}$ Boltzmann's constant

$\underline{°K}$ a unit of energy- 1 °K = k ergs.

$\underline{K_T}$ isothermal compressibility

$\underline{K_{\overline{\alpha}}}$ weighted average of the characteristic $K\alpha_1$ and $K\alpha_2$
x radiation

$\underline{l}$ path length of x-ray through irradiated material

$\underline{m}$ mass of the electron

$\underline{n}$ density
n_a argon density
n_{He} helium density
n_{Be} beryllium density
n_i (i= 1 or 2) refers to the density of the first
or second scattering medium in double scattering.

$\underline{N_a}$ conversion factor from electron units per atom to
counts per second/ cm for argon scatter

N_{Be} conversion factor for beryllium scatter.

$\underline{N_T}$ number of Monte Carlo estimates

NOMENCLATURE

P count rate of diffracted radiation, = intensity times cross sectional area

subscript notation:

P_{ca} count rate from cell and argon

P_{cHe} count rate from cell and helium

P_c count rate from cell

P_a count rate from argon

P_{He} count rate from helium

additional subscripts (c) and (i) are the same notation as for A*- thus $P_{c(i)}$ indicates the count rate of incoherent scatter from the cell.

$\left\{ P_{jk}(2\theta) \right\}_i$ raw data point equal to $\left\{ C_{jk}(2\theta) \right\}_i$ divided by 30 seconds

$P(2)$ count rate for twice scattered x-rays

P° total incident x-ray count rate in argon experiments

$P^{\circ\,\prime}$ total incident x-ray count rate for empty cell

$P^\circ(\lambda)$ normalized wavelength distribution of incident count rate

P°_1 $K\alpha$ component of $P^\circ(\lambda)$

$P^\circ_2(\lambda)$ continuous wavelength component of $P^\circ(\lambda)$

p width of argon cavity in cell

p_s range of i(s) perturbed by the error analysis function

Pol polarization factor for single scattering

Pol_2 polarization factor for double scattering

r intermolecular separation

r_{min} value of r at pair potential minimum

$\vec{r}_i$ (i= 1 or 2) position vector to the location of the i th event in double scattering

$r_{12} = \left| \vec{r}_1 - \vec{r}_2 \right|$

R distance from sample to detector

R^{BD} electron recoil factor $(\lambda/\lambda')^3$

NOMENCLATURE

$\underline{s}$ magnitude of the scattered wave vector

$\underline{S_c}$ normalizing constant to match the solid angle subtended by counter 1 to the solid angle subtended by counter 2

$\underline{t}$ thickness of one beryllium window

$\underline{T}$ temperature (absolute unless otherwise specified)

$\underline{u(r)}$ intermolecular pair potential

   $u^{eff}(r)$ effective potential including non-additive forces

   $u(r)[I]$ experimental estimate of the pair potential

   $u(r)[II]$ experimental estimate of the pair potential up to r= 4.625 A°, theoretical $C_6 r^{-6}$, $C_8 r^{-8}$, $C_{10} r^{-10}$ potential for r > 4.625A°.

$\underline{w}$ distance from center line of sample (horizontally) to point of diffraction

$\underline{W}$ width of irradiated volume of sample

$\underline{y}$ horizontal distance from the center of the vertical receiving slit to the point at which the diffracted x-ray enters the receiving slit

$\underline{Y}$ width of receiving slit

$\underline{z(2\theta)}$ error function modifying $P_a(2\theta)$ resulting from an error in the determination of P°'/P°

NOMENCLATURE

α_{max} maximum vertical divergence angle of the incident or diffracted beam

ϵ well depth of the pair potential

ϵ_r error in the determination of $P°'/P°$

ϵ_2 magnitude of the perturbation applied to the features of $i(s)$

ϵ_i actual uncertainty in the feature of $i(s)$

λ wavelength of x radiation

λ' wavelength of diffracted incoherent radiation

$\lambda_{K\alpha}$ wavelength of characteristic Ag K radiation

Ω effective solid angle subtended by a receiving slit system

σ value of r at which the pair potential is zero

2θ diffraction angle

$2\theta_0$ angle at which a Kα beryllium peak appears

$2\theta_i$ ($i = 1$ or 2) angle for the i th diffraction event in double scattering

$2\theta'$ actual diffraction angle of a divergent ray at goniometer position 2

μ linear coefficient for absorption of x rays

subscript notation: a and c denote absorption in the argon or in the cell. (i) denotes that the scattering absorbed is incoherent. Thus:

μ_c absorption, by the cell, of coherent scatter

μ_a absorption, by the argon, of coherent scatter

$\mu_{c(i)}$ absorption, by the cell, of incoherent scatter

$\mu_{a(i)}$ absorption, by the argon, of incoherent scatter

$\omega(r_{12}, r_{13}, r_{23})$ non-additive three body potential

NOMENCLATURE

Mayer Cluster Integrals

$\underset{i}{\circ}$ indicates a coordinate which is fixed
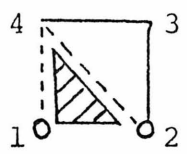
$\underset{i}{\bullet}$ indicates a coordinate over which the cluster function is integrated.

$i \underline{\hspace{2cm}} j$ indicates a term $e^{-u(r_{ij})/kT} - 1$

$i - - - - - j$ indicates a term $e^{-u(r_{ij})/kT}$

$i \overset{k}{\triangle} j$ indicates a term $e^{-\omega(r_{ij}, r_{jk}, r_{ik})/kT} - 1$

example

$$
\begin{array}{c}
\overset{4 \quad \quad 3}{\underset{1 \quad \quad 2}{\boxtimes}}
\end{array}
\;=\;
\int \left(e^{-u(r_{23})/kT} - 1 \right) \left(e^{-u(r_{34})/kT} - 1 \right) \cdot
$$

$$
\left(e^{-u(r_{24})/kT} \cdot e^{-u(r_{14})/kT} \right)
$$

$$
\left(e^{-(r_{12}, r_{24}, r_{14})/kT} - 1 \right) d\vec{r}_3 \, d\vec{r}_4
$$

If the cluster integral is being used to describe a system of identical particles, the numerical identification of the coordinates is unnecessary and the graph may be written: $\boxtimes$
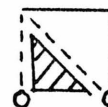
CHAPTER 1   INTRODUCTION

This thesis describes an x-ray diffraction experiment
designed to measure the intermolecular potential function,
also called the pair potential, of argon.

Chapter Outline

Part A of this chapter describes the present state
of knowledge of the pair potential as well as its
significance in liquid state theory.   Recent reviews of
this subject have been published[1,2,3].

Part B describes the basic theory involved in obtain-
ing u(r), the argon pair potential, from x-ray scattering
data.   r is the internuclear separation.

Part C places this experiment in the context of other
x-ray diffraction studies of argon.

Part A   Present Knowledge of the Pair Potential

Knowledge of intermolecular forces is clearly
essential to the understanding of material properties.   In
particular, an accurately known pair potential is necessary
to determine the magnitude of many-body forces, to

extrapolate data beyond presently available experimental results, and to test the various simplified theories which are approximations to the exact but insoluble statistical mechanical equations that describe liquids.

The present state of knowledge of the pair potential of argon is illustrated by three of the more recent potentials derived from fitting experimental data. (The best quantum mechanical calculations to date for the argon potential are still to be considered as estimates of the well depth and repulsive region[4] but are quite accurate (5%) for the limiting behavior of u(r) at large r [5,6].) These potentials, obtained by simultaneous fit to diverse types of experimental data, are the Dymond-Alder potential[7], the Klein-Hanley potential[8], and the Barker-Fisher-Watts potential[9]. T he Dymond-Alder is a numerically tabulated potential, the Klein-Hanley is a four parameter m-6-8 potential, and the Barker-Fisher-Watts is a multi-parameter analytic curve which represents the latest estimate in a series of potential functions based on the original Barker-Pompe[10] potential. Previous forms include the Barker-Pompe and Barker-Bobetic[11] potentials.

Upon examination, these potentials exhibit several difficulties. The Dymond-Alder potential has an unrealistic behavior at large separations. The Klein-Hanley and Barker-Fisher-Watts are constrained to a predetermined

analytic form.   The major point here is that there is a
question of uniqueness in determining a pair potential from
macroscopic data.   As pointed out by Kestin et al[12,13],
the inversion of the second virial coefficient integral and
the collision integral for viscosity and thermal conduc-
tivity lead to mathematically indeterminate problems.

In contrast, the various scattering experiments
(x-ray, neutron, molecular beam) uniquely determine, at
least in theory, the potential function or the distribution
functions from which the potential function may be derived.

Previous x-ray studies have not been able to accurately
determine the pair potential for reasons discussed in
part C of this chapter.

Neutron diffraction may also be used to determine
i(s), the structure factor in reciprocal space, and hence
the distribution functions, but no one has yet taken
sufficiently accurate data in the experimental region
which would be useful for obtaining the pair potential.
Most of the work has been done in the dense liquid or
three-phase region, where the structure depends mostly on
the hard-sphere properties of the potential. A neutron
scattering experiment[14] in the appropriate region of P-V-T
space (see part C, this chapter) produced an unrealistic
pair potential due to difficulties in correcting for multi-
ple scattering.

In principle, the intermolecular potential can be uniquely determined by inversion of differential cross section molecular beam data[15], but in practice this has proved impossible for inert gas scattering. Because of the finite experimental resolution of beam energy and scattering angle, molecular beam data, including the most recent work by Lee and co-workers[16,17], must be interpreted by using an assumed potential form.

Part B   Obtaining the Pair Potential from X-ray Data

The x-ray diffraction pattern from fluid argon may be used to derive $u(r)$ in the following manner:

The experimental intensity of diffracted x-rays is converted to the structure factor $i(s)$ by the equation:

$$i(s) = \frac{P_{a(c)}(s) - N_a f^2(s) \, Pol(s) \, A_{a(c)}(s)}{N_a f^2(s) \, Pol(s) \, A_{a(c)}(s)} \tag{1}$$

In equation (1) s is the magnitude of the scattered wave vector and is defined by

$$s = \frac{4\pi \sin\theta}{\lambda} \tag{2}$$

where 2θ is the scattering angle and λ is the wavelength

of the incident radiation. Because of the relationship

expressed in equation (2), any quantity expressed as a

function of s, such as $f^2(s)$, may be expressed as a function

of 2θ if λ is known. In equation (1) $P_{a(c)}$ is the

count rate for coherent scatter from the argon. f^2 is

the atomic scattering factor for argon. Pol is the polar-

ization factor for an unpolarized incident beam given by

$$Pol(2\theta) = \frac{1 + \cos^2(2\theta)}{2} \qquad (3)$$

$A_{a(c)}$ is the absorption correction for the absorption of

coherently scattered argon radiation by the cell and sample.

N_a is a normalization factor which converts the atomic

scattering in electron units to the laboratory units of

counts per second.

i(s) thus represents the difference between diffrac-

tion from the structured assemblage of atoms in the actual

fluid and the scattering from an unstructured collection

of argon atoms, and accordingly is a measure of this

structure.

The quantity si(s) can be Fourier transformed to give

the radial distribution function g(r) according to the

equation[18]

$$r(g(r)-1) = \frac{1}{2\pi^2 n} \int_0^\infty si(s)\sin rs \, ds \qquad (4)$$

where n is the density of argon.   In this laboratory,
a set of 13 argon states studied by Mikolaj[19,20] using
x-ray diffraction, 6 states studied by Smelser[21], and 5
states studied by Kirstein[22] were all transformed to give
radial distribution functions.   The quantity $si(s)/(1+i(s))$
may be Fourier transformed to give the direct correlation
function $c(r)$[23] according to the equation

$$rc(r) = \frac{1}{2\pi^2 n} \int_0^\infty \frac{si(s)}{1 + i(s)} \sin nrs \; ds \qquad (5)$$

The data of Mikolaj[19,24], Smelser[21], and Kirstein[22] were
transformed to obtain the corresponding $c(r)$ functions.

The radial distribution function may be expanded as a
power series in the density[25]

$$g(r) = \exp(-kT) \sum_{i=0}^\infty g_i(r) n^i \qquad (6)$$

where k is Boltzmann's constant and T is the absolute
temperature.   With the assumption of pairwise additivity
the first few coefficients, shown in terms of the Mayer
cluster integrals[26], are

$$g_0(r) = 1 \tag{7}$$

$$g_1(r) = \quad\bigwedge \tag{8}$$

$$g_2(r) = \frac{1}{2}\,\boxtimes + \,\square\, + 2\,\boxslash + \frac{1}{2}\,\boxtimes \tag{9}$$

Mikolaj and Pings[27] solved equation (6) iteratively including terms to the first order in the density and obtained estimates of u(r) from experimental g(r) values for two low density states. Pings[28] has further developed this expansion by showing that u(r) may be expressed, except for a very small cluster integral which must be calculated theoretically, as a function of various experimental integrals:

$$g(r) = I_1(r) + 1 = \exp(-kTu(r))[\, 1 + I_3(r) \tag{10}$$
$$+ \frac{1}{2}[I_3(r)]^2 + \frac{1}{2}n^2\,\boxtimes + ng_1^{(na)}(r) + O(n^3)\,]$$

where

$$I_1(r) = \frac{1}{2\pi^2 rn}\int_0^\infty si(s)\sin rs\,ds = g(r) - 1 \tag{11}$$

$$I_2(r) = \frac{1}{2\pi^2 rn}\int_0^\infty \frac{si(s)}{1+i(s)}\sin rs\,ds = c(r) \tag{12}$$

$$I_3(r) = \frac{1}{2\pi^2 rn} \int_0^\infty \frac{1}{1+i(s)} \text{sinrs } ds = g(r)-c(r)-1 \quad (13)$$

$g_1^{(na)}(r)$ is the non-additive first order term in the expansion of $g(r)$ and $O(n^3)$ indicates that some additive terms in n^3 and higher powers of the density are neglected. The data of Mikolaj[19] had too few points in the low density region to provide a strong test of equation (10), but there were enough to verify a fundamental step in the development of equation (10) by reproducing a theoretical value of the $g_1(r)$ term.

An alternative to the direct density expansion of $g(r)$ is the use of approximate integral equations in terms of the distribution functions. Two of the most prominent of these equations are the Percus-Yevick[29] (PY) equation

$$u^{eff}(r) = kT\ln\left(1 - \frac{c(r)}{g(r)} \right) \quad (14)$$

and the convoluted hypernetted chain (CHNC) equation[30]

$$u^{eff}(r) = kT(g(r)-1-c(r)-\ln(g(r))) \quad (15)$$

with the PY equation more widely used of the two. The potential function calculated from equation (14) or equation (15) is not the pair potential because the PY

and CHNC equations are inexact with respect to many-body forces. In general, $u^{eff}(r)$ will be a function of density and, less strongly, of temperature. Mikolaj and Pings[31] calculated effective potentials for 13 sets of distribution functions from the PY and CHNC equations. Smelser[21] and Kirstein[22] calculated effective potentials for their data using the PY equation.

Effective potentials calculated by the PY equation may be corrected for three-body effects to the second order in density according to a method developed by Rowlinson[32,33] to give the pair potential

$$kT(u^{eff}(r)-u(r)) = -n \; \triangle - n^2 (\; 2 \; \boxtimes + \boxtimes + \boxtimes \;) \tag{16}$$

Part C Other X-ray Studies of Argon

Two aspects of this study differentiate it from previous x-ray studies of argon:

1) As was demonstrated by Pings[28], there is a very specific region of P-V-T space in which the diffraction data can be successfully inverted to yield the pair potential. This region is shown in Figure 1 using the P-V-T data of Michels et al[34]. The lower limit of

density which can be studied is about .1 g/cm^3. Below
this density there is an insufficient number of scattering
units of argon and hence too low a signal-to-noise ratio.
An upper bound of about .4 g/cm^3 is set by the need to
study states in which three-body effects are small and in
which the largest additive terms omitted by equation (10)
are negligible. A lower limit of temperature is set a
few degrees above the critical temperature to assure that
the cluster integral expansions converge and that the
compressibility remains moderate. All aspects of this
experiment were designed with the intent of taking data in
this narrowly defined region.

2) This experiment represents the currently most
advanced state of refinement in the measurement of x-ray
diffraction from fluid argon at high pressures and cryogenic
temperatures. Specifically, this study makes use of the
best available methodology developed by previous investiga-
tors[19,21,22,35] with additional improvements in the
accumulation and analysis of the data. These improvements
are pointed out in the chapters on experimental aspects of
this work(Chapter II) and data analysis (Chapter III).

CHAPTER II   APPARATUS

The data analyzed to obtain the pair potential were taken in the eight experiments listed in Table I. The helium experiments and the empty cell experiment were used to measure the cell scatter as a function of pressure. The data used to correct the argon studies for the presence of cell scatter were derived by a linear interpolation between the two helium experiments. The evacuated cell data were used to verify that the (very small) amount of scatter due to helium was being subtracted correctly. Argon state 4, the lowest density state, was used to obtain a set of experimental atomic scattering factors for argon. Argon states 1, 2, 3, and 1R were analyzed to determine the effective argon potential as a function of density. State 1R is a repeat of the state 1 conditions and was used to establish the reproducibility of the experiments. In addition to the experiments listed in Table 1, experiments were performed to study the alignment of the system, the matching of dual counters, Soller slit uniformity, stability of the x-ray source, and balancing of dual filters. The conditions of alignment, collimation, and data collecting format which were followed in the eight experiments listed in Table 1 were selected as optimal based on these preliminary studies.

Sample

The argon used was obtained from Cryogenic Service Corporation[36] and was claimed to be 99.9999% pure, but samples analyzed on the Caltech mass spectrometer and by West Coast Technical Service Inc.[37] were found to be 99.86% pure (by mole) with principal

contaminants being .13% N_2 and .01% O_2.

The helium used was supplied by the Linde Corporation and was analyzed at Caltech to be 99.53 mole % He with .28% N_2, .12% H_2O, and .07% A.

Sample Containment

The cell and cryostat used in these experiments are of a new design and are shown in Figures 2 and 3. The most important differences in the cell's design from that used by Mikolaj,[19] Smelser,[21] and Kirstein[22] are the flat windows and the 7 mm path length through the sample. The cell used by the previous investigators was cylindrical with a path length of $\sim$ .77 mm. Because of the flat windows it is possible to remove the term representing the intensity distribution of the incident beam from the basic scattering integral (see Chapter III) and to calculate the absorption factors analytically. In addition, the flat cell is less sensitive to small misalignments than the cylindrical cell. The 7 mm path length is designed to optimize the **signal-to-noise** ratio for the low densities being studied.

The cell consists of a split Monel block held together with machine screws and a gold gasket. Each half has one of the sintered beryllium windows held in a Bridgmann-type unsupported area seal by Epoxylite type 8839 low temperature epoxy. The cell was designed to withstand 2500 psi internal pressure and was tested to 1600 psi for 24 hours at -100°C without detectable helium leakage.

The cell is mounted in a cylindrical evacuated (10^{-4} Torr) cryostat by Lucite support pieces and is surrounded by a copper and aluminized Mylar radiation shield. As in Kirstein's[22] work, the argon is fed into the cell through 3 feet of stainless steel capillary tubing. Slots in the cryostat for the entrance and exit of x-rays are covered with .002" Saran Wrap. The entire cryostat is attached by a micrometer driven compound lathe rest to a shaft which fits into the center of rotation of the Norelco wide angle goniometer. Thus it is possible to move the cell (that is, to move the cryostat) up and down or left and right relative to the goniometer axis.

The pressure measurement and control uses a Hart dead weight balance and Pace diaphragm pressure transducer as described in previous experiments.[38]

The use of cold N_2 gas to cool the cell was adopted from previous work.[21,22] In this work primary temperature control was attained by adjusting the flow rate through a pair of baffled cavities on each side of the cell. A major change here is the use of two Cambion model 800-3953-03 thermoelectric annular rings between the cell and the baffled heat sinks to achieve the final temperature adjustment. These devices were powered by a proportional-integral controller.[39] The sensing device is a platinum resistance thermometer imbedded in the Monel cell. A second platinum thermometer was used to measure and record the absolute temperature, and a network of four copper-constantan thermocouples was used to measure the temperature differences within the cell. It was not possible to measure these temperature differences more precisely

than a few tenths of a degree because of temperature differences between the electrically insulated thermocouples and the Monel block. However, the temperature differences within the Monel block could be estimated from the thermocouple potentials and thermal flux calculations, and have a maximum value of $.1^{o}C$. Table II lists the maximum and minimum values of the pressure and the temperature as measured by the platinum thermometer during the duration of each experiment.

X-Ray Source

The x-ray source was a Rigaku-Denki Rota unit model Ru-3V rotating anode x-ray machine with a silver target run at 60 kV and 100 mA electron current.

The spot focus at 5.7^{o} takeoff angle was used to irradiate the sample. This effective focal spot was photographically measured to be 1.1 mm wide and .7 mm long. The spot focus rather than line focus was used in order to be able to design the cell with minimum diameter (hence minimum thickness) of the beryllium windows and in order to minimize the horizontal divergence of the diffracted beam.

Silver radiation ($K\bar{\alpha}$ = .5608 A^{o}) was used in order to minimize the absorption and to obtain a maximum range of the scattering parameter, s, for a given range of 2θ.

As in previous experiments,[21,22] monochromatization of the incident beam was achieved by using a pair of balanced filters and pulse height discrimination using a Canberra model 6031 Single Channel analyzer. For silver $K\bar{\alpha}$ radiation the alpha filter is molybdenum and the beta filter is rhodium. These filters were

experimentally matched for identical β absorption and the transmitted spectrum was measured using a lithium fluoride analyzer crystal in the Bragg-Bretanno geometry. This spectrum is shown in Figure 4.

Collimation and Alignment

The optical geometry is shown in Figure 5. The incident beam is collimated by vertical Soller slits (1.174" long, spaced .0078" apart) and horizontal Soller slits (1.174" long and .0052" apart) with corresponding maximum angular dispersions of $\pm.38^O$ in the horizontal plane and $\pm.25^O$ in the vertical plane.

This beam passes through the cell at an angle of 45°.

The diffracted beam is collimated by horizontal Soller slits (1.32" long spaced .0051" apart) and a 3/16" wide vertical slit. These Soller slits are stacked high enough (9/16") to view the entire irradiated volume of cell and sample at all values of 2θ. The maximum dispersions of the diffracted beam are $\pm1.58^O$ in the horizontal plane and $\pm.22^O$ in the vertical plane.

The distance from the focal spot to the center of the cell is $8\frac{1}{2}$" and from the center of the cell to the vertical receiving slit is $6\frac{1}{4}$".

Whenever possible, the alignment of a coordinate was made optically, using the actual x-ray beam to determine the positioning. Three coordinates--the takeoff angle of 5.7^O, the cell rotation position of 45° and the distance from the center of the cell to the goniometer face--were aligned mechanically using a variable level indicator and vernier calipers. The exact value of the takeoff angle is not critical. The latter two coordinates were checked optically

after the alignment.

The result of the alignment was to have the x-ray beam come off at an angle of 5.7° below the horizontal and parallel to the goniometer and through the center of the receiving slits when the counter is positioned at $2\theta = 0.00°$.

The cell was then aligned to be centered on the axis of rotation of the goniometer and tilted at 45° relative to the incident beam.

The reproducibility of the measured zero of the goniometer after realignment was found to be ~ .02°.

A basic change from previous experiments was the use of two counters offset by a fixed angle and counting simultaneously. While counter 1 scans from $2\theta = .50°$ to $2\theta = 26.50°$ in steps of .25°, counter 2 scans from $2\theta = 19.00°$ to 45.00°. The data from counter 1 are used in the range .50° to 26.50°. The data from counter 2 are used in the range 26.75° to 45.00°. The overlap region from 19.00° to 26.50° is used to normalize the output of the second counter system to the first.

By using two counters in this manner, the statistical precision obtained by counting for a time t was as good as that obtained by counting for 1.69t with a single counter.

Each counter system, except for the receiving slits, is essentially the same as that used by Kirstein[22]--an Amperex XP1010 photomultiplier with a Horiba 4HG2 thallium activated sodium iodide crystal. The dynode chain is 1500 K ohms and is powered by an Alfred 218B high voltage power supply at 1200 volts. The signal from the phototube is amplified by a Canberra model 805 pre-

amplifier and Canberra model 6018 amplifier. Resolution for both counters was 23%. This increase in resolution over that found by previous investigators[19, 21, 22] is due to the fact that the energy of the $K\alpha$ radiation from silver is higher than that from molybdenum.

The same Canberra Industries DATANIM system and CIPHER tape recorder used by Kirstein were used to automate the goniometer positioning, data accumulation, and alternation of filters placed in the incident beam.

Data Collection Sequence

For each experiment the data were accumulated in a series of 12 scans. Each scan consisted of stepping the goniometer from $2\theta = .50°$ to $26.50°$ in steps of $.25°$ (counting for 30 seconds at each position) with the alpha filter in place, repositioning to $.50°$ and repeating the stepping pattern with the β filter in place. The empty cell experiment of 10/24/72 was an exception to this sequence in that the entire range from $.50$ to $45.00°$ was scanned by both counters (goniometer stepped from $-18.00°$ to $45.00°$) to verify that there was no error caused by the two counter normalization procedure.

Thus, the intensity at each angle is counted for a total of 360 seconds with each filter in place. The repetitive scanning technique (which was used by Kirstein) serves to minimize variation due to long term drift and acts as a multi-channel analyzer in averaging out short term noise.

CHAPTER III   DATA ANALYSIS

In this chapter the complete set of data for all the experiments
is presented at the stages of development which appear to be most
significant and/or useful.   At intermediate stages of development
the data from only one state, state 1R, will be presented for pur-
poses of illustration.   State 1R was chosen because its density is in
the middle of the range studied.   Unless otherwise specified, the
characteristics of the data for state 1R are typical of the entire set
of states.   Where exceptions occur they **are**   pointed out.

Determining $P(2\theta)$

The raw data for each experiment listed in Table I consist
of the count rates $\{P_{\alpha 1}(2\theta)\}_i$, $\{P_{\beta 1}(2\theta)\}_i$, $\{P_{\alpha 2}(2\theta)\}_i$, and $\{P_{\beta 2}(2\theta)\}_i$,
where i denotes the number of the scan (i = 1 to 12),   the subscripts
1 and 2 denote counters 1 and 2,   and the subscripts α and β denote
the count rate with the alpha filter in place and the count rate with
the β filter in place.   Each of the quantities $\{P_{jk}(2\theta)\}_i$ is determined
by dividing the counts accumulated during a thirty-second interval,
$\{C_{jk}(2\theta)\}_i$,   by 30 seconds:

$$\left\{P_{jk}(2\theta)\right\}_i = \frac{\left\{C_{jk}(2\theta)\right\}_i}{30 \text{ sec}} \tag{17}$$

The individual scans must be averaged to obtain $P_{\alpha 1}(2\theta)$,
$P_{\alpha 2}(2\theta)$, $P_{\beta 1}(2\theta)$, and $P_{\beta 2}(2\theta)$ the alpha and beta count rates for
each counter.   The procedure adopted here was to normalize the
individual scans by the total alpha and beta intensity during each
scan before averaging:

$$P_{jk}(2\theta) = \sum_{i=1}^{12} \frac{(NS)_{ik}\{P_{jk}(2\theta)\}_i}{12} \tag{18}$$

where

$$(NS)_{ik} = \frac{\sum_{2\theta}\{P_{\alpha k}(2\theta)\}_i + \{P_{\beta k}(2\theta)\}_i}{\frac{1}{12}\sum_i \sum_{2\theta}\{P_{\alpha k}(2\theta)\}_i + \{P_{\beta k}(2\theta)\}_i} \tag{19}$$

These normalization factors for the 1R state are listed in Table III. They indicate a drift of about 2% in the x-ray tube output of the characteristic $K\bar{\alpha}$ radiation over the 24 hours during which x-rays were counted, after a warmup time of 3 hours. The difference between the normalized mean from equation (18) and the simple mean given by

$$P_{jk}(2\theta) = \frac{\sum_{i=1}^{12}\{P_{jk}(2\theta)\}_i}{12} \tag{20}$$

is completely negligible, being on the order of .0005 counts per second. This averaging produces a set of numbers $P_{\alpha 1}(2\theta)$, $P_{\beta 1}(2\theta)$, $P_{\alpha 2}(2\theta)$, and $P_{\beta 2}(2\theta)$ for each experiment, where, for example, $P_{\alpha 1}(2\theta)$ is the count rate for counter 1 with the alpha filter in place.

The diffracted intensity for each counter corresponding to the incident intensity distribution in Figure 4 is then given by

$$P_k(2\theta) = P_{\beta k}(2\theta) - P_{\alpha k}(2\theta) \tag{21}$$

At this point there is a pattern from $2\theta = .50°$ to $2\theta = 26.50°$ for counter 1, and from $2\theta = 19.00°$ to $2\theta = 45.00°$ for counter 2. Counter 2 is normalized to counter 1 by measuring a scale factor

using the counts in the overlap region from 19.00° to 26.50°

$$S_c = \sum_{2\theta=19.00°}^{2\theta=26.50°} \frac{P_2(2\theta)}{P_1(2\theta)} \tag{22}$$

The complete diffraction pattern for an experiment is then found by:

$$P(2\theta) = P_1(2\theta) \qquad .50° \le 2\theta \le 26.50° \tag{23}$$

and

$$P(2\theta) = P_2(2\theta)/S_c \qquad 26.75° \le 2\theta \le 45.00° \tag{24}$$

S_c for the eight experiments is listed in Table IV. S_c is significantly different from 1 because the foils in receiving Soller set 2 are .004" thick, while those in Soller set 1 are .002" thick. The thicker foils in Soller set 2 do not change the collimating properties but they decrease Ω, the effective solid angle of diffracted radiation accepted by the receiving slit system. $P(2\theta)$ for the eight experiments is presented in Table V. $P(2\theta)$ for state 1R is illustrated by the filled circles in Figure 6. In the following discussion $P(2\theta)$ from the empty cell will be denoted by $P_c(2\theta)$, $P(2\theta)$ from the helium experiments by $P_{cHe}(2\theta)$, and $P(2\theta)$ from the argon experiments by $P_{ca}(2\theta)$.

Determining the Argon Scatter

It is now necessary to interpret the $P_{ca}(2\theta)$ scattering pattern in terms of the scatter from the argon, $P_a(2\theta)$, and the scatter from the cell, $P_c(2\theta)$, and remove the latter.

The intensity of radiation scattered from a volume element dx dy dz of material located at x, y, and z and irradiated with a monochromatic source of x-rays is[18]

$$dI(2\theta) = I^0(y,z)\frac{e^4}{m^2c^4R^2}Pol(2\theta)nJ(2\theta)A^*(x,2\theta)dxdydz \qquad (25)$$

The coordinate system is established with x being the axis along the line of the incident beam, y is the vertical axis in the goniometer counting plane (see Figure 5) and z is the third Cartesian coordinate. $I^0(y, z)$ is the intensity incident on the face of the material irradiated. R is the distance from the sample to the detector. $\frac{e^4}{m^2c^4}$ is a constant which combines the charge and mass of the electron and the speed of light in vacuum and has the value 7.939×10^{-26} cm^2. J is the scattering per atom in electron units. $A^*(x, 2\theta)$ is the factor which corrects for absorption of the incident beam to the scattering center and absorption of the diffracted beam after scattering. For coherent scattering

$$A^*(x,2\theta) = e^{-\mu l(x,2\theta)} \qquad (26)$$

where 1 is the total path length of the incident and diffracted beam through the sample and cell and μ is the linear absorption coefficient for the material through which the beam travels. In general, 1 and hence A^*, are functions of x, y, and z. For the cylindrical cell used by previous workers in this lab they are functions of x and y, but not z. For a flat plate cell as used here, 1 and A^* are only

functions of x. Because of this very important fact it is possible to separate the x variables from the y, z variables and write the integrated form of equation (25) as

$$I_{ca}(2\theta) = \frac{e^4}{m^2 c^4 R^2} Pol(2\theta) \int_{y,z} I^0(y,z)\,dydz \left\{ n_c J_c(2\theta) \right.$$

$$\int_x A_c^*(x,2)\,dx + n_a J_a(2) \left. \int_x A_a^*(x,2)\,dx \right\} \qquad (27)$$

$I_{ca}(2\theta)$ is the intensity from the cell and sample. The subscripts c and a on A^* indicate absorption of radiation scattered by the cell and by the argon respectively. The integration of A_c^* is performed over the cell path irradiated by the incident beam, the integral of A_a^* is evaluated over the sample path irradiated by the incident beam. The expression $\int_{y,z} I^0(y,z)\,dydz$ is just P^0, the total power (counts per second) incident on the cell. Define

$$A_a(2\theta) = \int_x A_a^*(x,2\theta)\,dx \qquad (28)$$

for absorption of the argon scatter by the cell and sample, and

$$A_c(2\theta) = \int_x A_c^*(x,2\theta)\,dx \qquad (29)$$

for absorption of the cell scatter by the cell and sample. Note that while the (A^*)'s are true absorption coefficients, the (A)'s have dimensions of length and are a combination of the absorption coefficient and irradiated path length. The effective integrated true absorption coefficients are given by $\dfrac{A_a}{\sqrt{2}\,p}$ for the sample scatter and $\dfrac{A_c}{\sqrt{2}\cdot 2\,t}$ for the cell scatter, where p is the width of the cell

cavity and t is the thickness of one beryllium window. The quantity actually measured in the laboratory is a power (or count rate) rather than an intensity

$$P(2\theta) = I(2\theta) \cdot XA \tag{30}$$

where XA is the effective cross-sectional area of the receiving slit system on counter 1. The effective solid angle subtended by the slit system is

$$\Omega = \frac{XA}{R^2} \tag{31}$$

Combining equations (27) to (31) gives the count rate of scattered radiation from the cell and sample as

$$P_{ca}(2\theta) = \frac{e^4}{m^2 c^4} \Omega \ P^0 Pol(2\theta) \left\{ n_c J_c(2\theta) A_c(2\theta) \right.$$

$$\left. + n_a J_a(2\theta) A_a(2\theta) \right\} \tag{32}$$

In a similar manner, the equation for the count rate of scattered radiation from the empty cell is seen to be

$$P_c(2\theta) = \frac{e^4}{m^2 c^4} \Omega \ P^{o'} Pol(2\theta) \left\{ n_c J_c(2\theta) A'_c(2\theta) \right\} \tag{33}$$

The use of $P^{o'}$ indicates that there may be a change of incident intensity between the empty cell experiment which determined P_c and the cell + sample experiment which determined P_{ca} because of variation of the x-ray tube output. The prime on the absorption factor in equation (33) indicates that the scatter is to be corrected

for absorption by the cell alone.

The argon scatter from a cell + sample experiment can be written in a form analogous to equations (32) and (33) as

$$P_a(2\theta) = \frac{e^4}{m^2 c^4} \, \Omega \, P^{o\prime} Pol(2\theta) \left\{ n_a J_a(2\theta) A_a(2\theta) \right\} \qquad (34)$$

Equations (32), (33), and (34) may be combined to give the count rate for the argon scatter.

$$P_a(2\theta) = \frac{P^{o\prime}}{P^o} P_{ca}(2\theta) - P_c(2\theta) \left\{ \frac{A_c(2\theta)}{A_c^\prime(2\theta)} \right\} \qquad (35)$$

The determination of $\frac{P^{o\prime}}{P^o}$ as well as the fairly involved calculation of $\frac{A_c(2\theta)}{A_c^\prime(2\theta)}$ are described in Appendix A. The values of $\frac{P^{o\prime}}{P^o}$ for the various experiments are listed in Table VI using the cell scatter from the helium 2 state as the reference state for $P^{o\prime}$. These numbers indicate a maximum variation of about 6% in the $K\bar{\alpha}$ x-ray output from one run to the next.

In equation (35), $P_c(2\theta)$ is the scatter from the cell at the pressure of the argon state at which $P_{ca}(2\theta)$ is measured. It was considered possible that the $P_c(2\theta)$ values might not be independent of pressure because of pressure-induced stresses in the cell. Accordingly, the helium scatter was subtracted from the total scatter for each of the two helium states to obtain the cell scatter as a function of pressure. To do this equation (35) was written in the form

$$P_c(2\theta) = \left(\frac{P^{o\,\prime}}{P^o}\, P_{cHe}(2\theta) - P_{He}(2\theta) \right) \frac{A_c'(2\theta)}{A_c(2\theta)} \qquad (36)$$

$P_{He}(2\theta)$ was calculated from theory and is small because of the low density and low intrinsic scattering power of helium. Because μ for helium is very small, $\dfrac{A_c'(2\theta)}{A_c(2\theta)}$ is very close to one. Thus $P_c(2\theta)$ is close to $P_{c\,He}(2\theta)$. This is seen in Table VII which compares $P_c(2\theta)$ and $P_{c\,He}(2\theta)$ for the helium 1 state. The corrections for the helium 2 state (for which $P_c(2\theta)$ is also shown in Table VII) are about one-half as large as those for helium 1. Linear inter-polation is used to find $P_c(2\theta)$ at some pressure other than the 900 psi or 376.6 psi of the helium 1 and helium 2 states. The open circles in Figure (6) illustrate the value of $P_c(2\theta)$ at 778.81 psi, the pressure of state 1R. The peaks in $P_c(2\theta)$ agree with the values expected from the tabulated[40] 2d spacings for beryllium. The rise in intensity below $2\theta = 5^o$ is due to scattering from the air and from the Saran wrap windows of the empty cryostat. This empty cryostat scattering is shown in Figure 7. $P_a(2\theta)$ for state 1R from equation (35) is presented in Table VIII.

Correction for Double Scatter

$P_a(2\theta)$ as defined in equation (34) is the count rate of singly scattered radiation. However, the quantity obtained from the experimental data by equation (35) contains significant amounts of twice scattered x-rays.[41] In the experimental data from the empty cell there is cell-cell double scatter, while in the cell + sample data

there is cell-cell, sample-sample, sample-cell, and cell-sample

double scattering. The cell-cell double scatter is removed from

the cell+sample data by the cell subtraction so that $P_a(2\theta)$ as deter-

mined by equation (35) contains sample-sample, sample-cell, and

cell-sample double scatter. The amount of this double scatter was

calculated by Monte Carlo methods (Appendix B) and subtracted from

the $P_a(2\theta)$ obtained from equation (35). This corrected $P_a(2\theta)$ is now

the count rate of singly scattered radiation from argon. $P_a(2\theta)$

corrected for double scatter is presented for state 1R in Table VIII.

Divergence Correction

$P_a(2\theta)$ can now be corrected for divergence of the incident

and diffracted beams by a method based on that used by Kirstein[22]

to correct for his horizontal divergence. The method has been

further developed to include vertical divergence of the incident and

diffracted beams. The correction is accomplished by the inversion

of the matrix equation relating the experimental quantity $P_a^D(2\theta)$

{heretofore called $P_a(2\theta)$} to the ideal (non-divergent) $P_a(2\theta)$.

$$
\begin{bmatrix}
1 & \dfrac{1}{WY}\int(2\theta'-2\theta)\,dw\,dy + \dfrac{1}{3}\alpha_{max}^2\dfrac{1}{WY}\int\dfrac{\partial^2 2\theta'}{\partial 2\theta^2}dw\,dy & \dfrac{1}{2WY}\int(2\theta'-2\theta)^2 dw\,dy + \dfrac{1}{3}\alpha_{max}^2\cdot\left\{\dfrac{1}{WY}\int\left(\dfrac{\partial 2\theta'}{\partial 2\theta}\right)^2 + (2\theta'-2\theta)\dfrac{\partial^2 2\theta'}{\partial 2\theta^2}dw\,dy\right\} \\[4mm]
0 & \dfrac{1}{WY}\int\dfrac{\partial 2\theta'}{\partial 2\theta}dw\,dy & \dfrac{1}{WY}\int(2\theta'-2\theta)\dfrac{\partial 2\theta'}{\partial 2\theta}dw\,dy \\[4mm]
0 & \dfrac{1}{WY}\int\dfrac{\partial^2 2\theta'}{\partial 2\theta^2}dw\,dy & \dfrac{1}{WY}\int\left(\dfrac{\partial 2\theta'}{\partial 2\theta}\right)^2 + (2\theta'-2\theta)\dfrac{\partial^2 2\theta'}{\partial 2\theta^2}dw\,dy
\end{bmatrix}
\times
\begin{bmatrix}
P_a(2\theta) \\[4mm]
\dfrac{\partial P_a(2\theta)}{\partial 2\theta} \\[4mm]
\dfrac{\partial^2 P_a(2\theta)}{\partial 2\theta^2}
\end{bmatrix}
=
\begin{bmatrix}
P_a^D(2\theta) \\[4mm]
\dfrac{\partial P_a^D(2\theta)}{\partial 2\theta} \\[4mm]
\dfrac{\partial^2 P_a^D(2\theta)}{\partial 2\theta^2}
\end{bmatrix}
\quad (37)
$$

2θ is the nominal angle of the goniometer positioning. $2\theta'$ is the actual diffraction angle of the divergent ray. w is the horizontal distance across the sample from the center to the actual point of diffraction. y is the distance from the center of the receiving slit to the point where the diffracted beam enters the slit. W is the width of the irradiated volume of sample. Y is the width of the receiving slit. The vertical divergence of the incident and diffracted beams is $\pm\alpha_{max}$. If $\alpha_{max} = 0$ equation (37) reduces to Kirstein's[22] equation (9) Appendix G. $2\theta'$ is given in terms of 2θ by Kirstein's[22] equation (3) Appendix G:

$$
2\theta' = \sin^{-1}\left\{\left[\frac{R^2\sin^2 2\theta + (w-y)^2}{R^2 + (w-y)^2}\right]^2\right\}
\quad (38)
$$

Table VIII lists $P_a(2\theta)$ for state 1R before and after the divergence correction. Table IX lists the divergence corrected

single scatter count rates $P_a(2\theta)$ for the five argon experiments. $P_a(2\theta)$ for state 1R is also shown by the filled circles in Figure 8.

Determining the Coherent Scatter

$P_a(2\theta)$ consists of coherent and incoherent scatter. The argon scatter in electron units per atom (see equation (34)) can be written

$$J_a(s) = (1+i(s))f^2(s) + \mathcal{J}_{inc} \tag{39}$$

where the first term on the right represents the coherent scattering and the second term is the incoherent scattering. The terms in equation (34) which are independent of angle may be grouped

$$N_a = \frac{e^4}{m^2 c^4}\Omega P^{\circ\prime}n_a \tag{40}$$

and equation (34) can be rewritten

$$P_a(s) = N_a Pol(s)\left\{(1+i(s))f^2(s)A_{a(c)}(s) + \mathcal{J}_{inc}(s)A_{a(i)}(s)\right\} \tag{41}$$

where the subscripts (c) and (i) refer to coherent and incoherent scatter. Because the wavelength of the coherent and incoherent scattered radiation are different, $A_{a(c)} \neq A_{a(i)}$. At high angles (large s) the coherent argon scatter is just the atomic scatter f^2. ($i(s) = 0$). Thus N_a is determined by fitting the experimental quantity $P_a(s)$ (where s and 2θ are related by equation (2)) to the calculated quantity on the right side of equation (41) with $i(s)$ set equal to zero. Then, with N_a known, $i(s)$ is determined from a simple rearrangement of equation (41).

$$i(s) = \frac{P_a(s) - N_a Pol(s) \mathcal{J}_{inc}(s) A_{a(i)}(s)}{N_a Pol(s) f^2(s) A_{a(c)}(s)} - 1 \tag{42}$$

Correction for Incident Wavelength Distribution

Equation (42) as it is written implies that the experimental $P_a(2\theta)$ may be expressed as $P_a(s)$ by converting 2θ to s via equation (2). This is completely true only if the incident radiation is mono-chromatic. Previous investigators[19, 20, 22] have made this assumption and treated $P_a(2\theta)$ as if it was diffraction from an incident beam of pure $K\bar{\alpha}$ radiation. With a finite spread of incident wavelengths equation (42) is correctly written

$$i(2\theta) = \frac{P_a(2\theta) - N_a Pol(2\theta) \int_\lambda P^o(\lambda) \mathcal{J}_{inc}(2\theta,\lambda) A_{a(i)}(2\theta,\lambda) d\lambda}{N_a Pol(2\theta) \int_\lambda P^o(\lambda) f^2(2\theta,\lambda) A_{a(c)}(2\theta,\lambda) d\lambda} \tag{43}$$

where $P^o(\lambda)$ is the wavelength distribution of the incident radiation and is normalized such that

$$\int_\lambda P^o(\lambda) d\lambda = 1 \tag{44}$$

This distribution in non-normalized form is shown in Figure 4. N_a is determined by fitting $P_a(2\theta)$ at high angles to

$$P_a(2\theta) = N_a Pol(2\theta) \left\{ \int_\lambda f^2(2\theta,\lambda) A_{a(c)}(2\theta,\lambda) P^o(\lambda) d\lambda \right.$$
$$\left. + \int_\lambda \mathcal{J}_{inc}(2\theta,\lambda) A_{a(i)}(2\theta,\lambda) P^o(\lambda) d\lambda \right\} \tag{45}$$

which is the correct form of equation (41) for non-monochromatic radiation.

The f^2 used to reduce $P_a(2\theta)$ was determined experimentally. The determination is discussed in Appendix C. The values for $\mathscr{I}_{inc}(s)$ were taken from the calculations of Cromer and Mann.[42] These are tabulated in the form I_{inc}/R where I_{inc} is in energy units and

$$R \overset{BD}{=} \left(\frac{\lambda}{\lambda'}\right)^3 \tag{46}$$

where λ and λ' are the wavelengths of the incident and incoherently scattered x-rays. For quantum flux counting $\mathscr{I}_{inc}$ is given by

$$\mathscr{I}_{inc} = \frac{I_{inc}}{R}\left(\frac{\lambda}{\lambda'}\right)^2 = I_{inc}\frac{\lambda'}{\lambda} \tag{47}$$

λ' is determined from the equation[43]

$$\lambda' - \lambda = .02426 \ \mathring{A} \ (1-\cos 2\theta) \tag{48}$$

$f^2(s)$ and $\mathscr{I}_{inc}(s)$ are listed in Tables X and XI. The 2θ values are those which correspond to s according to equation (2) for Ag $K\bar{\alpha}$ radiation.

Finally, it is necessary to convert $i(2\theta)$ from equation (43) to $i(s)$ while allowing for the finite wavelength spread of incident radiation. From the definition of $i(2\theta)$ (equation (43)) one can write

$$i(2\theta) = \int_\lambda P^\circ(\lambda)\, i(\lambda, 2\theta)\, d\lambda \tag{49}$$

The incident intensity distribution is decomposed into the mono-

chromatic $K\bar{\alpha}$ and the continuous contribution as follows:

$$P^o(\lambda) = P_1^o(\lambda) + P_2^o(\lambda) \tag{50}$$

where the monochromatic part can be written as a delta function

$$P_1^o(\lambda) = P_1^o \delta(\lambda - \lambda_{K\bar{\alpha}}) \tag{51}$$

where P_1^o is a constant.

Substituting equations (50) and (51) into (49) gives

$$i(2\theta) = P_1^o i(\lambda_{K\bar{\alpha}}, 2\theta) + \int_\lambda P_2^o(\lambda) i(\lambda, 2\theta) d\lambda \tag{52}$$

The experimental values of $i(2\theta)$ were smoothed using a cubic spline least squares regression routine and equation (52) was solved iteratively to obtain $i(\lambda K\bar{\alpha}, 2\theta)$. $i(\lambda K\bar{\alpha}, 2\theta)$ gives $i(s)$ directly by equation (2) with $\lambda = \lambda K\bar{\alpha}$. Table XII lists the smoothed values of $i(2\theta)$ and $i(s)$ for the 1R state.

Note:

In one case experimental points were rejected in the process of smoothing $i(2\theta)$. In the $i(2\theta)$ data from state 1, 7 points from $2\theta = 18.00^o$ to $2\theta = 19.50^o$ were discarded as being inaccurate due to faulty subtraction of the very large beryllium peak at 18.75^o.

Obtaining the Distribution Functions

In order to obtain the distribution functions from equations (4) and (5), $i(s)$ must be known from $s = 0$ to $s = \infty$.

Below $2\theta = 1.00^o$, the main beam impinges on the detector system and $i(s)$ must be extrapolated theoretically from $s = .1955$

to $s = 0$. The value of i(s) at $s = 0$ is given by the isothermal compressibility K_T

$$i(s)\Big|_{s=0} = kTn_a K_T - 1 \tag{53}$$

Because i(s) is an even function of s, the additional specification is made

$$\frac{\partial i(s)}{\partial s}\Big|_{s=0} = 0 \tag{54}$$

Table XIII lists K_T and i(0) for the densities used to calculate $u(r)$. K_T is determined from the data of Michels.[34]

The maximum value of s realizable in a scattering experiment is found from equation (2) to be

$$s_{max} = \frac{4\pi \sin 90°}{\lambda} = \frac{4\pi}{\lambda} \tag{55}$$

which for $Ag\,K\bar{\alpha}$ radiation ($\lambda = .5608 \text{ A}°$) is $s_{max} = 22.41 \text{ A}°^{-1}$. In this experiment, however, the oscillations in i(s) become smaller than the uncertainty in the data after about $s = 4 \text{ A}°^{-1}$. A larger error can be incurred in the integrals in equation (4) and (5) by using these uncertain data than is incurred by setting $i(s) = 0$ after $s = 4 \text{ A}°^{-1}$. This latter procedure was used by previous investigators[19, 20, 22] and is known to cause errors in the transformed functions.[25, 44] The procedure used here was to truncate the experimental i(s) after two complete oscillations (at $s \sim 3.5 \text{ A}°^{-1}$) and to extrapolate from this point by calculating the high s oscillations which are consistent with the experimental data in the region from $s = 0$ to $s = 3.5 \text{ A}°^{-1}$. The details of this procedure are as follows:

Equation (6) was evaluated for a Lennard-Jones potential including terms up to n^2 to obtain $g(r)$. (The cluster integrals had been previously evaluated by Henderson and Oden.[45, 46]) This $g(r)$ was transformed to give $i(s)$ by

$$si(s) = 4\pi n \int_0^\infty r(g(r)-1)\sin sr \, dr \qquad (56)$$

which is the inverse transformation of equation (4). The experimental data for $i(s)$ were truncated after the second complete oscillation and the high s oscillations from equation (56) were added to the experimental data by matching the crossover points (points at which $i(s) = 0$) of the two curves.

Normalization - At this point the experimental $i(s)$ was renormalized according to the criterion, derived by taking the limit of equation (4) as $r \to 0$,

$$\int_0^\infty s^2 i(s) \, ds = -2\pi^2 n \qquad (57)$$

This complete renormalized curve (experimental $i(s)$ + extrapolated tail) was then transformed to give $g(r)$, $c(r)$, and $u^{eff}(r)$ (PY) from equations (4), (5), and (14). This $u^{eff}(r)$ (PY) was then used as the leading term in equation (6) along with the Lennard-Jones cluster integrals to recalculate $g(r)$. This new $g(r)$ was transformed again to a new estimate of $i(s)$ and the procedure was repeated until the value of $u^{eff}(r)$ converged to within $.1^\circ K$ in the well depth. This occurred after 1 transformation of the Lennard-Jones $i(s)$ and 2

subsequent transformations.

The final normalizing constants obtained from this procedure are listed in Table XV along with the normalization constants previously obtained by fitting to the atomic scatter at high s (equation 45). The complete normalized i(s) for each state is presented in Table XV and i(s) for state 1R is illustrated in Figure 9. (The intercept i(s) = 1.075 at s = 0, $\frac{\partial i(s)}{\partial s}$ = 0 at s = 0, is off the scale of Figure 9.) Note that state 4 was used to determine the atomic scattering factors $f^2(s)$ used in equation (45) (see Appendix C), and accordingly has not been subsequently analyzed to produce a potential function. Table XVI presents c(r), g(r), and u^{eff}(PY) for the four states analyzed. c(r), g(r), and u^{eff}(PY) for state 1R are illustrated in Figures 10, 11, and 12.

Correction for Non-Additivity

Equation (16) is now used to correct u^{eff}(PY) for many-body effects. It was found that the n^2 term in equation (16) could be neglected, its effect on the pair potential being of the order of .1°K in the well depth. Therefore equation (16) was rewritten as

$$u(r) = \frac{n_o \overbrace{\cdot}^{} b}{kT} + u^{eff}(r)(P\ Y) \tag{58}$$

and the $u^{eff}(r)$ (PY) for each state was corrected to give the pair potentials, u(r). u(r) for the four states is given in Table XVII. The prominent features of these potentials are listed in Table XVIII.

Comparison of Equation (10) and the PY Equation

Pings[28] suggested that equation (10) be rearranged into the

form
$$\frac{1+I_3(r,n,T)+\frac{1}{2}[I_3(r,n,T)]^2+\frac{1}{2}n^2\ \boxtimes}{1+I_1(r,n,T)} =$$

$$\exp\left\{kTu(r)\right\} \quad - \quad \frac{ng_1^{(NA)}(r)}{I_1(r,n,T)+1} \tag{59}$$

One would then use equation (59) by obtaining the experimental integrals for a range of densities and plotting the quantity on the left as a function of density. The slope of the function would give the $g_1^{(NA)}(r)$ term and the intercept at zero density would give the pair potential. However, no systematic trend of $u^{eff}(r)$ with density was found for the present experiments, and the aforementioned procedure could not be used. This indicates that the variation of the three-body effects at these densities is smaller than the imprecision of the data, which is consistent with the calculated three-body corrections of Rowlinson.[32, 33] However, equation (59) can be rewritten in terms of an effective two-body potential

$$\frac{1+I_3(r,n,T)+\frac{1}{2}[I_3(r,n,T)]^2+\frac{1}{2}n^2\boxtimes}{1+I_1(r,n,T)}=\exp\left\{kTu^{eff}(r)\ (eq.10)\right\} \tag{60}$$

Using the definitions in equations (11), (12), and (13), equation (60) can be rewritten

$$u^{eff}(r) = kT\ln\left[1 - \frac{c(r)}{g(r)} + \frac{\frac{1}{2}[g(r)-1-c(r)]^2 + \frac{1}{2}n^2 \; \boxtimes}{g(r)}\right] \qquad (61)$$

By comparing this with the Percus-Yevick equation (equation 14), it can be seen that equation (61) may be regarded as a corrected P Y equation which now becomes exact to the second order of density. (A cluster integral expansion of the P Y equation shows that the PY equation begins to be inexact in the n^2 and subsequent terms, as evidenced by the absence of some 4-body cluster integrals of the type shown in equation (9).) The term in equation (61) which corrects the PY equation for the missing n^2 integrals, $(\frac{1}{2}(g(r)-1-c(r))^2 + \frac{1}{2}n^2 \; \bowtie /g(r))$, has a maximum value for the densities studied of -.0014 at $r = r_{min}$, the separation at the potential minimum. This term produces a difference between the u^{eff}(PY) and u^{eff} (equation 10) of ϵ(PY) - ϵ(10) = .22°K for states 1 and 1R, .43°K for state 2, and .20°K for state 3. $u^{eff}(r)$ (equation 10) was evaluated for state 2, the most dense state, and is compared with $u^{eff}(r)$ (PY) in Table XVIX.

Averaging the Four States

The final estimate of u(r) is obtained by averaging the u(r)'s for the four states studied. An error analysis (see Chapter IV) showed that the final precision of u(r) for a given state was approximately proportional to the density of the state. Accordingly, the average u(r) was determined by weighting the contributions from each state (i) by the density:

$$u(r) = \frac{\sum_i \left\{ u(r) \right\}_i n_i}{\sum_i n_i} \tag{62}$$

u(r) from equation (61) is tabulated in Table XX and shown in Figure 13. The difference between u(r) obtained from equation (61) and from the average

$$u(r) = \frac{\sum_i \left\{ u(r) \right\}_i}{4} \tag{63}$$

is (at $r = r_{min}$), u(r) (equation 63) - u(r) (equation 62) = .15°K. The prominent features of the average u(r) from equation (62) are σ = 3.389 A°, ϵ = -146.3°K , r_{min} = 3.86 A°. These features are also listed in Table XXV.

CHAPTER IV   ERROR ANALYSIS

The method used here to determine the confidence limits on the estimates of the pair potential is as follows: The effect of various sources of error on i(s) are calculated or estimated. These effects are combined to give total error bounds on the i(s) curve. Next, a perturbation technique is used to estimate the error limits on u(r) corresponding to the error limits on i(s). Finally, the error limits on u(r) from each state are combined to give the confidence limits on the averaged u(r). Throughout this chapter, the error limits referred to are those which correspond to a two-sigma or 95% confidence interval. (Sigma as used here is the statistical measure of variation, and should not be confused with the sigma used to denote the intermolecular separation at u(r) = 0.)

The estimate of the error corresponding to this confidence interval is, in the case of some of the sources of error, somewhat subjective. The validity of these estimates can be judged by comparing the resultant calculated error with the internal consistency of the data (including the agreement among the final set of potential functions) and the ability of the final estimate of u(r) to predict other experimental data within the error limits on this estimate of u(r). This latter point will be discussed in Chapter V.

Error Limits on i(s)

Before examining the sources of error, it is necessary to comment on two procedures in the data analysis which have the effect of cancelling certain types of error. These procedures are 1) the experimental determination of f^2 (discussed in Appendix C)

and 2) the integral renormalization of i(s) by equation (56).

1) The experimental determination of f^2 has the effect of cancelling any errors which are reproducible functions of the scattering angle 2θ. This is demonstrated by the following development: The coherent scattering components of equations (39) and (41) may be written

$$J_{a(c)}(2\theta) = (1+i(2\theta))f^2(2\theta) \tag{64}$$

and

$$P_{a(c)}(2\theta) = N_a Pol(2\theta)(1+i(2\theta))f^2(2\theta)A_{a(c)}(2\theta) \tag{65}$$

so that

$$i(2\theta) = \frac{J_{a(c)}(2\theta)}{f^2(2\theta)} - 1 \tag{66}$$

and

$$J_{a(c)}(2\theta) = \frac{P_{a(c)}(2\theta)}{N_a Pol(2\theta)A_{a(c)}(2\theta)} \tag{67}$$

Assume that instead of measuring the true $P_{a(c)}(2\theta)$ one measures an erroneous quantity given by

$$P'_{a(c)}(2\theta) = d(2\theta)P_{a(c)}(2\theta) \tag{68}$$

The difference between $d(2\theta)$ and 1 is a measure of the error under consideration. Then the erroneous $J'_{a(c)}(2\theta)$ determined from (67) will be

$$J'_{a(c)}(2\theta) = \frac{P'_{a(c)}(2\theta)}{N_a Pol(2\theta) A_{a(c)}(2\theta)} \tag{69}$$

Now, because f^2 was obtained under the identical experimental conditions as $P'_{a(c)}(2\theta)$, the quantity used in equation (66) will not be the true $f^2(2\theta)$, but an erroneous $f^{2'}(2\theta)$ given by

$$f^{2'}(2\theta) = d(2\theta) f^2(2\theta) \tag{70}$$

Combining equations (66), (68), (69), and (70) produces the erroneous $i'(2\theta)$

$$i'(2\theta) = \frac{J'_{a(c)}(2\theta)}{f^{2'}(2\theta)} - 1 = \frac{d(2\theta) J_{a(c)}(2\theta)}{d(2\theta) f^2(2\theta)} - 1 \tag{71}$$

The $d(2\theta)$ functions cancel, giving the correct structure function

$$i'(2\theta) = i(2\theta) \tag{72}$$

2) The integral normalization of $i(s)$ by equation (57) has the effect of cancelling any errors in $P_a(2\theta)$ which act as a multiplicative constant over the range $s = 0$ to $s = 3.5$ A^{o-1}. This is seen as follows: If the measured $P'_a(2\theta)$ differs from the true $P_a(2\theta)$ by a constant b (which is allowed to vary from state to state)

$$P'_a(2\theta) = bP_a(2\theta) \tag{73}$$

Then N'_a (the erroneous normalization factor) will be determined to be bN_a, so that equation (42) becomes

$$i'(2\theta) = \frac{bP_a(2\theta) - bN_a Pol(2\theta) \mathcal{J}_{inc}(2\theta) A_{a(i)}(2\theta)}{bN_a Pol(2\theta) f^2(2\theta) A_{a(c)}(2\theta)} - 1 \qquad (74)$$

The (b)'s cancel and, again, $i'(2\theta) = i(2\theta)$. As one might expect, none of the sources of error produce a $P_a'(2\theta)$ which can be exactly written as $P_a(2\theta)$ multiplied by a constant. The important fact, however, is that the effect on $i(s)$ of an error which modifies $P_a(2\theta)$ by $h(2\theta, state)$, an arbitrary function of angle and state:

$$P_a'(2\theta) = h(2\theta, state) P_a(2\theta) \qquad (75)$$

depends on the <u>variation</u> of $h(2\theta)$ over the range $s = 0$ to $s = 3.5 \, \text{A}^{\circ -1}$ ($2\theta = 0$ to $2\theta = 18^\circ$). This is one of the reasons the integral normalization is a preferable method of determining N_a. If N_a is determined by fitting to the atomic scatter at high s then the error propagated to $i(s)$ depends on the variation of $h(2\theta)$ between the low s data and the high s data ($2\theta = 0$ to $2\theta = 45^\circ$), which will, in general, be significantly larger than the variation of $h(2\theta)$ over the low s range.

Cancellation of errors by integral normalization is illustrated by analysis of the error produced in $i(s)$ by an error in the quantity $(\frac{P^{o\prime}}{P^o})$ used to internormalize the cell and cell + sample data. Assume that instead of the correct $(\frac{P^{o\prime}}{P^o})$ one uses an incorrect $\left(\frac{P^{o\prime}}{P^o}(1 + \epsilon_r)\right)$. Then, from equation (35), the incorrect $P_a'(2\theta)$ obtained is

$$P_a'(2\theta) = P_a(2\theta) + \epsilon_r P_{ca}(2\theta) \qquad (76)$$

Substituting this value into equation (42) with the incorrect N_a' determined from equation (57) gives

$$i'(s) = \frac{z(2\theta)P_a(2\theta) - \bar{z}P_{a(i)}(2\theta) - \bar{z}A_{a(c)}(2\theta)\text{Pol}(2\theta)f^2(2\theta)N_a}{\text{Pol}(2\theta)A_{a(c)}(2\theta)f^2(2\theta)N_a}$$

(77)

where

$$z(2\theta) = P_a(2\theta) + \epsilon_r P_{ca}(2\theta)$$

(78)

and

$$\bar{z} = \langle z(2\theta)\rangle\bigg|_{2\theta=.50°\text{to}18.00°}$$

(79)

Rewriting (77) produces

$$i'(s) = i(s) + \left[\frac{z(2\theta)}{\bar{z}} - 1\right]\frac{P_a(2\theta)}{A_{a(c)}(2\theta)\text{Pol}(2\theta)f^2(2\theta)N_a}$$

(80)

where, for these densities, the term $(P_a(2\theta)/A_{a(c)}(2\theta)\text{Pol}(2\theta)f^2(2\theta)N_a)$ is close to one. For state 1R, for example, a 1% error in ($\frac{P^{o'}}{P^o}$) produces about a 1.2% error in $P_a(2\theta)$. $z(2\theta)$ ranges from 1.010 to 1.016 over the lower s domain and the errors in i(s) from equation (80) are about .2%.

The other sources of error used to estimate the error limits on i(s) are uncertainty in the atomic scattering factors $f^2(2\theta)$, and uncertainty in $P_c(2\theta)$ and $P_{ac}(2\theta)$ due to the statistically random nature of the scattering process. The uncertainty in f^2 is estimated (from the details of the f^2 determination, Appendix C) to have a variation of 2% (an absolute confidence of about 2% in $f(2\theta)$, 4% in

$f^2(2\theta)$). As previously explained, it is the imprecision in the deter-
mination of f^2 which affects $i(s)$, not the absolute accuracy of the
of the resultant f^2.

The statistical imprecision of $P_c(2\theta)$ and $P_{ca}(2\theta)$ was cal-
culated during the initial data averaging from the standard deviation
of the 12 scans and agreed with the precision predicted for a Poisson
process. This measured precision was carried through all the data
analyses. The precision of $P_a(2\theta)$ was determined by combining the
precision of cell and cell+ sample data according to statistical rules.
The final uncertainty in $i(s)$ per point ranged from about .008 at
$2\theta = .50^{\circ}$ to .035 at $2\theta = 45^{\circ}$. The corresponding uncertainties in
the value of the smooth regression line drawn through the experi-
mental points are presented for all four states in Table XXI. The
error limits on $i(s)$ from all errors are presented in Table XXII and
shown for state 1R in Figure 9.

Perturbation Technique

The error limits on $u(r)$ are now calculated from the error
limits on $i(s)$. The features in $i(s)$ were perturbed by adding a cali-
brated amount of error, $\Delta i(s)$, in the form

$$\Delta i(s) = \epsilon_2 \sin\frac{\pi}{p_s}(s-s_{min}) \tag{81}$$

from $s = s_{min}$ to $s = s_{min} + p_s$. p_s, the range perturbed, was
chosen so that the total amount of distortion accumulated by the
perturbation of various features in $i(s)$ was somewhat greater than
the uncertainty in $i(s)$ over its entire range. The features perturbed

were the large peak, the two minima, the four crossover points
$(i(s) = 0)$ and the approach to $s = 0$. By comparing $u^{eff}(PY)$ for the
perturbed $i(s) + \Delta i(s)$ with $u^{eff}(PY)$ for the unperturbed $i(s)$, the
effect of a given error in $i(s)$ on $u(r)$ could be determined. It was
verified that the changes induced in $u(r)$ were linear with ϵ_2. The
changes in $u(r)$ for the actual error limits of $i(s)$, ϵ_i, were found
by scaling the changes for the calibrated perturbation by ϵ_i/ϵ_2. As
an example, the effect of perturbing the second minimum in $i(s)$ with
$\epsilon_2 = .03$ is shown in Figure 14. For state $1R$, $\epsilon_i = .0214$ at this
feature, so the error induced in $u(r)$ from state $1R$ by the perturbation
is given by the values in Figure 14 multiplied by .713. In all the
perturbations the error in $u(r)$ diverged for values of r somewhat
below 3.20 A^o, and the conclusion is that these experiments provide
no information about $u(r)$ below $r = 3.20$ A^o.

The error limits from the various perturbations were com-
bined by taking the root-mean-square of the deviations to arrive at
the final error limits on $u(r)$. These limits are presented for each
state in Table XXIII.

The error limits for the average $u(r)$ are found by taking the
root-mean-square of the error limits on the individual states:

$$\Delta u(r) = \sqrt{\sum_i \left(\frac{n_i \{\Delta u(r)\}_i}{\sum_i n_i} \right)^2} \tag{82}$$

and are presented in Table XXIV and Figure 13. Table XXV sum-
marizes the main features and error limits of the individual

estimates of u(r) as well as the average u(r).

Other Sources of Error

The other possible sources of error do not appear to be large enough to significantly change the error limits on u(r) derived in the preceding section.

The error due to use of a non-monochromatic beam is eliminated by analyzing the data using the equations which involve integrals over the wavelength and do not assume the incident beam is monochromatic.

The total divergence correction is small, and appears to be complete at this point. The application of this correction to these experiments has the effect of deepening the potential well by $2.71^{O}K$ (for state 1R).

Errors incurred in correcting for absorption and double scatter have been minimized and are of the type which are largely cancelled by the experimental determination of f^{O} and the integral normalization.

The addition of high s extrapolated oscillations to i(s) has a large effect on the well depth (ϵ is decreased by $19^{O}K$), but the change is not sensitive to the form of the potential used to calculate these oscillations. The difference between ϵ calculated from oscillations added using a Lennard-Jones potential and ϵ from the self-consistent potential for state 1R was $2.5^{O}K$.

Internal Consistency of Data

The internal consistency of the data is an indication of the

validity of the error limits on u(r). The agreement among the final estimates of u(r) is seen to be considerably better than the calculated error limits and there are no observable trends with density.

The values of N_a are related to the incident power by equation (4). The values for $\Omega P^{O'}$ determined from equation (40) and the integral normalization constants are: State 1: 9166.7 cps, state 2: 9484.5 cps, state 3: 9197.5 cps and state 1R: 9115.8 cps. This agreement is quite satisfactory, especially when it is considered that the normalization constants used here are the values of N_a' which have absorbed the largest part of errors in the determination of $\frac{P^{O'}}{P^O}$, errors in the absorption correction, and errors in the double scattering correction. As a rough check on the absolute magnitude of the N_a values, the incident beam $K\bar{\alpha}$ power was measured directly, by absorption in palladium and rhodium foil, to be 1.7×10^8 counts per second. This agrees, within the experimental accuracy of the determination, with the value 1.16×10^8 cps obtained from the average of the four values of $P^{O'}\Omega$ and the calculated Ω value of 8×10^{-5} steradians.

Mountain's Criterion

Mountain[47] has developed a criterion for determining the accuracy of structure factor data by examining the spurious low r structure in g(r). He correlates the root-mean-square value of $r \frac{\partial g(r)}{\partial r}$ at values of r less than about .8 sigma with the accuracy of the i(s) data. Application of this criterion to the present data produces a "range of uncertainty" on the order of .6% for i(s),

which is a somewhat optimistic estimate of the 95% confidence level precision of the data points for i(s) compared to the value of .9% as determined from the scan averages.

CHAPTER V   COMPARISON WITH OTHER INFORMATION
ABOUT THE ARGON POTENTIAL

This chapter examines the agreement of the argon potential derived from this set of x-ray experiments with other available information about the pair potential.

Theoretical Calculations

Figure 13 shows the final estimate of $u(r)$ from equation (62) along with the error limits and the theoretical behavior of $u(r)$ at large r calculated from the most recent values[5,6] for the dispersion forces:

$$u(r) = - \frac{C_6}{r^6} - \frac{C_8}{r^8} - \frac{C_{10}}{r^{10}} \qquad (83)$$

with $C_6 = 4.694 \times 10^5 \, ^\circ K \, A^{\circ 6}$, $C_8 = 2.191 \times 10^6 \, ^\circ K \, A^{\circ 8}$ and $C_{10} = 1.34 \times 10^7 \, ^\circ K A^{\circ 10}$. Except for a small disagreement at $r \approx 5 \, A^\circ$ and $r \approx 6.70 \, A^\circ$. (The theoretical $u(r)$ from equation (64) is $2.3 \, ^\circ K$ below the lower error bound at $r = 5 \, A^\circ$, and $1.2 \, ^\circ K$ below the lower error bound at $6.70 \, A^\circ$.) The theoretical curve falls entirely within the experimental error limits, and converges to the experimental estimate in the region $r = 4.4 \, A^\circ$ to $r = 4.7 \, A^\circ$.

The experimental and theoretical curves coincide at $r = 4.625 A^\circ$. The most recently calculated[4] potential parameters ($\sigma = 3.28 \, A^\circ$, $\epsilon = 127 \, ^\circ K$, and $r_{min} = 3.63 \, A^\circ$) agree, within the accuracy of the theoretical model, with the results for these experiments.

Under these considerations it is worthwhile to examine the experimental potential function in two forms: $u(r)(I)$ will be the

experimental potential from 3.20 A° to 10.00 A°. $\mu(r)(II)$ combines

the experimental $\mu(r)$ from 3.20 to 4.625 A° and the theoretical potential

from eq. (64) for r = 4.625 A° to r = 10 A°. $\mu(r)(II)$ is equivalent to the re-

sult one would get by smoothing the kink at 5.3 A° out of the experimental

$\mu(r)$ within the calculated experimental error.

Second Virial Coefficient

The second virial coefficient is given in terms of the pair po-

tential by

$$B(T) = -2\pi \int_0^\infty (e^{-u(r)/kT} - 1) r^2 \, dr \qquad (84)$$

Prediction of the correct second virial coefficient is a necessary

condition for the credibility of a potential function. B(T) was calcu-

lated from $u(r)(I)$ and $u(r)(II)$ and compared with the smoothed exper-

imental estimates, compiled by Dymond and Smith,[48] of B(T) for

argon, and with the more recent data of Pope, Chappelear and

Kobayashi.[49] In the calculation of equation (65) values of $u(r)$ ob-

tained from the dilute gas transport coefficient data and presented

in the paper by Dymond and Alder[7] were used for the segment of

$u(r)$ from r = 0 to r = 3.20 A°. These values are presented in Table

XXVI. At low and intermediate temperatures (<800°K) B(T) is in-

sensitive to the value of $u(r)$ in this repulsive region. The theoretical

curve (equation (64)) was used for r > 10 A° in both cases. The re-

sults of these calculations of B(T) are presented in Table XXVI and

Figure 15. The following are significant aspects of this comparison

with experimental data:

1) There is some question about the error limits on $B_{exp}(T)$

as determined by Dymond and Smith in that some of the data of Pope

and coworkers falls outside of these limits.

2) The agreement with the experimental data is better for u(r)(II) than for u(r)(I).

3) If u(r)(I) is decreased by 35% of the error limits in the negative well region, the calculated values of B(T) agree with the experimental values.

Vibrational Energy Levels

The Schrödinger equation was solved[50] for the bound vibrational states of the argon dimer using u(r)(I) and u(r)(II). Seven stationary states were found for u(r)(I) and eight states for u(r)(II). The eigenvalues of these states and the energies of the transitions between these states are presented in Table XXVII and Figure 16 and compared with the experimental values of Tanaka and Yoshino,[51] with the experimental error limits on the transitions set by Bruch and McGee.[52] Note that u(r)(II) agrees with the experimental values better than u(r)(I) does.

Molecular Beam Data

A private communication has been received from Professor Donald Fitts[53] in which he reports the results of a comparison between the spacing of the glory extrema calculated from various potentials and his experimentally determined values. For a potential with the reduced form of u(r)[II] his experiments predict a product $\epsilon r_{min} =$ 592 °K A° to $\epsilon r_{min} = 605$ °K A°. The value determined in this thesis

is $\epsilon r_{min} = 564.7$ °K A°, with maximum and minimum values of 591.2 °K A° and 538.7 °K A°. Interestingly, this agreement is better than the agreement for the potentials derived by Lee and co-workers[16] from their molecular beam studies. The values for the Barker-type potentials[9,10,11] give somewhat better agreement than the median estimate of $u(r)$[II], but the ϵr_{min} products are still too low. The best agreement is obtained for the original Barker-Pompe potential.

Further discussion awaits the calculation of total cross sections for the various potentials.

CHAPTER VI   DISCUSSION AND CONCLUSIONS

This chapter discusses the contributions of this thesis work in terms of improved methods of x-ray data analysis, information about the argon pair potential, and information about three-body forces in argon. These contributions are discussed with respect to this thesis work, studies by other experimenters, and possible applications outside of this thesis. The chapter concludes with recommendations for improving the accuracy of the argon potential as determined from x-ray scattering data.

Improved Methods of X-Ray Scattering Data Analysis

1) <u>Divergence Correction</u> - The divergence correction developed by Kirstein[22] is now complete in that it corrects an experimental set of data for horizontal and vertical divergence (Chapter III, equations (37) and (38)). With appropriate modifications, the general technique is applicable to other types of data in which the experimental quantities are averages of some zero-divergence quantity sampled over a finite range, for example, molecular beam scattering. An observation from the divergence correction which could be of use in planning a scattering experiment is the fact that the effect of horizontal divergence depends on the first derivative of the data $\partial P(2\theta)/\partial 2\theta$, while the effect of the vertical divergence depends on the second derivative of the data, $\partial^2 P(2\theta)/\partial 2\theta$.

2) <u>Wavelength Correction</u> - Previously, x-ray data has been analyzed by assuming monochromatic incident radiation. [19, 21, 22] The methods developed and presented in Chapter III and Appendix A allow the actual spread of incident radiation to be taken into account. This result could also be applied to analysis of molecular beam data.

3) <u>High S Oscillations</u> - The method developed for extrapolating the experimental data to high values of s should be considerably more accurate than the simple truncation of data used previously.

4) <u>Effective Potentials from Pings' Treatment</u>[28] and the P-Y <u>Equation</u> - The difference between the effective potential calculated from the Percus-Yevick equation and the effective potential calculated from equation (61) is a direct measure of the contributions to $u(r)$ of the leading terms neglected by the Percus-Yevick equation. In an alternate form, the correct $u(r)$ could be used in the two equations to determine the effect of these leading terms on $c(r)$ and $g(r)$, and thus estimate the range of validity of the Percus-Yevick equation for a particular potential.

5) <u>Double Scattering</u> - The results of the Monte Carlo calculations of double scattering add information to that previously available concerning double scatter.[B1] Because the double scattering is such a sensitive function of many geometric and atomic variables, this low density information, particularly for the cross terms in the double scatter, should be a useful contribution.

6) <u>Atomic Scattering</u> - Experimental measurements of the coherent atomic scattering factors for argon are presented and compared with the Hartree-Fock calculations. These measurements are

sufficiently precise to reduce the other experimental data, but more work would have to be done before any definite conclusions could be drawn concerning the absolute validity of the Hartree-Fock scattering factors.

Pair Potential for Argon

The measured pair potential from this set of x-ray studies is consistent, within the error limits calculated by the perturbation analysis (Chapter IV), with the measured second virial coefficient data for argon, the spectroscopic data for the argon dimmer, and the theoretical calculations of $u(r)$. The agreement with $B(T)$ and the spectroscopic data is better for $u(r)$ [II] than for $u(r)$ [I]. It thus appears that the kink in $u(r)$[I] at $r = 5.3 \, A^\circ$ is spurious. This kink is associated with the spurious low r oscillations and "subsidiary peak"[21, 22, 54, 55] in $g(r)$. Kirstein has shown that this kink could be made to appear and disappear by small variations in $i(s)$. The perturbation analysis of Chapter IV has shown that errors in the features of $i(s)$ produce spurious oscillations in $u(r)$, $g(r)$ and $c(r)$. From these considerations, the best estimate of $u(r)$ is $u(r)$ [II], the combination of experimental data to $r = 4.625 \, A^\circ$ and the theoretical value from equation (64) for $r > 4.625 \, A^\circ$.

Table XXIX (taken largely from the review article by Maitland and Smith[3]) summarizes the estimates of the pair potential parameters for argon from various sources. In addition to the work previously referenced in this thesis, Table XXIX includes potentials determined by Guggenheim and McGlashan,[56] Sherwood and Prausnitz,[57] Munn and Smith,[58]

Dymond, Rigby and Smith,[59,60] and Maitland and Smith.[61] The agreement among the Barker-Bobetic, Maitland-Smith, and BFW parameters in Table XXIX is at least partly attributable to the fact that they assume the same multi-parametric analytical form. Figure 17 shows u(r) [II] along with the potentials derived by Dymond and Alder,[7] Klein and Hanley,[8] and Barker-Fisher-Watts.[9]

For the reasons discussed in the introduction, I believe the present work provides the best individual estimate of the argon potential parameters. In addition, there is a good measure of the accuracy of this estimate. This has not been presented for previous determinations because of the difficulty in determining error propagation when simultaneously fitting different types of data, and because of the impossibility of estimating the error incurred by presupposing the potential form.

The final error limits on u(r) could be significantly collapsed by determining the range of potentials within the x-ray determination error limits which fit all the known macroscopic and spectroscopic argon data.

Three-Body Forces

As explained in Chapter III, the density range covered by the experimental work of this thesis is insufficient to enable the effect of three-body forces to be determined by these experiments alone. However, three-body forces could be determined in two ways by using these experiments along with other data:

1) u(r)[II] could be used to calculate the two-body-additive part of C(T), the argon third virial coefficient. This calculated C(T)

could be compared with the experimental C(T) to determine the non-additive contributions. This was done by Sherwood and Prausnitz[57,62] for a variety of potentials, but the results were sensitive to the form of the pair potential used, and it was impossible to conclude anything definite about the three-body forces. (It would appear that more accurate experimental C(T) data than is presently available would be needed. The current tabulated[48] results vary by 20% for argon.)

2) Kirstein's[22] measurements of $u(r)^{eff}$[PY] for high densities could be combined with the present low density data to yield the effective $u(r)$ over a large density range and, consequently, information about the non-additive effects. There are no discrepancies between the two sets of data and it would only be necessary to extrapolate Kirstein's i(s) functions to high s by calculating the self-consistent oscillations according to the method of Chapter III.

Recommended Improvements in Obtaining X-Ray Data

There do not appear to be any significant improvements or additions to be made in the data analysis scheme. The limiting factors on the final accuracy of the data are experimental.

The largest source of experimental error at these low densities appears to be the presence of cell scattering. As recommended by Kirstein, a single crystal beryllium cell would appear to solve this problem by restricting the cell scatter to a few well defined peaks.

The use of an incident beam of more monochromatic radiation than that provided by dual filters would considerably facilitate the data analysis, as well as eliminate the statistical error caused by

subtraction of the alpha filter count rate, $P_\alpha(2\theta)$, from the beta filter count rate, $P_\beta(2\theta)$ (equation (21)). Monochrometers are one possible solution but there are difficulties with respect to alignment, chemical stability of the monochrometer crystal, polarization corrections, and loss of incident intentisy. A recent development is the production of lithium activated silicon detectors.[63] These detectors, operating at cryogenic temperatures, have extremely high resolving properties compared to the Na I (Th) crystals, and provide a complete separation of the $K\bar\alpha$ and $K\beta$ peaks. With these detectors it would be possible to irradiate the sample with a direct beam from the x-ray tube and restrict the wavelength range of the diffracted beam to be counted by using pulse height discrimination.

References

1. A. D. Buckingham and B. D. Utting, Ann. Rev. Phys. Chem. $\underline{21}$, 287 (1970)

2. T. M. Reed and K. E. Gubbins, Applied Statistical Mechanics (McGraw-Hill Book Co., N.Y., 1973)

3. G. C. Maitland and E.B. Smith, Chem. Soc. Rev. $\underline{2}$, 181 (1973)

4. R. G. Gordon and Y. S. Kim, J. Chem. Phys. $\underline{56}$, 3122 (1972)

5. G. Starkschall and R. G. Gordon, J. Chem. Phys. $\underline{54}$, 663 (1971)

6. G. Starkschall and R. G. Gordon, J. Chem. Phys. $\underline{56}$, 2801 (1972)

7. J. H. Dymond and B. J. Alder, J. Chem. Phys. $\underline{51}$, 309 (1969)

8. M. Klein and H.J.M. Hanley, J. Chem. Phys. $\underline{53}$, 4722 (1970)

9. J. A. Barker, R. A. Fisher and R. O. Watts, Mol. Phys. $\underline{21}$, 657 (1971)

10. J. A. Barker and A. Pompe, Aust. J. Chem. $\underline{21}$, 1683 (1968)

11. M. V. Bobetic and J. A. Barker, Phys Rev. B $\underline{2}$, 4169 (1970)

12. J. Kestin, S. T. Ro and W. Wakeham, Physica $\underline{58}$, 165 (1972)

13. J. Kestin (ed.), Transport Phenomena - 1973 (American Institute of Physics, N.Y., 1973) AIP Conference Proceedings Number 11, pp. 140,141

14. C. D. Andriesse and E. Legrand, Physica $\underline{57}$, 191 (1972)

15. W. H. Miller, J. Chem. Phys. $\underline{51}$, 3631 (1969), and references cited therein

16. J. M. Parson, P.E. Siska and Y. T. Lee, J. Chem. Phys. $\underline{56}$, 1511 (1972)

17. J. Kestin (ed.), <u>Transport Phenomena - 1973</u>, (American Institute of Physics, N.Y., 1973) AIP Conference Proceedings Number 11, pp. 279-296

18. R. W. James, <u>The Optical Principles of the Diffraction of X-rays</u> (G. Bell and Sons, London 1962)

19. P. G. Mikolaj, " An X-Ray Diffraction Study of the Structure of Fluid Argon ", doctoral thesis, California Institute of Technology, Pasadena, California, (1965)

20. P. G. Mikolaj and C. J. Pings, J. Chem. Phys. <u>46</u>, 1401 (1967)

21. S. C. Smelser, " An X-ray Diffraction Study of the Structure of Argon in the Dense Liquid Region" , doctoral thesis, California Institute of Technology, Pasadena, California (1969)

22. B. E. Kirstein, " The Structure of Liquid Argon as Determined by X-ray Diffraction", doctoral thesis, California Institute of Technology, Pasadena, California (1972)

23. L. Goldstein, Phys. Rev. <u>84</u>,466 (1951)

24. P. G. Mikolaj and C. J. Pings, J. Chem. Phys. <u>46</u>, 1412 (1967)

25. H. N. V. Temperley, J. S. Rowlinson and G. S. Rushbrooke (ed.), <u>Physics of Simple Liquids</u>, (North-Holland Publishing Co., Amsterdam, 1968) Chapter 10

26. G. S. Rushbrooke and H. I. Scoins, Proc. Roy. Soc. A <u>216</u>, 203 (1953)

27. P. G. Mikolaj and C. J. Pings, Phys. Rev. Letters <u>16</u>, 4 (1965)

28. C. J. Pings, Discussions Faraday Soc., 89 (1967)

29. J. K. Percus and G. J. Yevick, Phys. Rev. <u>110</u>,1 (1958)

30. J. S. Rowlinson, Mol. Phys. <u>9</u>, 217 (1965)

31. P. G. Mikolaj and C. J. Pings, Phys. Rev. Letters <u>15</u>, 849 (1965)

32. G. Casanova, R.J. Dulla, D. A. Jonah, J. S. Rowlinson and G. Saville, Mol. Phys. 18,589 (1970)

33. R. J. Dulla, J.S. Rowlinson and W. R. Smith, Mol. Phys. 21, 299 (1971)

34. A. Michels, J. M. Levelt and W. DeGraaff, Physica 24, 659 (1958)

35. W. I. Honeywell, " X-ray Diffraction Studies of Dense Fluids ", doctoral thesis, California Institute of Technology, Pasadena, California (1964)

36. Cryogenic Service Corporation, 3539 Ocean View Blvd., Glendale, California 91208

37. West Coast Technical Service Inc., 1049 South San Gabriel Blvd., San Gabriel, California 91776

38. S. Y. Wu, " Study of Equilibrium Critical Phenomena in Fluid Argon", doctoral thesis, California Institute of Technology, Pasadena, California (1971)

39. This controller was built at Caltech by John Yehle with the design based on a unit built by Electro-Optical Systems, Pasadena, California.

40. W. B. Pearson, A Handbook of Lattice Spacings and Structures of Metals and Alloys (Pergamon Press, New York, 1958)

41. The possibility that the double scatter from a flat cell might be significantly larger than the (negligible) double scatter from a cylindrical cell was pointed out in a personal communication from G.D.Wignall, present address: Imperial Chemical Industries Ltd., Corporate Laboratory, P.O. box 11, the Heath, Runcorn, Cheshire WA7 4QE England.

42. D. T. Cromer and J. B. Mann, J. Chem. Phys. 47, 1892 (1967)

43. K. Lonsdale (ed.), International Tables for X-Ray Crystallography (The Kynoch Press, Birmingham England, 1962)

44. R. Kaplow, S.L. Strong and B. L. Averbach, Phys. Rev. 138, A 1336 (1965)

45. D. Henderson, Mol. Phys. $\underline{10}$, 73 (1965)

46. D. Henderson and L. Oden, Mol. Phys. $\underline{10}$, 405 (1966)

47. R. D. Mountain, J. Chem. Phys. $\underline{57}$, 4346 (1972)

48. J. H. Dymond and E. B. Smith, <u>Virial Coefficients of Gases</u> (Oxford, 1969)

49. G. A. Pope, P. S. Chappelear and R. Kobayashi, J. Chem. Phys. $\underline{59}$, 423 (1973)

50. These calculations were performed with the assistance of Barry Olafson using a matrix-finite differences program developed at Caltech by R.C. Ladner, D.L. Huestis and B. Olafson.

51. Y. Tanaka and K. Yoshino, J. Chem. Phys. $\underline{53}$, 2012(1970)

52. L. W. Bruch and I. J. McGee, J. Chem. Phys. $\underline{53}$, 4711 (1970)

53. D. D. Fitts, private communication. Address-Department of Chemistry, University of Pennsylvania, Philadelphia, Pennsylvania

54. P. L. Fehder, J. Chem. Phys. $\underline{52}$, 791 (1970)

55. D. Stripe and C. W. Thompson, J. Chem. Phys. $\underline{36}$, 3921 (1962)

56. E. A. Guggenheim and M. L. McGlashan, Proc. Roy. Soc. $\underline{A255}$, 456 (1960)

57. A. E. Sherwood and J. M. Prausnitz, J. Chem. Phys. $\underline{41}$, 429 (1964)

58. R. J. Munn and F. J. Smith, J. Chem. Phys. $\underline{43}$, 3998 (1965)

59. J. H. Dymond, M. Rigby and E. B. Smith, Physics of Fluids $\underline{9}$, 1222 (1966)

60. J. H. Dymond, M. Rigby and E. B. Smith, J. Chem. Phys. $\underline{42}$, 2801 (1965)

61. G. C. Maitland and E. B. Smith, J. Chem. Phys. $\underline{52}$, 3848 (1970)
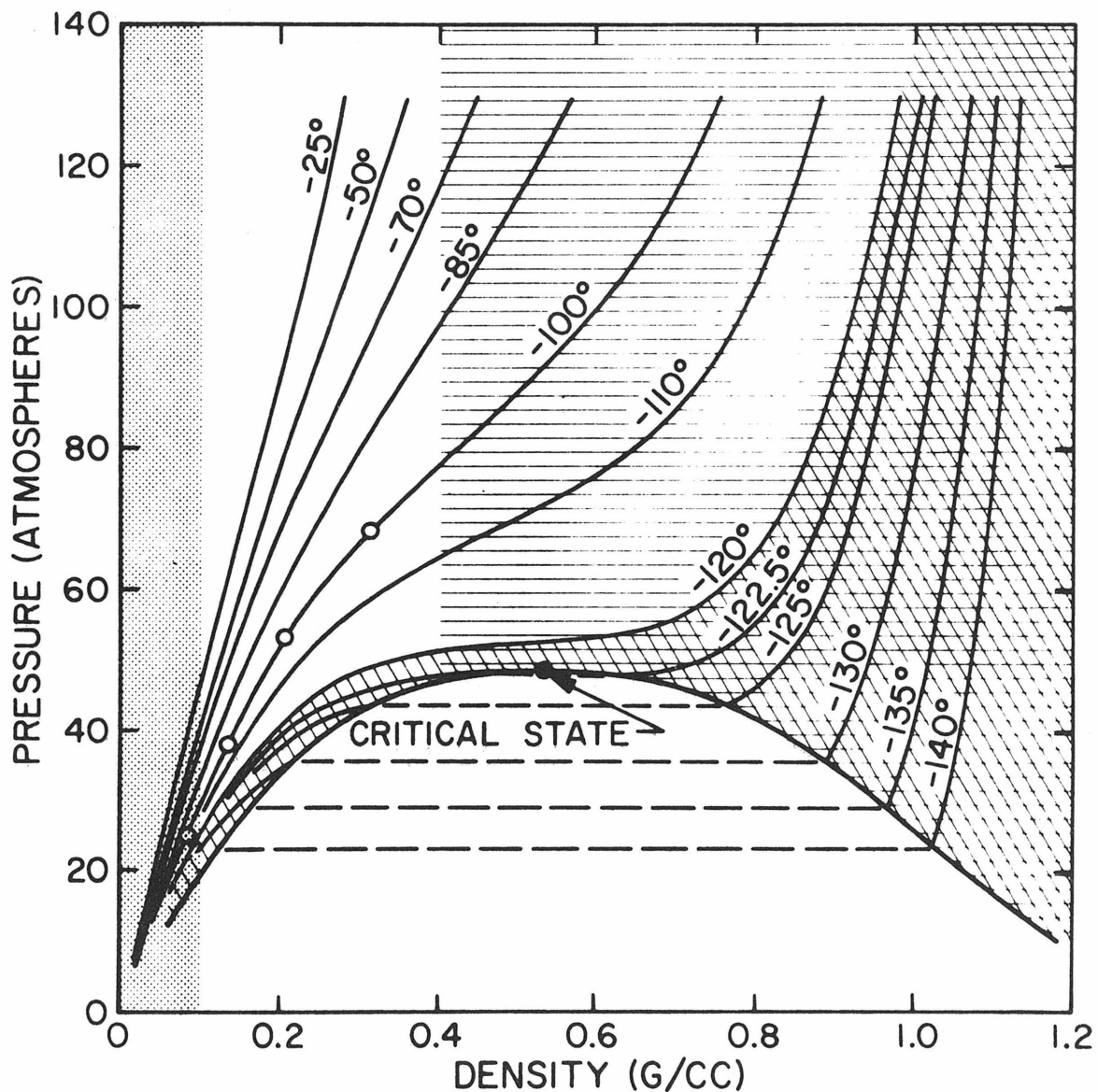
Figure 1. Thermodynamic Plane for Argon. P-V-T data is
from Michels and co-workers[34]. O indicate experimental
states studied in this work; Shaded areas indicate regions
where x-ray data cannot be inverted to obtain pair potential
information. Temperatures are in °C.

1/16" SWAGELOCK FITTING

S.S. TUBING

0.035" Be WINDOWS

MONEL SKT. HD. SCREWS

HR MONEL

0.005" GOLD WASHER

1 3/8 IN.
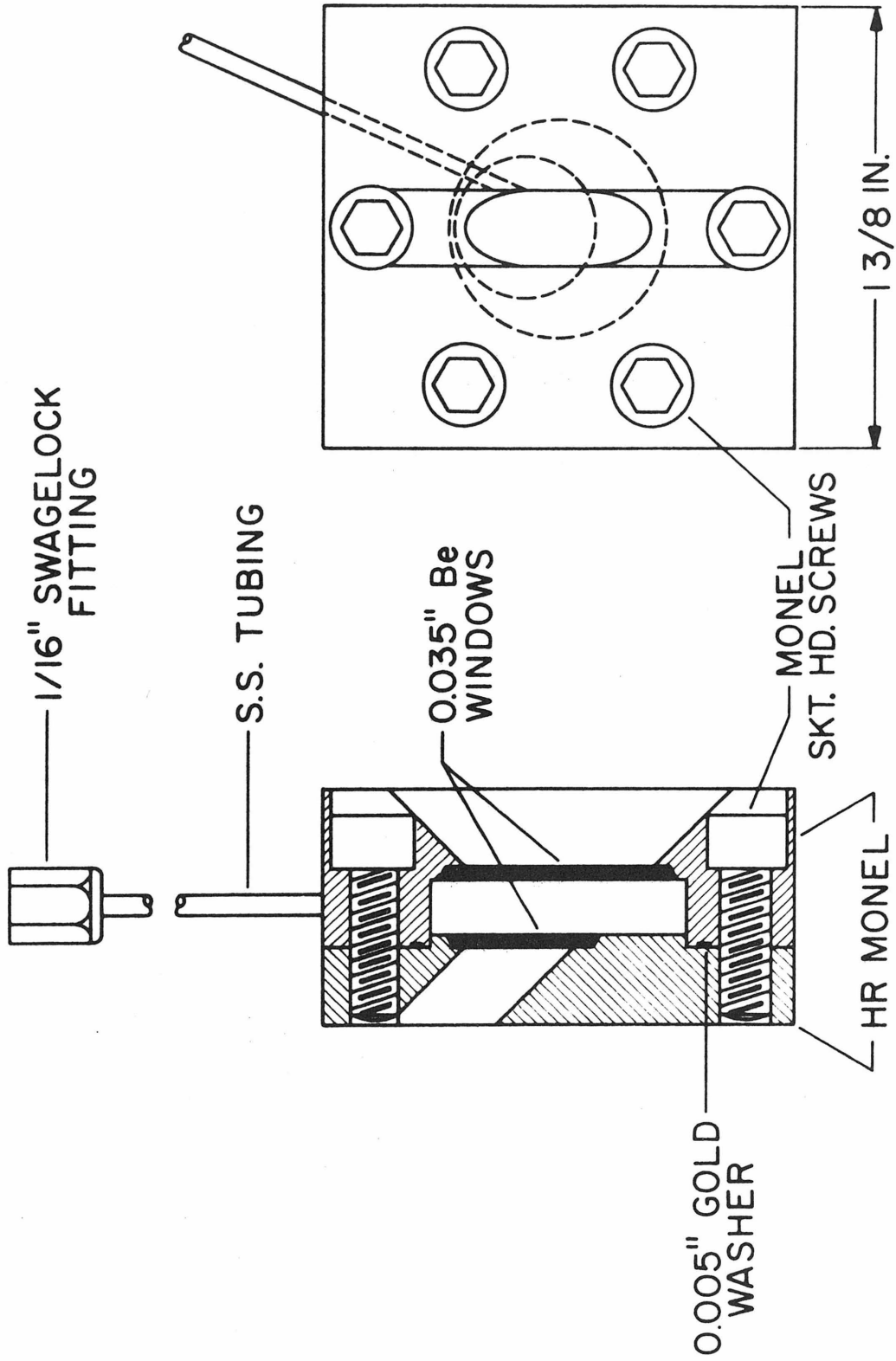
Figure 2. High Pressure, Low Temperature, X-Ray Diffraction Cell.

DIFFRACTED RADIATION

CU RADIATION SHIELD

INCIDENT RADIATION

PELTIER DEVICE

CELL

SARAN WRAP ENTRY PORT

SARAN WRAP EXIT SLOT

304 S.S. CRYOSTAT

ARGON FILLING LINE

PT THERM.

COMPOUND LATHE REST

TO VACUUM PUMP

CELL

GONIOMETER SHAFT

N_2 COLD SINK

PELTIER DEVICES

N_2 COLD SINK

ARGON

N_2 FLOW

6 3/4"
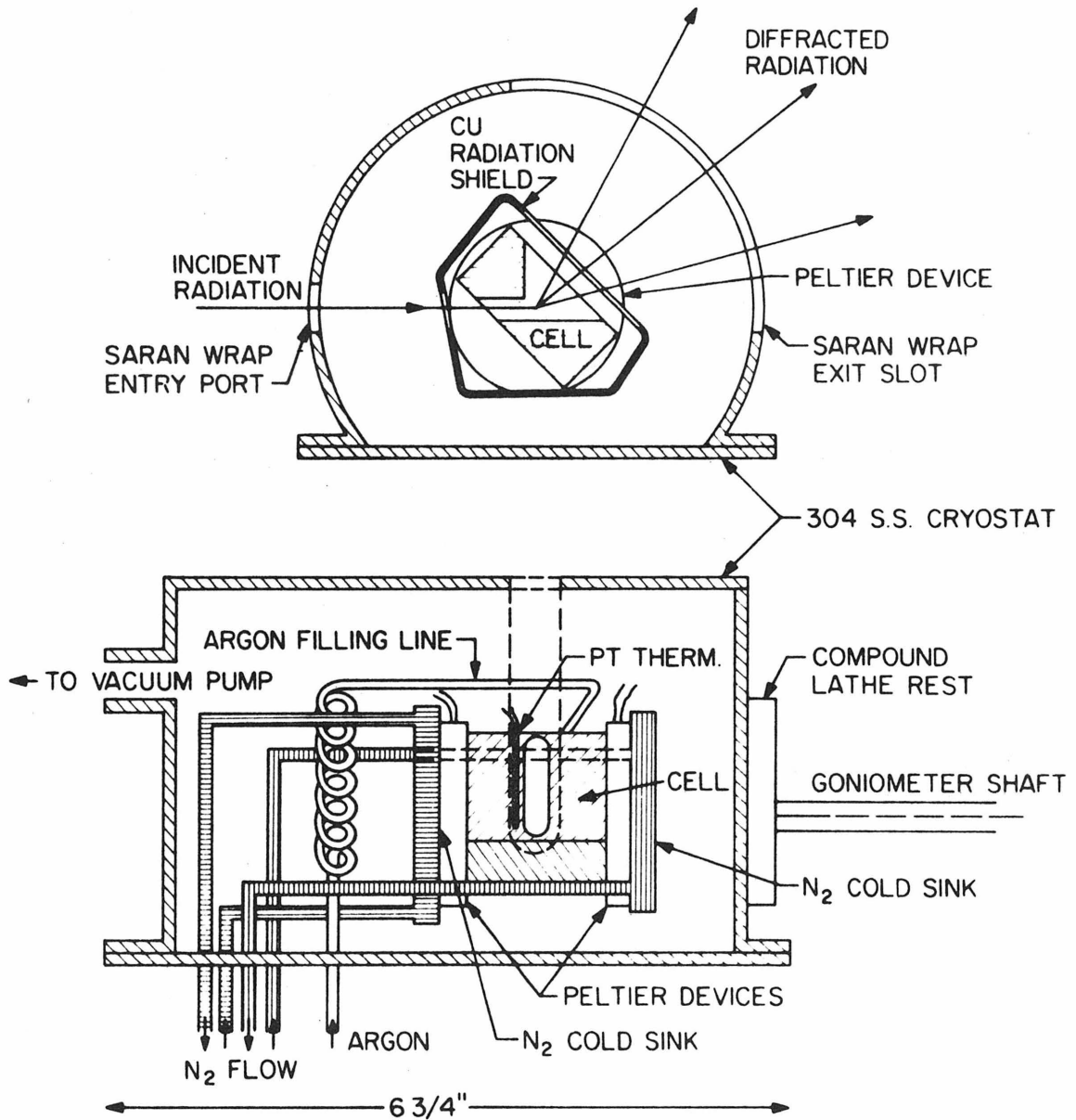
Figure 3. Cryostat used in These Experiments.
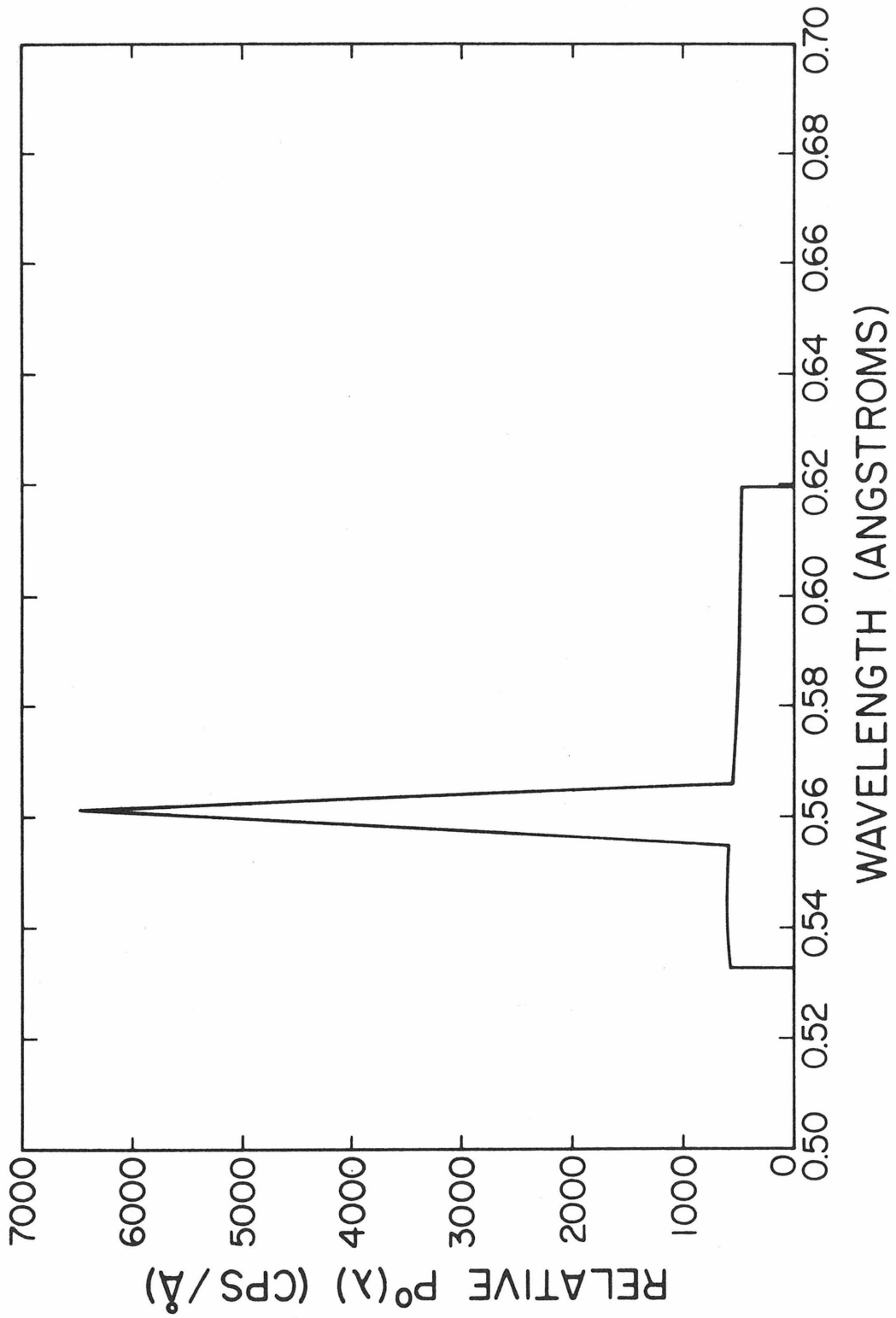
Figure 4. Differential Intensity Spectrum from Balanced Dual Filters for Silver K-alpha radiation.
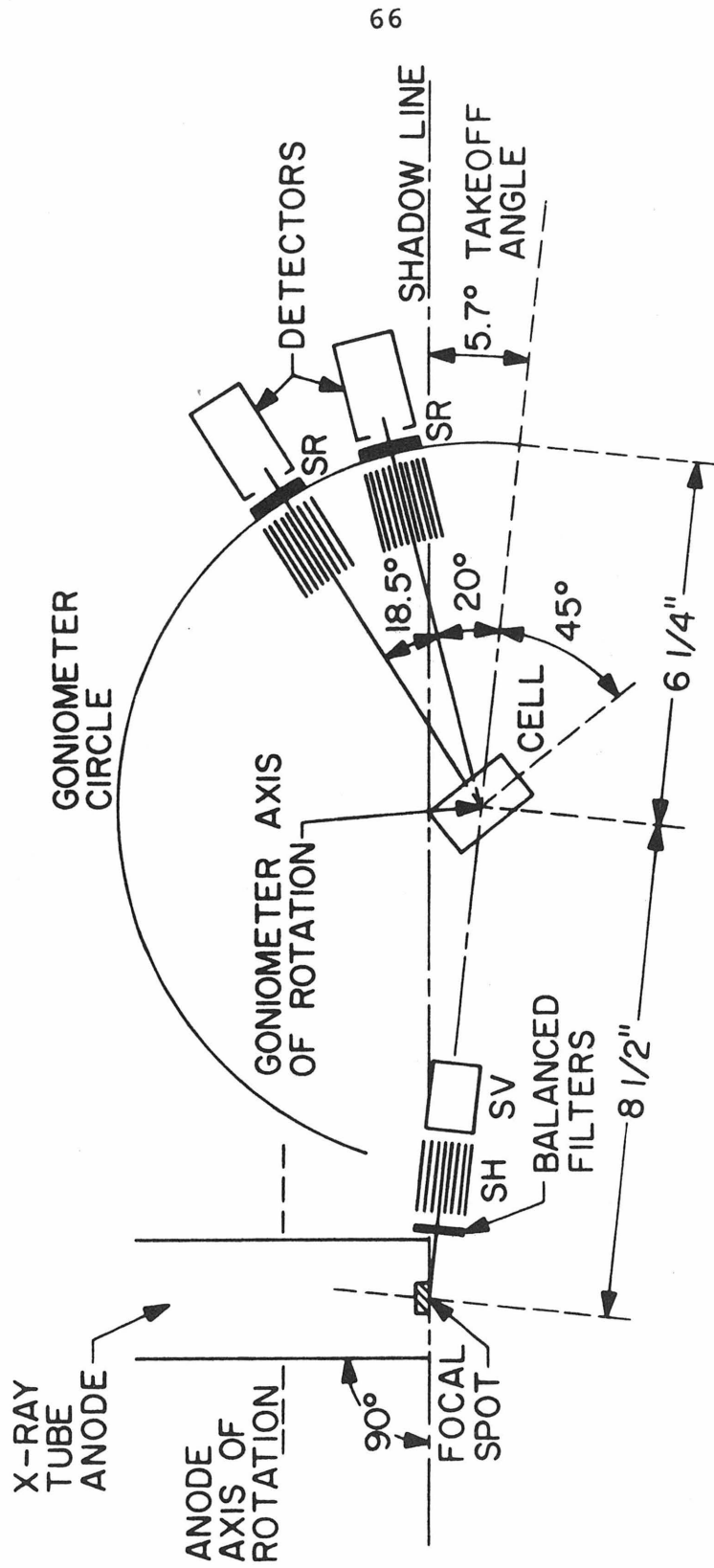
Figure 5. Optical Geometry in the Vertical Plane for the X-Ray Diffraction Experiments.
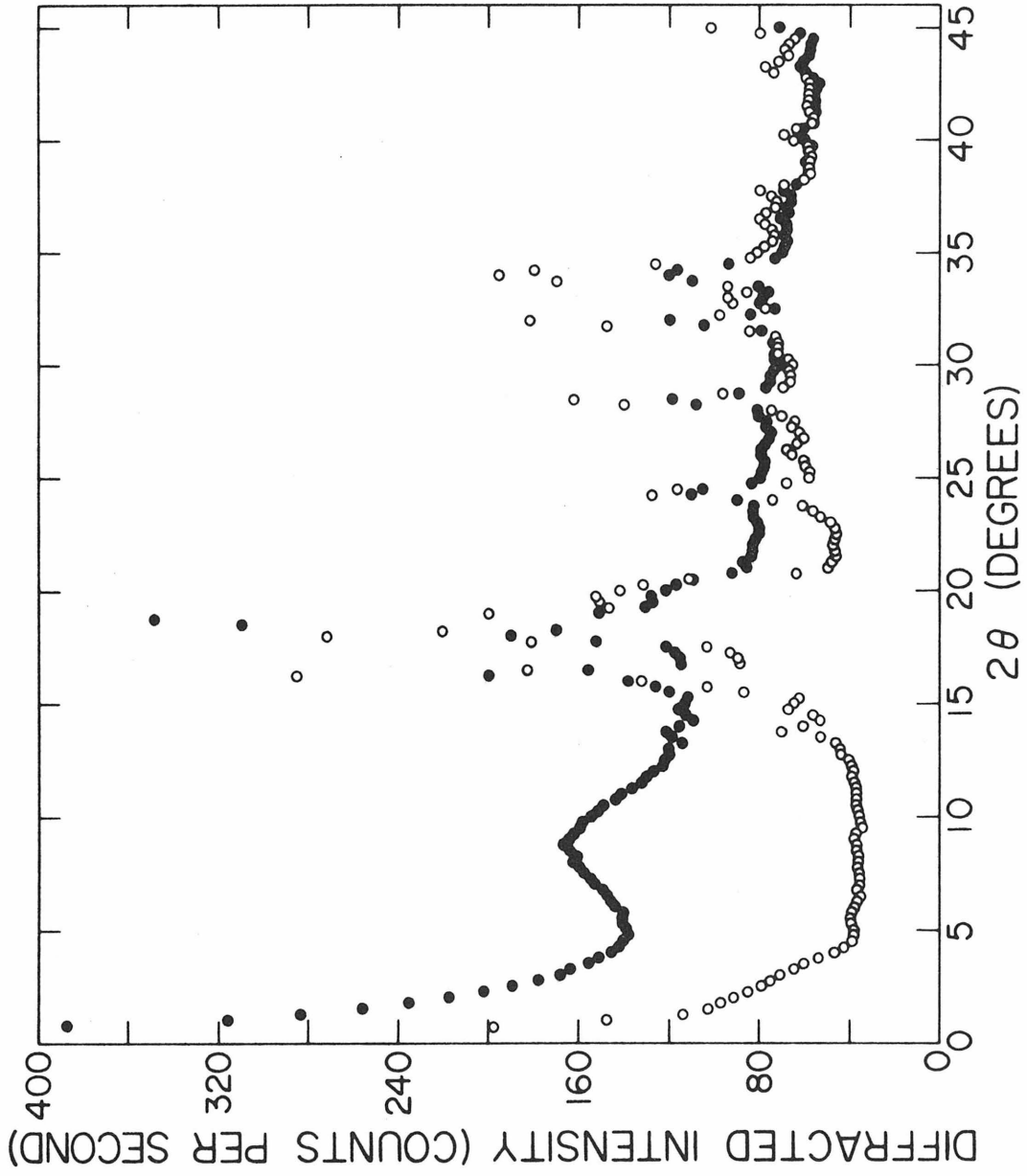
Figure 6. Diffraction Patterns for Empty Cell and Cell+Sample Experiments, State 1R.
○ empty cell count rate. ● cell+sample count rate. Off scale empty cell data:
561.22 cps at 18.50°, 654.46 cps at 18.75°.
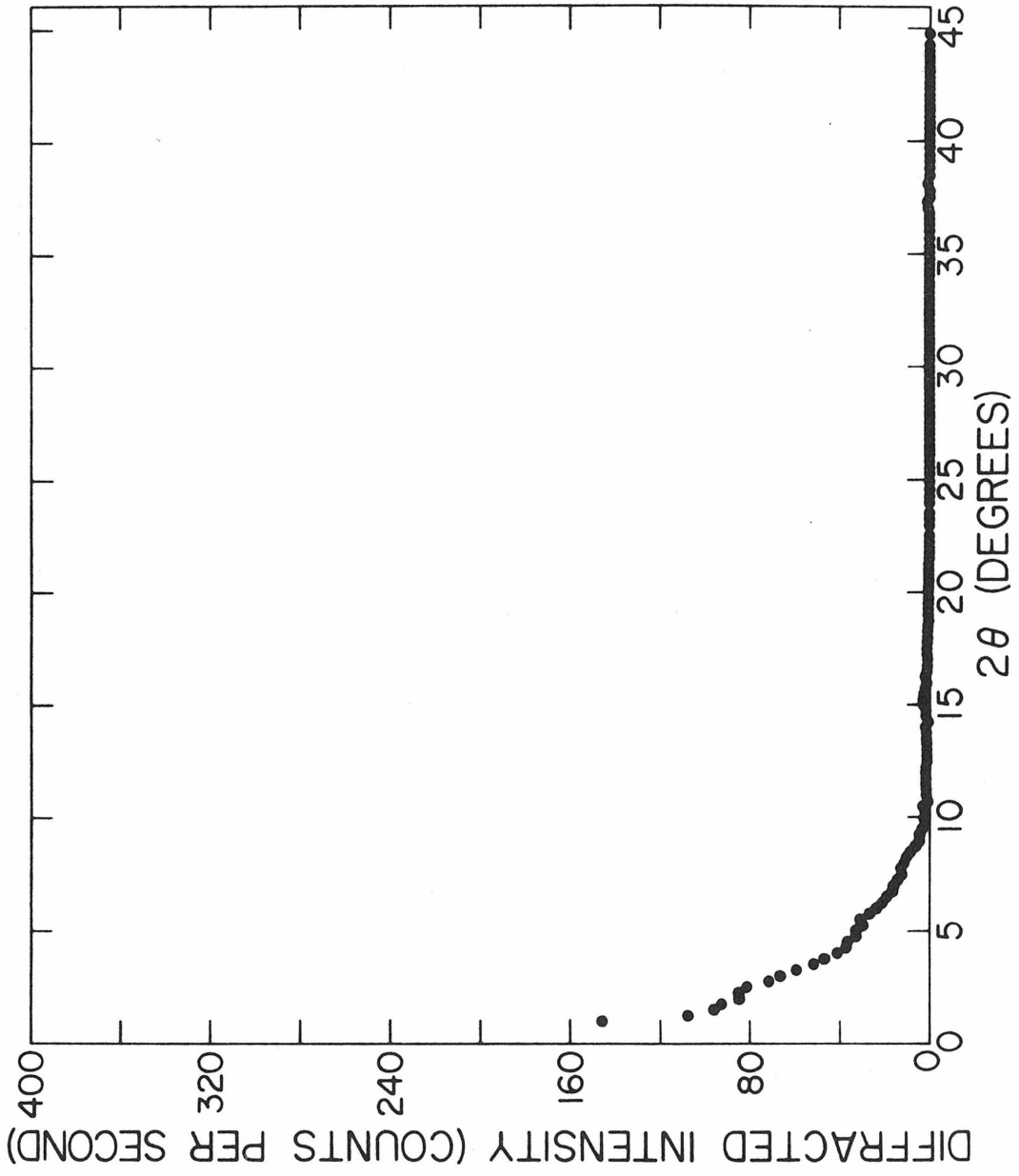
Figure 7. Diffraction from the Empty Cryostat.
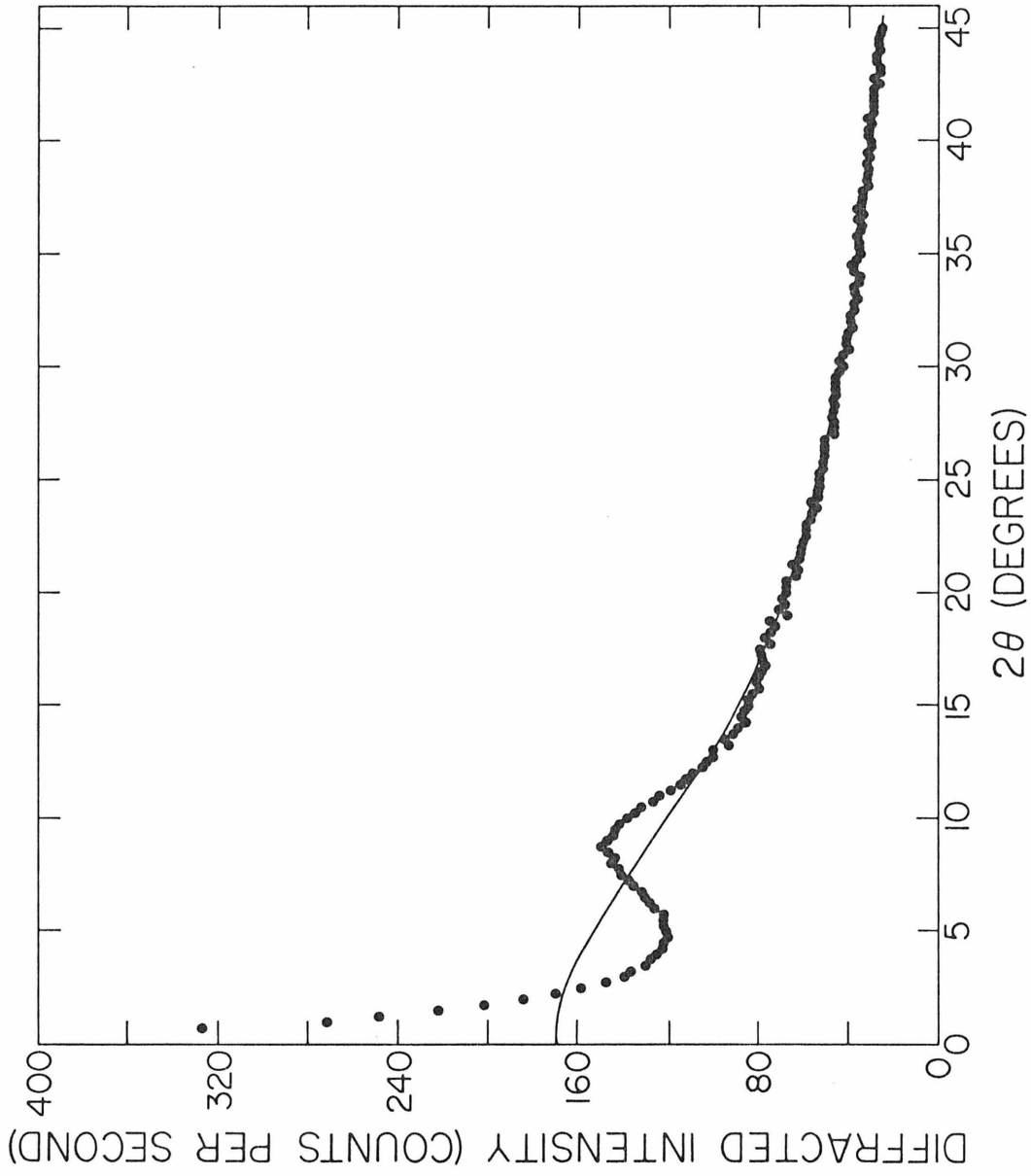
Figure 8. Argon Diffraction Pattern, State 1R. ● Experimental count rate.
—atomic scatter, coherent plus incoherent, corrected for absorption and polarization.
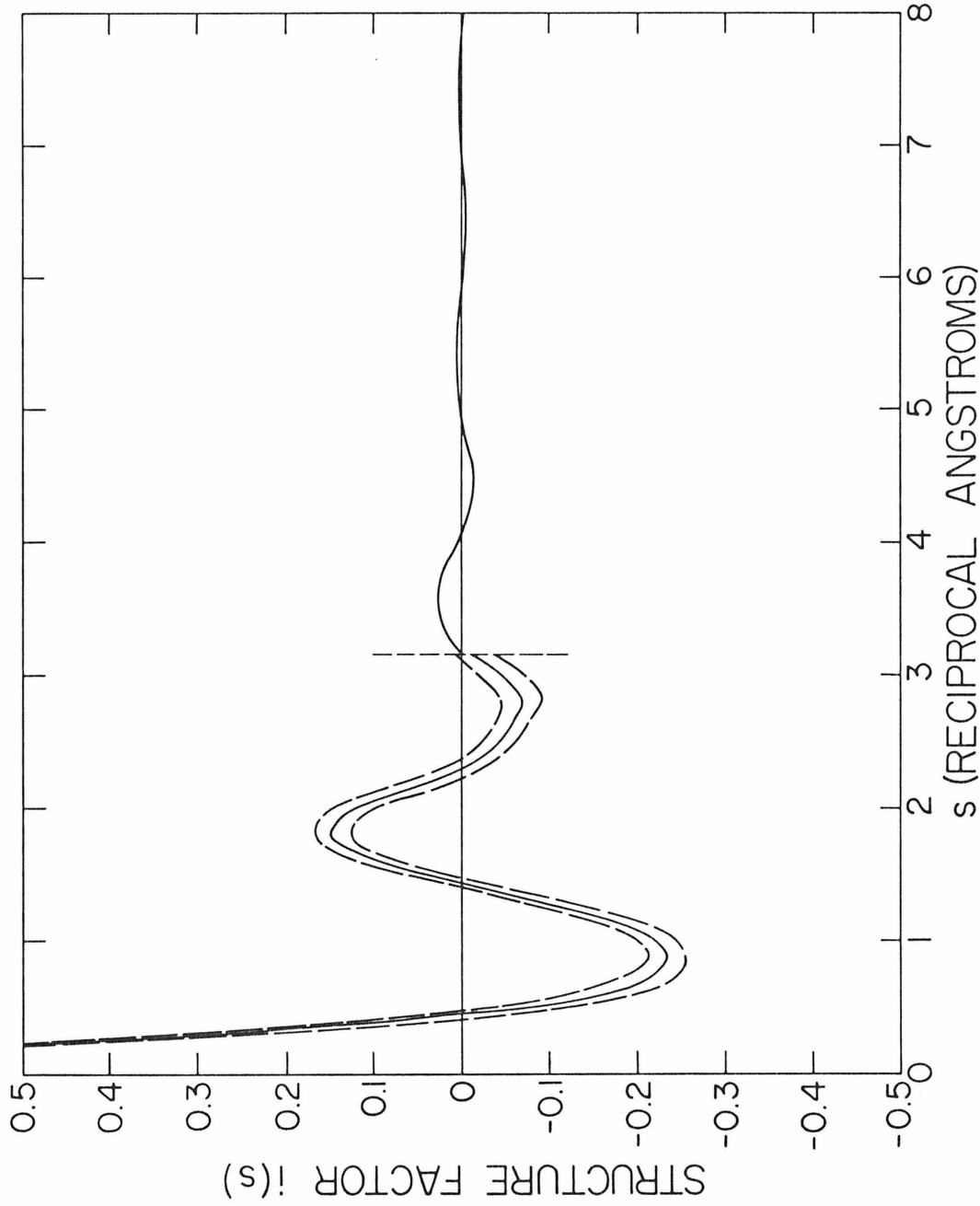
Figure 9. Structure Factor for State 1R. —— experimental data for s < 3.12 Å^{-1}; self-consistent extrapolated oscillations for s > 3.12 Å^{-1}; — — error limits; At s=0: i(0) = 1.075, $\partial i(s)/\partial s = 0$.
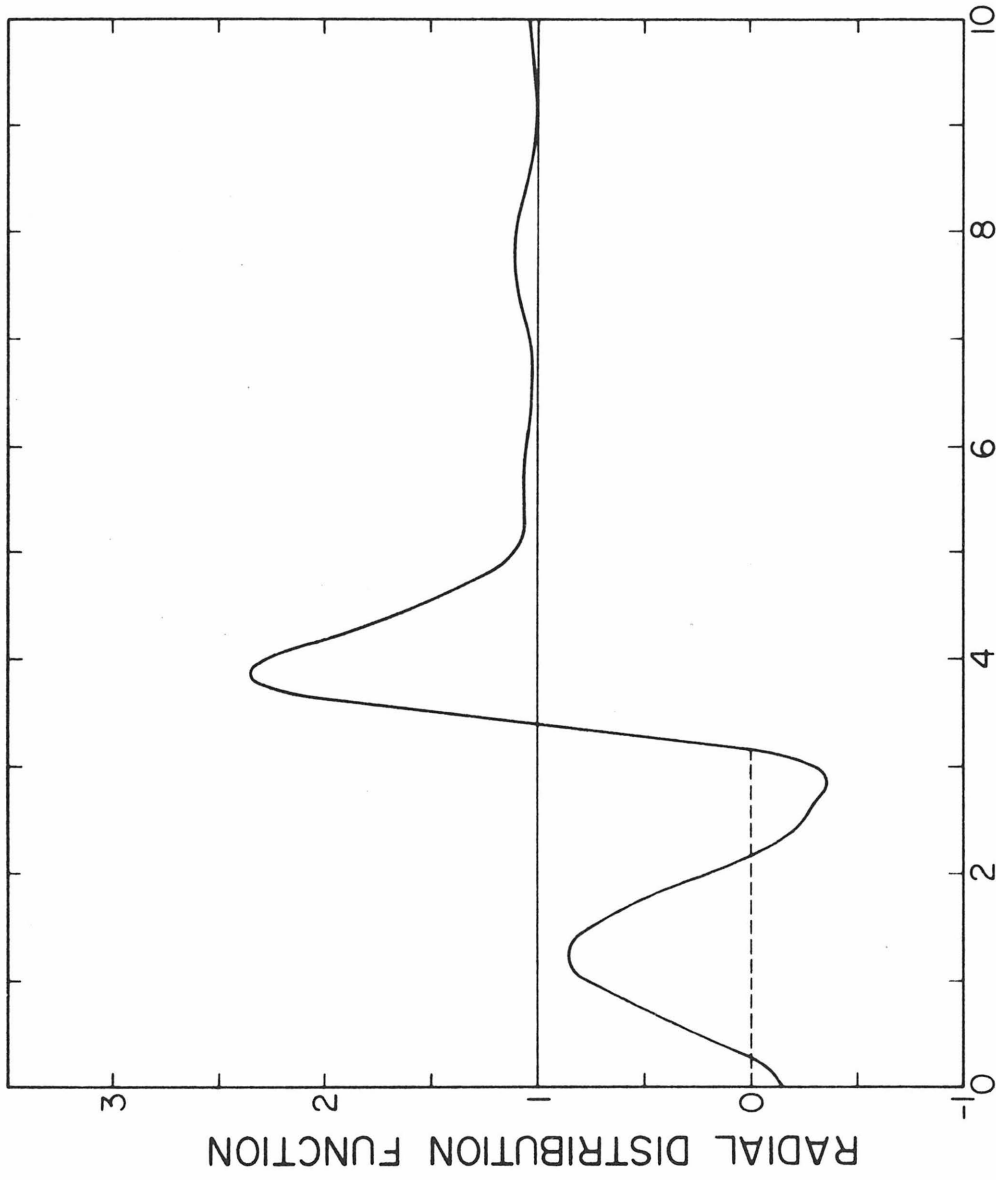
Figure 10. Radial Distribution Function, State 1R. ——— experimental value, eq.(4); --- expected behavior of g(r) for r<σ.
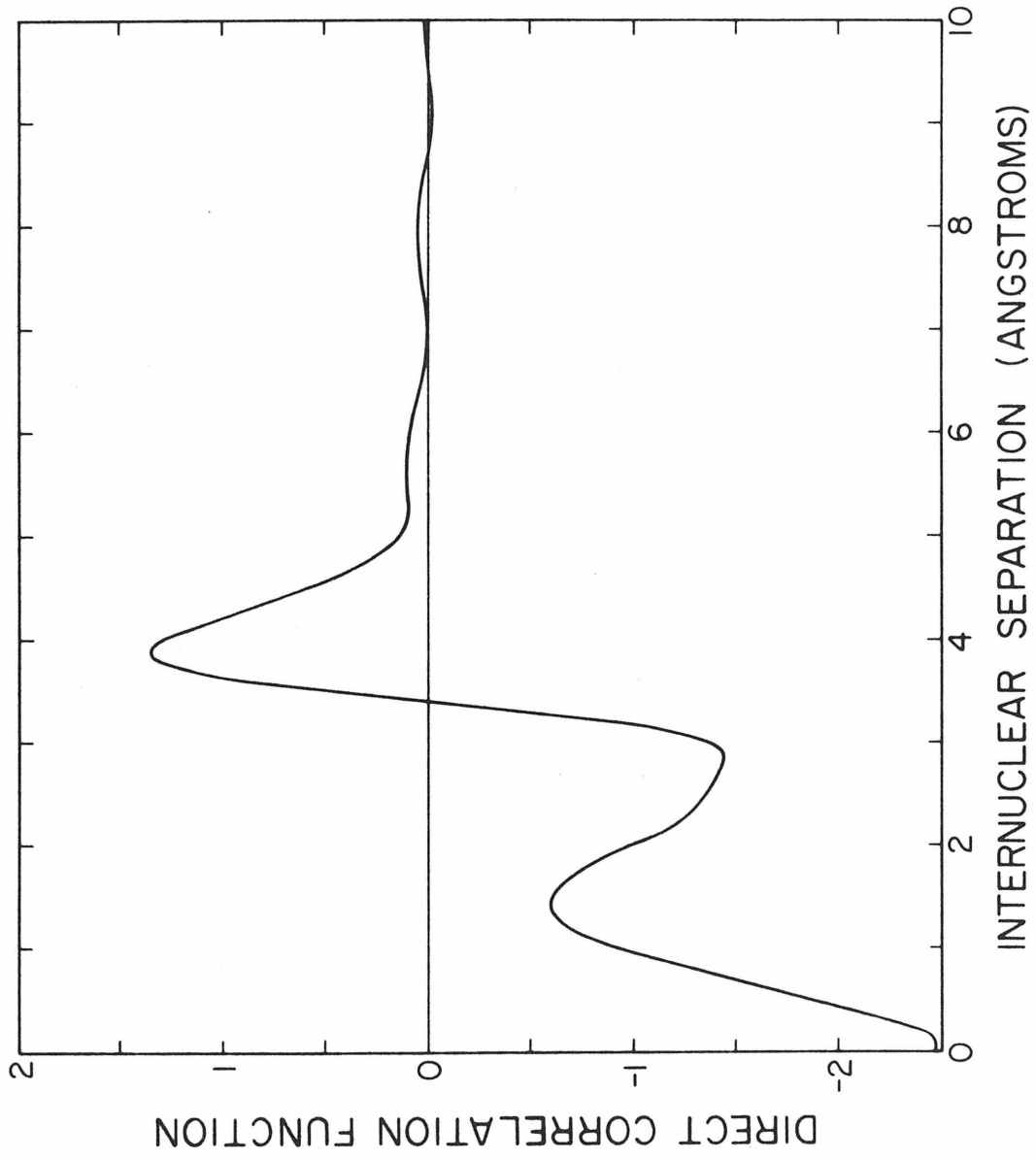
Figure 11. Direct Correlation Function, State 1R, equation (5).
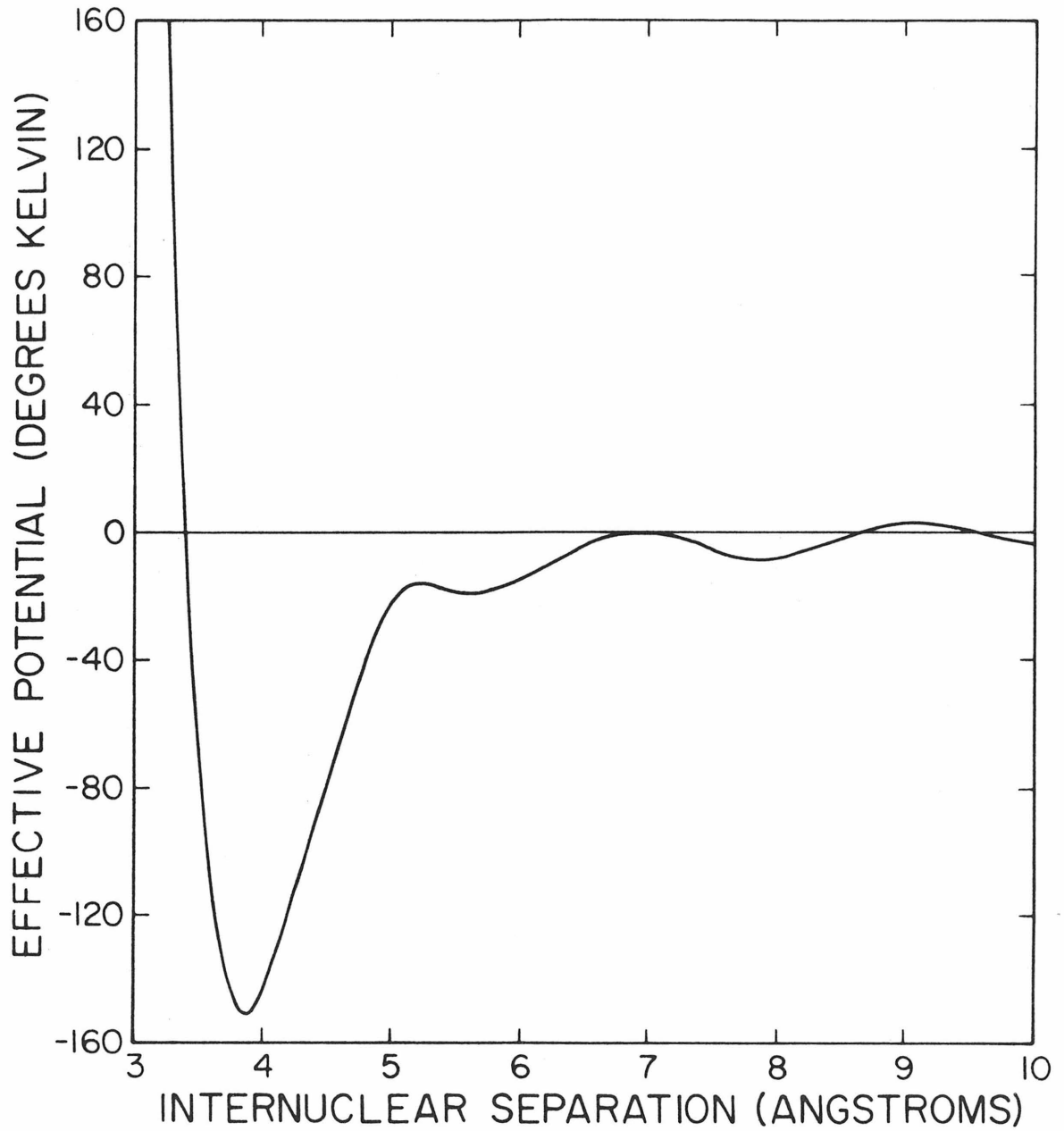
Figure 12.   Effective Pair Potential from the Percus-Yevick equation, State 1R.
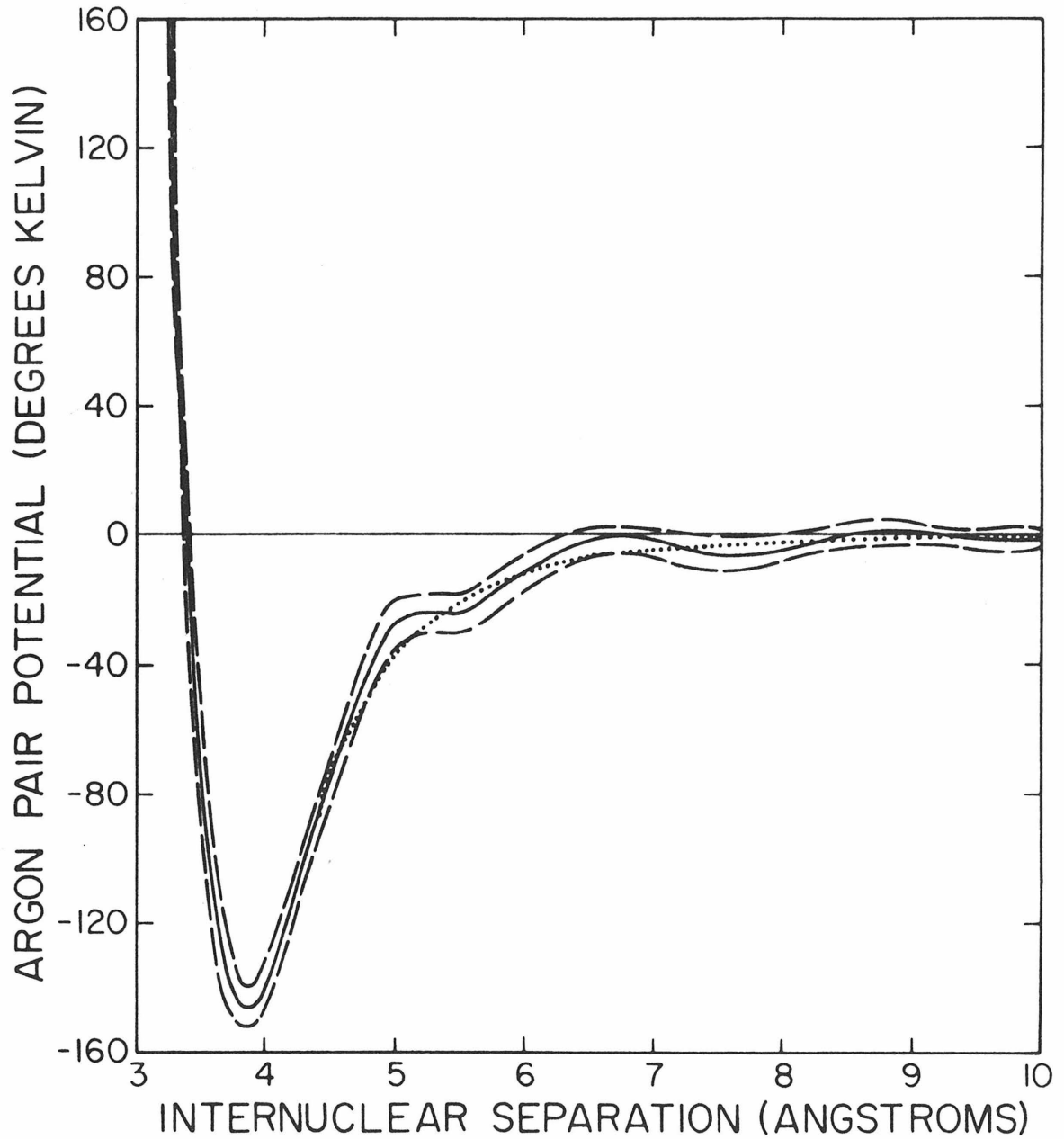
Figure 13.   Average Argon Pair Potential from X-Ray Data.
———— pair potential from eq.(62); --- error
limits; •••• theoretical dispersion potential
from eq.(83)
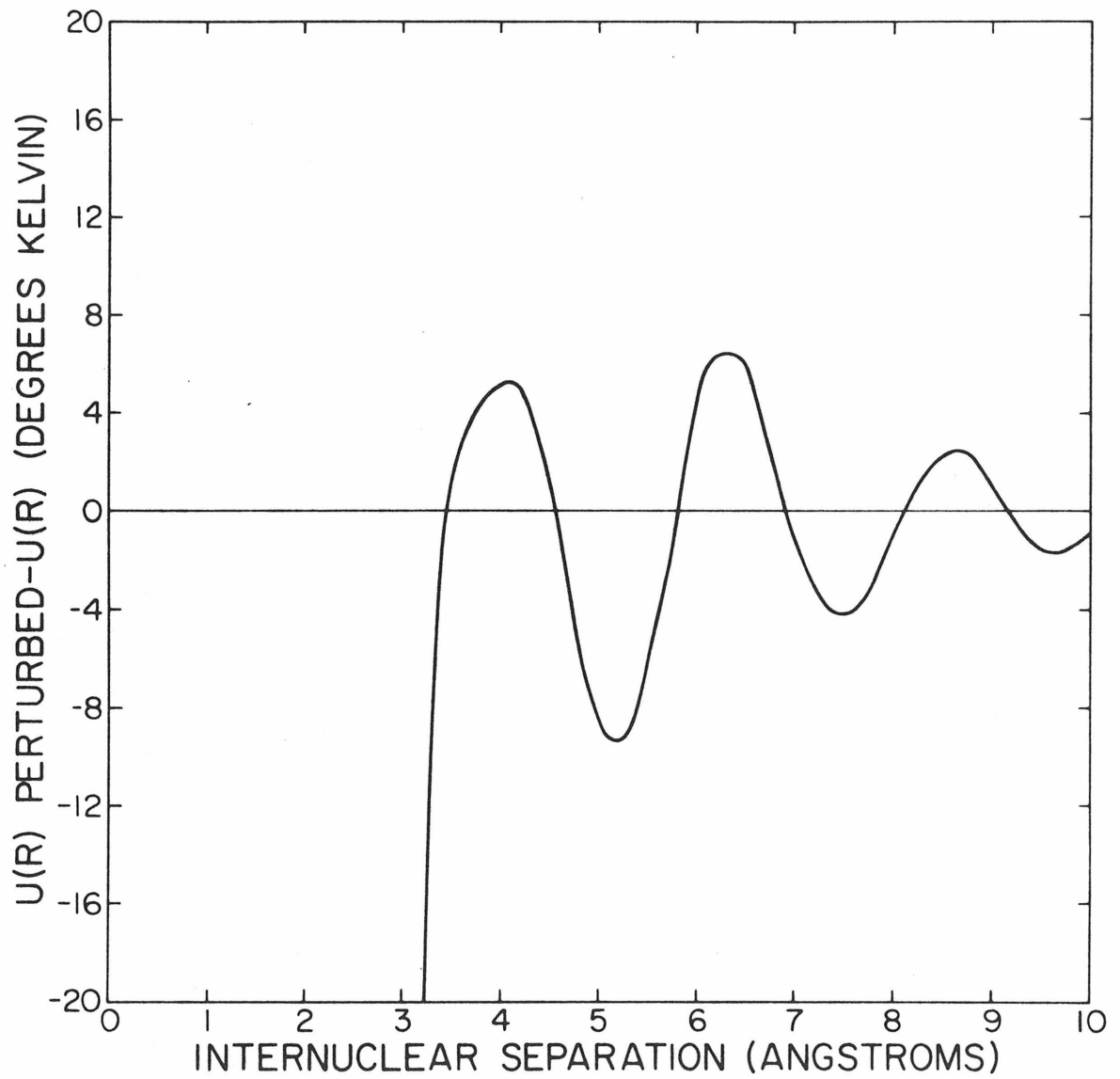
Figure 14. Effect of Perturbing the Second Minimum in i(s)
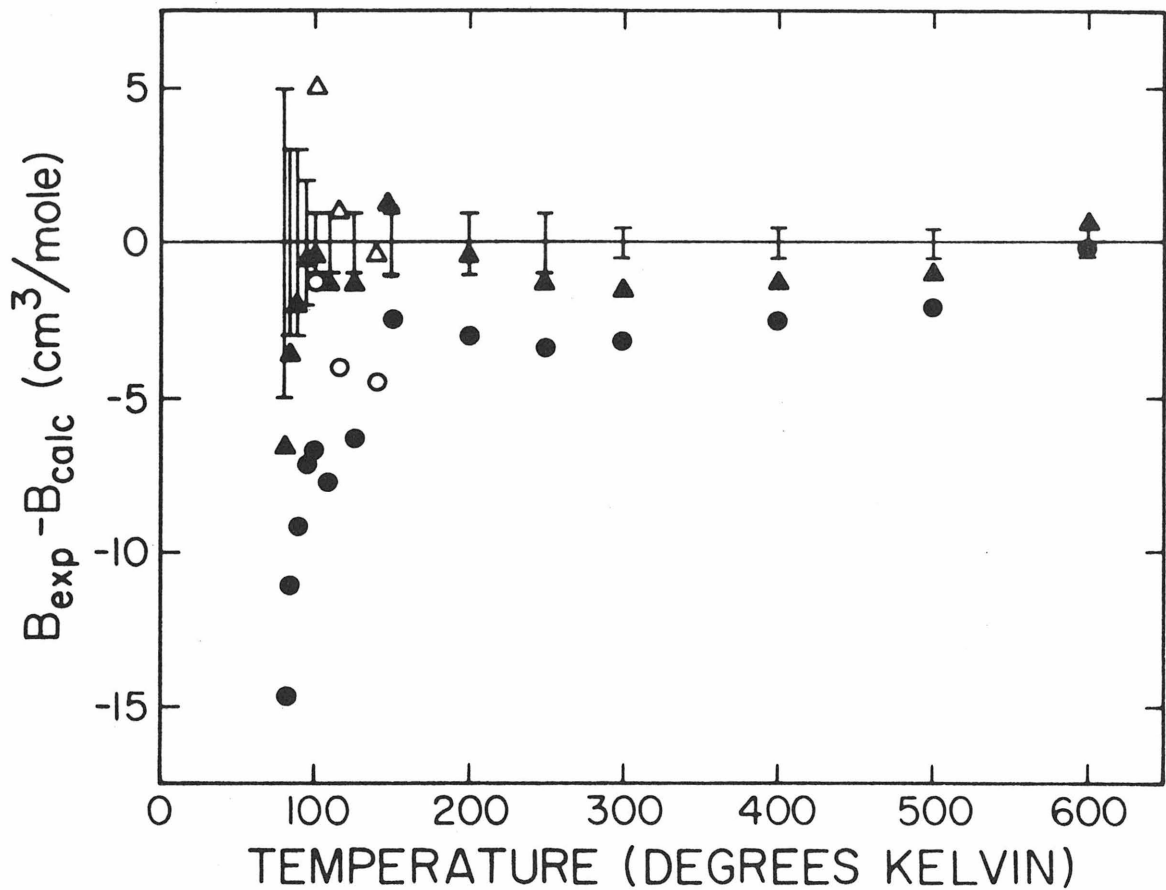
Figure 15. Comparison of Experimental and Calculated second virial coefficients. ● u(r)[I], exptl. data from Dymond and Smith[47]. O u(r)[I], exptl. data from Pope et al.[48] ▲ u(r)[II], exptl. data from Dymond and Smith. △ u(r)[II], exptl. data from Pope et al. Error limits on the experimental data are those set by Dymond and Smith.
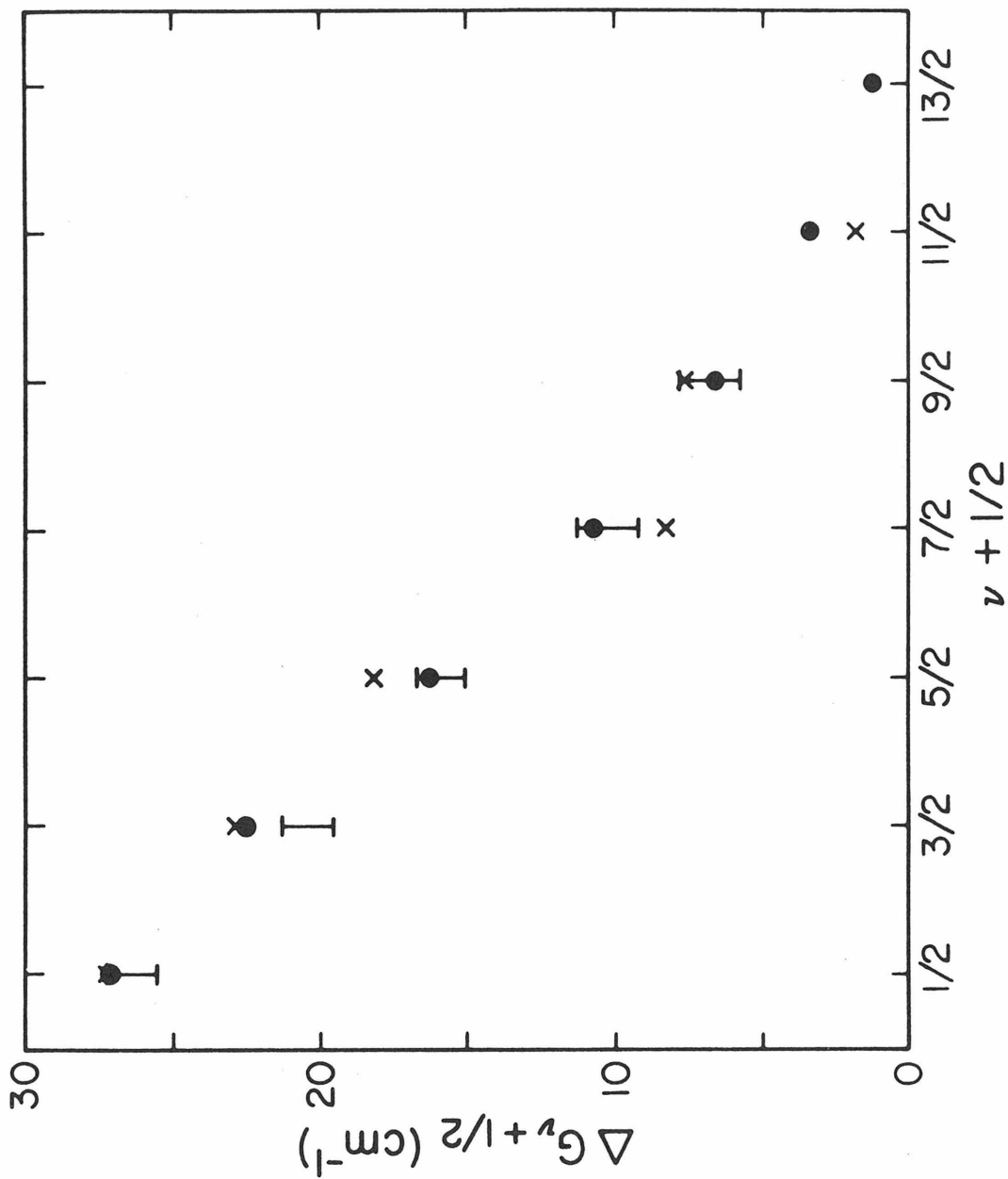
Figure 16. Vibrational Energy Level Transitions for the Argon Dimer. [Experimental data of Tanaka and Yoshino. **x** Calculated from u(r)[I]. ● Calculated from u(r)[II].
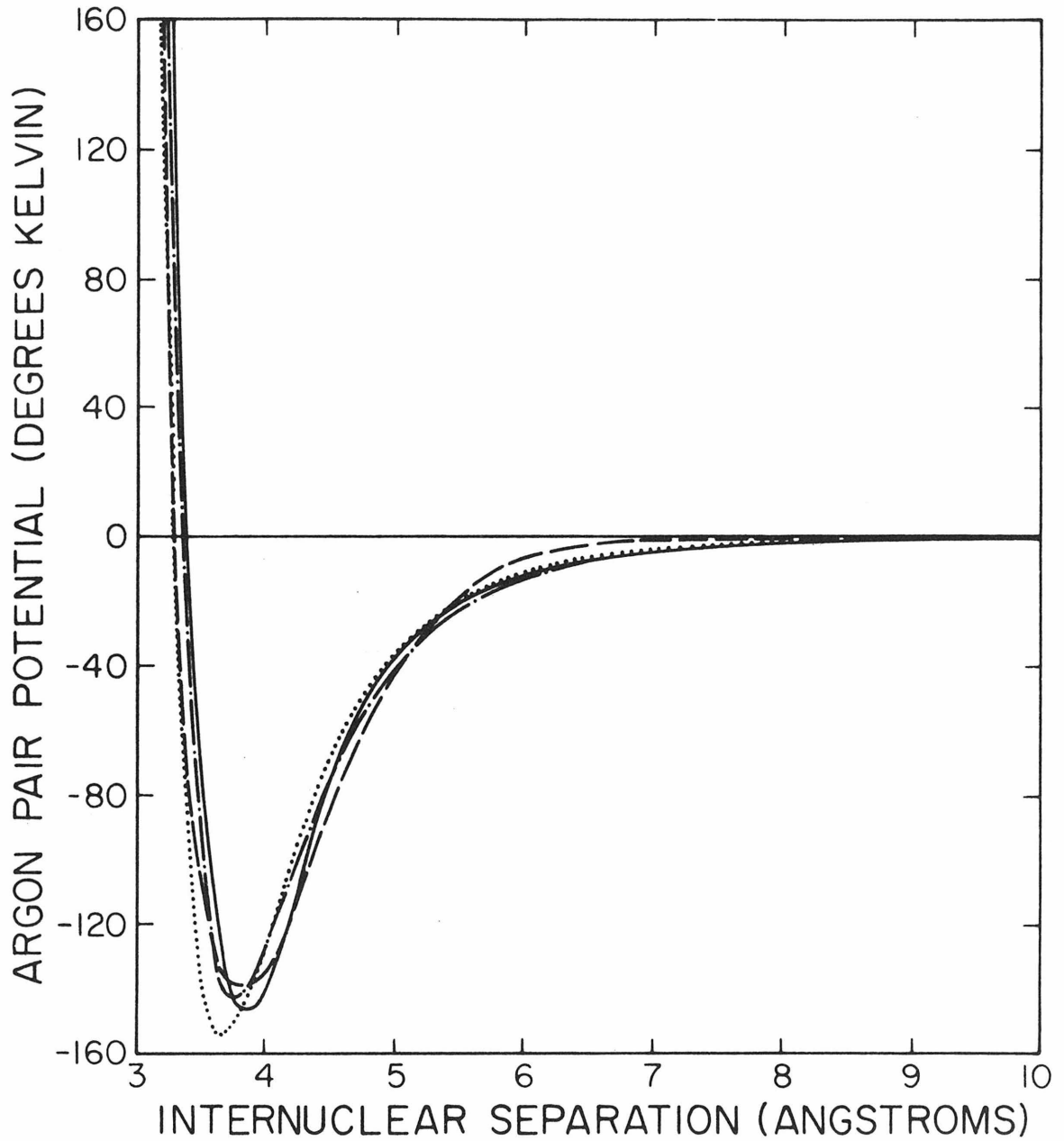
Figure 17. Comparison of Various Argon Potentials.
——— u(r)[II]; --- Dymond-Alder[7]; ••• Klein-Hanley[8];
—•— Barker-Fisher-Watts[9].

Table I

Summary of Experiments

STATE NAME	DATE	TEMP.	PRESSURE		SAMPLE DENSITY
empty cell	10/24/72	-100°C	0.00atm	0.00psi	.0000g/cm^3
argon 1	11/13/72	-100	52.995	778.81	.2087
argon 2	1/8/73	-100	67.860	997.27	.3111
argon 3	1/22/73	-100	38.133	560.40	.1331
helium 1	2/5/73	-100	61.241	900.00	.0164
argon 1R	2/21/73	-100	52.995	778.81	.2087
argon 4	3/5/73	-100	25.626	376.60	.0824
helium 2	3/12/73	-100	25.626	376.60	.0070

Table II

Temperature and Pressure Extremes for Each Experiment

EXPERIMENT	T_{max} (°C)	T_{min} (°C)	P_{max} (psi)	P_{min} (psi)
empty cell	-99.83	-99.95	0.00	0.00
argon 1	-99.996	-100.019	778.69	778.41
argon 2	-99.988	-100.012	997.44	997.13
argon 3	-99.986	-100.013	560.58	560.39
helium 1	-99.95	-100.09	900.09	899.95
argon 1R	-99.992	-100.011	778.99	778.78
argon 4	-99.992	-100.010	376.67	376.54
helium 2	-99.990	-100.009	376.65	376.56

Table III

Normalization Factors for Quick-Scan Averaging of State 1R

SCAN #	NS, COUNTER 1	NS, COUNTER 2
1	1.0111	1.0102
2	1.0039	1.0011
3	1.0017	1.0024
4	.9951	.9977
5	.9993	.9987
6	.9959	.9985
7	1.0013	1.0044
8	.9973	.9997
9	.9956	.9951
10	.9958	.9948
11	.9980	.9953
12	1.0054	1.0025

Table IV

Normalization Factors for Dual-Counter Matching

EXPERIMENT	S_c
empty cell	.7958
argon 1	.8064
argon 2	.8175
argon 3	.7919
helium 1	.8048
argon 1R	.8035
argon 4	.7957
helium 2	.7797

Table V (A)

EXPERIMENTAL COUNT RATE FOR   EMPTY CELL

TWO THETA	P(2θ) (CPS)	TWO THETA	P(2θ) (CPS)	TWO THETA	P(2θ) (CPS)
0.50	2153.875	11.00	37.778	21.50	46.536
0.75	173.957	11.25	36.374	21.75	47.525
1.00	142.567	11.50	38.040	22.00	48.312
1.25	109.426	11.75	39.211	22.25	50.904
1.50	98.603	12.00	37.967	22.50	48.790
1.75	94.069	12.25	39.673	22.75	49.109
2.00	88.836	12.50	42.515	23.00	53.495
2.25	81.959	12.75	44.335	23.25	54.730
2.50	77.715	13.00	42.988	23.50	58.573
2.75	74.672	13.25	46.249	23.75	60.941
3.00	69.363	13.50	51.200	24.00	73.575
3.25	62.212	13.75	68.962	24.25	122.824
3.50	59.016	14.00	60.682	24.50	117.562
3.75	53.346	14.25	52.358	24.75	69.113
4.00	47.203	14.50	56.320	25.00	59.194
4.25	43.436	14.75	65.584	25.25	59.665
4.50	39.460	15.00	64.606	25.50	59.485
4.75	37.514	15.25	63.294	25.75	60.573
5.00	37.822	15.50	86.316	26.00	64.646
5.25	39.460	15.75	102.637	26.25	67.299
5.50	38.085	16.00	123.663	26.50	62.097
5.75	39.358	16.25	299.225	26.75	59.699
6.00	38.923	16.50	188.185	27.00	60.929
6.25	37.599	16.75	85.680	27.25	62.740
6.50	35.020	17.00	87.645	27.50	63.838
6.75	33.214	17.25	92.237	27.75	68.119
7.00	34.923	17.50	100.596	28.00	75.776
7.25	34.650	17.75	169.472	28.25	150.995
7.50	35.581	18.00	263.952	28.50	162.099
7.75	35.570	18.25	216.764	28.75	96.898
8.00	36.304	18.50	491.819	29.00	71.288
8.25	36.073	18.75	584.476	29.25	66.335
8.50	35.867	19.00	188.021	29.50	66.563
8.75	37.340	19.25	135.084	29.75	65.001
9.00	36.769	19.50	143.178	30.00	67.943
9.25	38.062	19.75	152.761	30.25	69.163
9.50	34.987	20.00	141.230	30.50	71.741
9.75	34.289	20.25	129.750	30.75	72.288
10.00	36.643	20.50	107.628	31.00	69.608
10.25	37.111	20.75	61.816	31.25	71.888
10.50	36.197	21.00	51.671	31.50	83.213
10.75	35.611	21.25	50.025	31.75	144.440

Table V (A) (cont.)

EXPERIMENTAL COUNT RATE FOR   EMPTY CELL

TWO THETA	P(2θ) (CPS)	TWO THETA	P(2θ) (CPS)
32.00	165.919	42.50	56.372
32.25	95.443	42.75	60.984
32.50	75.317	43.00	74.672
32.75	89.057	43.25	76.452
33.00	92.749	43.50	70.915
33.25	83.830	43.75	65.138
33.50	94.323	44.00	69.569
33.75	170.475	44.25	68.015
34.00	201.276	44.50	68.308
34.25	193.857	44.75	77.257
34.50	121.124	45.00	96.922
34.75	84.611		
35.00	80.229		
35.25	78.711		
35.50	74.210		
35.75	73.314		
36.00	71.861		
36.25	74.688		
36.50	79.173		
36.75	73.202		
37.00	72.439		
37.25	72.210		
37.50	72.847		
37.75	78.069		
38.00	69.519		
38.25	62.100		
38.50	56.877		
38.75	58.225		
39.00	57.237		
39.25	57.179		
39.50	58.954		
39.75	57.740		
40.00	66.151		
40.25	66.589		
40.50	62.748		
40.75	59.788		
41.00	57.939		
41.25	59.252		
41.50	58.019		
41.75	57.142		
42.00	60.122		
42.25	57.799		

Table V (B)

EXPERIMENTAL COUNT RATE FOR   ARGON 1

TWO THETA	P(2θ) (CPS)	TWO THETA	P(2θ) (CPS)	TWO THETA	P(2θ) (CPS)
0.50	2915.766	11.00	142.527	21.50	84.009
0.75	397.944	11.25	140.548	21.75	84.406
1.00	321.522	11.50	135.360	22.00	83.810
1.25	285.916	11.75	132.650	22.25	83.094
1.50	258.372	12.00	128.423	22.50	81.409
1.75	236.836	12.25	125.773	22.75	81.466
2.00	219.506	12.50	124.443	23.00	80.357
2.25	205.154	12.75	125.147	23.25	83.419
2.50	193.085	13.00	118.930	23.50	84.722
2.75	183.256	13.25	120.005	23.75	82.260
3.00	173.743	13.50	119.375	24.00	90.651
3.25	167.279	13.75	127.274	24.25	115.811
3.50	158.464	14.00	119.781	24.50	107.855
3.75	154.552	14.25	114.082	24.75	84.389
4.00	147.951	14.50	115.419	25.00	80.907
4.25	143.662	14.75	117.904	25.25	80.056
4.50	142.605	15.00	116.166	25.50	78.883
4.75	140.926	15.25	115.662	25.75	78.195
5.00	140.781	15.50	123.829	26.00	80.007
5.25	141.928	15.75	129.878	26.25	79.222
5.50	144.082	16.00	143.886	26.50	79.383
5.75	143.429	16.25	205.665	26.75	77.693
6.00	146.170	16.50	161.553	27.00	78.179
6.25	147.759	16.75	118.024	27.25	78.011
6.50	150.398	17.00	118.219	27.50	79.129
6.75	151.800	17.25	116.920	27.75	79.003
7.00	155.869	17.50	120.646	28.00	81.814
7.25	156.133	17.75	154.135	28.25	111.960
7.50	159.495	18.00	186.754	28.50	119.724
7.75	160.317	18.25	165.386	28.75	92.179
8.00	164.917	18.50	306.635	29.00	80.237
8.25	164.925	18.75	343.454	29.25	76.062
8.50	169.362	19.00	153.595	29.50	74.887
8.75	167.416	19.25	131.342	29.75	72.774
9.00	168.379	19.50	128.868	30.00	73.664
9.25	165.213	19.75	129.274	30.25	73.698
9.50	161.568	20.00	124.407	30.50	76.120
9.75	159.629	20.25	117.774	30.75	74.972
10.00	155.824	20.50	110.029	31.00	74.843
10.25	154.035	20.75	94.028	31.25	74.438
10.50	151.027	21.00	87.988	31.50	79.601
10.75	146.262	21.25	87.732	31.75	105.462

Table V (B) (cont.)

EXPERIMENTAL COUNT RATE FOR   ARGON 1

TWO THETA	P(2θ) (CPS)	TWO THETA	P(2θ) (CPS)
32.00	119.865	42.50	56.876
32.25	88.624	42.75	57.576
32.50	73.814	43.00	64.301
32.75	80.993	43.25	63.580
33.00	81.533	43.50	60.867
33.25	77.976	43.75	57.636
33.50	82.598	44.00	60.261
33.75	111.077	44.25	57.588
34.00	124.277	44.50	57.430
34.25	118.557	44.75	61.431
34.50	96.002	45.00	74.060
34.75	74.923		
35.00	72.668		
35.25	72.125		
35.50	69.119		
35.75	69.648		
36.00	69.620		
36.25	69.610		
36.50	69.419		
36.75	68.975		
37.00	66.040		
37.25	67.381		
37.50	66.475		
37.75	69.325		
38.00	65.715		
38.25	62.180		
38.50	59.232		
38.75	58.546		
39.00	58.641		
39.25	58.649		
39.50	58.672		
39.75	58.577		
40.00	60.891		
40.25	64.885		
40.50	60.174		
40.75	55.639		
41.00	57.463		
41.25	58.130		
41.50	58.285		
41.75	55.873		
42.00	57.423		
42.25	56.805		

Table V (C)

EXPERIMENTAL COUNT RATE FOR ARGON 2

TWO THETA	P(2θ) (CPS)	TWO THETA	P(2θ) (CPS)	TWO THETA	P(2θ) (CPS)
0.50	1964.088	11.00	136.053	21.50	73.209
0.75	373.352	11.25	129.496	21.75	73.103
1.00	304.534	11.50	126.722	22.00	72.567
1.25	259.380	11.75	122.839	22.25	72.791
1.50	225.536	12.00	119.923	22.50	70.602
1.75	202.702	12.25	114.690	22.75	71.173
2.00	183.841	12.50	113.241	23.00	70.421
2.25	168.534	12.75	110.906	23.25	71.338
2.50	154.516	13.00	108.734	23.50	70.687
2.75	145.783	13.25	107.065	23.75	71.859
3.00	137.340	13.50	106.089	24.00	76.359
3.25	130.363	13.75	107.814	24.25	92.052
3.50	124.727	14.00	104.322	24.50	85.892
3.75	120.572	14.25	101.388	24.75	71.413
4.00	116.202	14.50	99.775	25.00	70.460
4.25	115.442	14.75	101.610	25.25	67.817
4.50	111.593	15.00	101.057	25.50	68.534
4.75	113.564	15.25	99.851	25.75	69.232
5.00	113.265	15.50	106.757	26.00	68.637
5.25	114.243	15.75	110.499	26.25	70.297
5.50	117.721	16.00	115.158	26.50	67.215
5.75	116.819	16.25	157.299	26.75	64.746
6.00	120.210	16.50	125.970	27.00	66.976
6.25	125.340	16.75	102.254	27.25	66.712
6.50	127.386	17.00	99.263	27.50	67.349
6.75	131.331	17.25	101.310	27.75	66.761
7.00	134.337	17.50	102.606	28.00	69.049
7.25	140.888	17.75	124.525	28.25	84.828
7.50	143.599	18.00	146.293	28.50	93.657
7.75	146.180	18.25	132.866	28.75	75.238
8.00	152.831	18.50	220.667	29.00	65.118
8.25	152.387	18.75	246.945	29.25	64.307
8.50	155.144	19.00	121.394	29.50	61.332
8.75	156.525	19.25	107.555	29.75	64.136
9.00	157.329	19.50	105.865	30.00	62.317
9.25	158.890	19.75	105.159	30.25	61.703
9.50	156.434	20.00	102.605	30.50	62.845
9.75	151.595	20.25	96.112	30.75	62.799
10.00	151.416	20.50	91.523	31.00	63.436
10.25	147.598	20.75	81.142	31.25	61.116
10.50	141.380	21.00	76.641	31.50	64.390
10.75	138.772	21.25	76.844	31.75	83.140

Table V (C) (cont.)

EXPERIMENTAL COUNT RATE FOR   ARGON 2

TWO THETA	P(2θ) (CPS)	TWO THETA	P(2θ) (CPS)
32.00	90.575	42.50	45.658
32.25	70.524	42.75	46.112
32.50	61.401	43.00	50.685
32.75	66.211	43.25	51.395
33.00	65.519	43.50	49.642
33.25	62.845	43.75	47.510
33.50	64.809	44.00	47.910
33.75	83.538	44.25	46.789
34.00	89.360	44.50	45.832
34.25	87.948	44.75	48.674
34.50	74.599	45.00	50.609
34.75	58.615		
35.00	58.085		
35.25	59.044		
35.50	55.899		
35.75	55.958		
36.00	55.445		
36.25	55.588		
36.50	56.831		
36.75	55.472		
37.00	54.237		
37.25	54.498		
37.50	53.487		
37.75	55.058		
38.00	52.237		
38.25	50.612		
38.50	49.669		
38.75	50.096		
39.00	49.374		
39.25	48.405		
39.50	49.567		
39.75	47.834		
40.00	49.757		
40.25	51.615		
40.50	48.727		
40.75	48.168		
41.00	47.022		
41.25	47.201		
41.50	46.230		
41.75	45.730		
42.00	47.113		
42.25	45.711		

Table V (D)

EXPERIMENTAL COUNT RATE FOR   ARGON 3

TWO THETA	P(2θ) (CPS)	TWO THETA	P(2θ) (CPS)	TWO THETA	P(2θ) (CPS)
0.50	4159.961	11.00	131.169	21.50	84.869
0.75	366.300	11.25	129.119	21.75	83.641
1.00	289.444	11.50	126.977	22.00	81.600
1.25	264.922	11.75	122.668	22.25	81.774
1.50	246.508	12.00	122.082	22.50	81.540
1.75	231.705	12.25	121.880	22.75	80.419
2.00	220.505	12.50	118.272	23.00	83.024
2.25	207.002	12.75	118.798	23.25	83.232
2.50	198.770	13.00	115.596	23.50	85.283
2.75	190.714	13.25	115.892	23.75	85.978
3.00	179.540	13.50	116.439	24.00	94.152
3.25	173.076	13.75	127.190	24.25	124.420
3.50	168.995	14.00	117.954	24.50	118.433
3.75	161.632	14.25	110.695	24.75	90.867
4.00	154.901	14.50	112.776	25.00	83.962
4.25	150.231	14.75	117.287	25.25	82.196
4.50	148.823	15.00	114.811	25.50	82.064
4.75	145.901	15.25	113.078	25.75	81.278
5.00	143.965	15.50	126.115	26.00	83.636
5.25	145.519	15.75	132.997	26.25	84.105
5.50	146.499	16.00	148.699	26.50	81.570
5.75	145.900	16.25	239.057	26.75	80.874
6.00	148.087	16.50	174.602	27.00	81.576
6.25	148.038	16.75	120.285	27.25	81.742
6.50	146.239	17.00	119.345	27.50	79.852
6.75	149.975	17.25	123.540	27.75	84.370
7.00	151.005	17.50	126.370	28.00	88.473
7.25	149.183	17.75	170.103	28.25	126.760
7.50	150.326	18.00	225.955	28.50	136.822
7.75	150.291	18.25	194.378	28.75	94.973
8.00	152.487	18.50	379.894	29.00	82.422
8.25	150.785	18.75	442.728	29.25	79.566
8.50	150.582	19.00	174.861	29.50	78.257
8.75	151.654	19.25	141.791	29.75	77.536
9.00	150.380	19.50	141.832	30.00	79.408
9.25	148.130	19.75	143.001	30.25	81.417
9.50	146.076	20.00	134.476	30.50	78.752
9.75	142.598	20.25	128.573	30.75	81.749
10.00	142.868	20.50	117.231	31.00	77.679
10.25	137.789	20.75	93.745	31.25	79.382
10.50	135.620	21.00	86.424	31.50	85.211
10.75	134.057	21.25	85.024	31.75	123.840

Table V (D) (cont.)

EXPERIMENTAL COUNT RATE FOR   ARGON 3

TWO THETA	P(2θ) (CPS)	TWO THETA	P(2θ) (CPS)
32.00	147.437	42.50	62.007
32.25	93.703	42.75	62.054
32.50	81.445	43.00	71.366
32.75	90.377	43.25	70.719
33.00	89.556	43.50	69.437
33.25	86.583	43.75	64.687
33.50	91.586	44.00	67.614
33.75	134.708	44.25	66.088
34.00	147.908	44.50	63.131
34.25	143.061	44.75	72.904
34.50	108.295	45.00	83.637
34.75	82.322		
35.00	78.549		
35.25	78.405		
35.50	75.655		
35.75	75.094		
36.00	73.942		
36.25	76.827		
36.50	79.967		
36.75	75.319		
37.00	73.058		
37.25	71.802		
37.50	73.236		
37.75	77.328		
38.00	69.884		
38.25	66.493		
38.50	66.501		
38.75	64.620		
39.00	63.985		
39.25	64.429		
39.50	63.159		
39.75	64.572		
40.00	66.986		
40.25	70.046		
40.50	65.383		
40.75	63.101		
41.00	60.923		
41.25	60.730		
41.50	61.719		
41.75	63.350		
42.00	61.823		
42.25	62.577		

Table V (E)

EXPERIMENTAL COUNT RATE FOR HELIUM 1

TWO THETA	P(2θ) (CPS)	TWO THETA	P(2θ) (CPS)	TWO THETA	P(2θ) (CPS)
0.50	2790.941	11.00	40.101	21.50	47.404
0.75	206.798	11.25	40.458	21.75	49.001
1.00	152.825	11.50	40.781	22.00	49.457
1.25	118.089	11.75	42.012	22.25	48.821
1.50	106.694	12.00	41.488	22.50	47.658
1.75	101.772	12.25	42.348	22.75	48.699
2.00	95.821	12.50	43.161	23.00	50.156
2.25	89.425	12.75	46.969	23.25	54.720
2.50	83.409	13.00	47.318	23.50	58.102
2.75	80.069	13.25	49.126	23.75	63.030
3.00	74.910	13.50	55.463	24.00	75.911
3.25	68.999	13.75	72.587	24.25	129.514
3.50	64.720	14.00	62.970	24.50	117.487
3.75	58.687	14.25	56.002	24.75	69.695
4.00	51.238	14.50	59.252	25.00	59.683
4.25	47.020	14.75	69.538	25.25	59.929
4.50	43.616	15.00	67.439	25.50	61.997
4.75	42.407	15.25	64.792	25.75	61.273
5.00	42.519	15.50	89.078	26.00	66.823
5.25	43.649	15.75	105.406	26.25	68.708
5.50	43.748	16.00	135.171	26.50	64.683
5.75	43.473	16.25	286.090	26.75	61.523
6.00	42.113	16.50	186.205	27.00	63.136
6.25	40.693	16.75	91.487	27.25	67.669
6.50	39.413	17.00	91.616	27.50	65.707
6.75	40.578	17.25	95.375	27.75	71.643
7.00	39.767	17.50	105.425	28.00	75.116
7.25	39.224	17.75	184.105	28.25	138.368
7.50	39.444	18.00	269.510	28.50	163.775
7.75	40.488	18.25	220.193	28.75	97.953
8.00	40.069	18.50	564.630	29.00	70.231
8.25	39.889	18.75	650.401	29.25	67.618
8.50	40.037	19.00	203.849	29.50	66.538
8.75	40.841	19.25	148.547	29.75	68.292
9.00	41.063	19.50	152.937	30.00	66.751
9.25	40.666	19.75	153.995	30.25	68.147
9.50	37.897	20.00	143.881	30.50	72.840
9.75	38.726	20.25	132.469	30.75	72.613
10.00	38.896	20.50	113.241	31.00	72.625
10.25	39.357	20.75	65.140	31.25	73.829
10.50	40.802	21.00	51.758	31.50	85.391
10.75	40.454	21.25	49.535	31.75	147.919

Table V (E) (cont.)

EXPERIMENTAL COUNT RATE FOR HELIUM 1

TWO THETA	P(2θ) (CPS)	TWO THETA	P(2θ) (CPS)
32.00	179.063	42.50	58.881
32.25	98.200	42.75	59.735
32.50	77.920	43.00	74.359
32.75	92.284	43.25	78.413
33.00	94.530	43.50	71.855
33.25	86.831	43.75	68.379
33.50	93.939	44.00	69.629
33.75	167.637	44.25	67.648
34.00	193.930	44.50	65.260
34.25	177.077	44.75	79.652
34.50	127.405	45.00	101.776
34.75	84.661		
35.00	81.957		
35.25	77.701		
35.50	74.855		
35.75	74.484		
36.00	74.955		
36.25	78.283		
36.50	80.171		
36.75	77.644		
37.00	73.298		
37.25	72.773		
37.50	75.259		
37.75	79.642		
38.00	69.628		
38.25	61.329		
38.50	58.559		
38.75	59.096		
39.00	58.782		
39.25	57.802		
39.50	58.746		
39.75	59.220		
40.00	65.773		
40.25	70.273		
40.50	64.440		
40.75	57.389		
41.00	56.419		
41.25	59.056		
41.50	59.919		
41.75	58.602		
42.00	58.521		
42.25	58.741		

Table V (F)

EXPERIMENTAL COUNT RATE FOR ARGON 1R

TWO THETA	P(2θ) (CPS)	TWO THETA	P(2θ) (CPS)	TWO THETA	P(2θ) (CPS)
0.50	3513.922	11.00	140.999	21.50	82.866
0.75	387.229	11.25	136.076	21.75	82.461
1.00	315.936	11.50	132.205	22.00	82.213
1.25	283.344	11.75	129.889	22.25	81.227
1.50	255.630	12.00	126.778	22.50	79.729
1.75	235.305	12.25	122.527	22.75	79.789
2.00	217.512	12.50	121.798	23.00	80.619
2.25	201.954	12.75	119.747	23.25	82.007
2.50	189.321	13.00	119.940	23.50	82.190
2.75	177.661	13.25	113.891	23.75	82.110
3.00	168.020	13.50	118.525	24.00	89.591
3.25	163.523	13.75	121.196	24.25	109.699
3.50	155.203	14.00	115.415	24.50	104.990
3.75	151.165	14.25	109.006	24.75	82.993
4.00	145.518	14.50	112.420	25.00	79.204
4.25	142.224	14.75	115.435	25.25	78.491
4.50	140.023	15.00	112.918	25.50	77.695
4.75	137.855	15.25	111.413	25.75	77.134
5.00	138.946	15.50	119.768	26.00	78.566
5.25	140.266	15.75	125.956	26.25	78.693
5.50	140.658	16.00	137.990	26.50	77.006
5.75	140.062	16.25	199.768	26.75	75.386
6.00	143.923	16.50	155.027	27.00	74.321
6.25	145.720	16.75	114.504	27.25	76.590
6.50	147.337	17.00	114.878	27.50	76.190
6.75	149.059	17.25	117.116	27.75	79.651
7.00	152.767	17.50	121.045	28.00	80.372
7.25	154.534	17.75	151.993	28.25	107.690
7.50	157.667	18.00	189.653	28.50	118.107
7.75	159.042	18.25	169.431	28.75	88.407
8.00	162.438	18.50	309.515	29.00	76.739
8.25	160.765	18.75	348.532	29.25	74.716
8.50	163.822	19.00	150.796	29.50	74.363
8.75	166.754	19.25	130.237	29.75	73.381
9.00	163.909	19.50	127.410	30.00	70.774
9.25	161.875	19.75	127.866	30.25	73.092
9.50	159.310	20.00	121.237	30.50	73.956
9.75	158.027	20.25	116.255	30.75	71.205
10.00	154.450	20.50	109.047	31.00	72.773
10.25	151.522	20.75	91.473	31.25	72.368
10.50	148.875	21.00	85.055	31.50	76.213
10.75	143.515	21.25	86.509	31.75	104.183

Table V (F) (cont.)

EXPERIMENTAL COUNT RATE FOR   ARGON 1R

TWO THETA	P(2θ) (CPS)	TWO THETA	P(2θ) (CPS)
32.00	119.211	42.50	53.335
32.25	83.520	42.75	56.369
32.50	72.615	43.00	59.719
32.75	79.361	43.25	61.665
33.00	78.162	43.50	60.299
33.25	75.548	43.75	58.014
33.50	79.862	44.00	57.438
33.75	109.587	44.25	56.850
34.00	119.902	44.50	56.002
34.25	115.909	44.75	62.217
34.50	93.164	45.00	71.162
34.75	72.425		
35.00	69.478		
35.25	68.464		
35.50	67.532		
35.75	68.392		
36.00	67.037		
36.25	67.651		
36.50	70.178		
36.75	66.714		
37.00	67.289		
37.25	65.066		
37.50	65.530		
37.75	68.610		
38.00	62.825		
38.25	59.888		
38.50	58.222		
38.75	57.916		
39.00	58.968		
39.25	57.050		
39.50	58.057		
39.75	56.818		
40.00	59.937		
40.25	62.902		
40.50	60.746		
40.75	55.940		
41.00	57.203		
41.25	55.556		
41.50	55.646		
41.75	55.450		
42.00	55.610		
42.25	55.220		

Table V (G)

EXPERIMENTAL COUNT RATE FOR ARGON 4

TWO THETA	P(2θ) (CPS)	TWO THETA	P(2θ) (CPS)	TWO THETA	P(2θ) (CPS)
0.50	3786.980	11.00	107.575	21.50	74.219
0.75	330.089	11.25	102.323	21.75	70.985
1.00	250.723	11.50	101.973	22.00	74.377
1.25	220.984	11.75	101.465	22.25	72.703
1.50	207.553	12.00	98.634	22.50	72.980
1.75	197.229	12.25	99.711	22.75	69.785
2.00	190.330	12.50	95.858	23.00	72.990
2.25	179.810	12.75	98.133	23.25	76.452
2.50	172.142	13.00	96.564	23.50	77.539
2.75	165.515	13.25	96.269	23.75	80.283
3.00	161.783	13.50	100.440	24.00	91.594
3.25	155.063	13.75	109.197	24.25	127.714
3.50	147.261	14.00	104.083	24.50	119.759
3.75	140.861	14.25	96.360	24.75	84.691
4.00	137.250	14.50	100.625	25.00	77.394
4.25	134.457	14.75	104.876	25.25	73.827
4.50	129.377	15.00	102.777	25.50	74.624
4.75	128.586	15.25	101.677	25.75	75.090
5.00	125.929	15.50	115.609	26.00	79.088
5.25	127.005	15.75	125.831	26.25	83.019
5.50	126.306	16.00	142.952	26.50	76.889
5.75	126.456	16.25	250.536	26.75	74.105
6.00	124.450	16.50	173.745	27.00	74.150
6.25	123.648	16.75	111.159	27.25	77.976
6.50	122.859	17.00	112.937	27.50	78.008
6.75	124.106	17.25	115.937	27.75	77.060
7.00	122.817	17.50	123.540	28.00	83.385
7.25	122.124	17.75	173.104	28.25	130.342
7.50	122.852	18.00	244.120	28.50	140.770
7.75	123.173	18.25	206.100	28.75	96.768
8.00	121.540	18.50	429.462	29.00	78.262
8.25	124.899	18.75	504.986	29.25	75.701
8.50	122.105	19.00	178.221	29.50	76.033
8.75	121.485	19.25	145.740	29.75	75.339
9.00	119.593	19.50	147.465	30.00	72.271
9.25	118.809	19.75	146.932	30.25	76.118
9.50	114.851	20.00	138.242	30.50	78.503
9.75	112.114	20.25	130.434	30.75	77.957
10.00	111.652	20.50	115.214	31.00	76.318
10.25	111.139	20.75	87.624	31.25	79.984
10.50	109.705	21.00	79.479	31.50	86.249
10.75	107.957	21.25	74.799	31.75	128.813

Table V (G) (cont.)

EXPERIMENTAL COUNT RATE FOR   ARGON 4

TWO THETA	P(2θ) (CPS)	TWO THETA	P(2θ) (CPS)
32.00	155.592	42.50	59.587
32.25	95.497	42.75	61.416
32.50	81.522	43.00	72.628
32.75	89.738	43.25	73.459
33.00	90.569	43.50	68.756
33.25	85.597	43.75	66.016
33.50	92.201	44.00	67.055
33.75	146.268	44.25	65.454
34.00	162.376	44.50	64.750
34.25	154.255	44.75	74.718
34.50	111.015	45.00	88.023
34.75	84.264		
35.00	80.926		
35.25	80.004		
35.50	74.139		
35.75	76.495		
36.00	75.083		
36.25	76.305		
36.50	79.619		
36.75	76.841		
37.00	75.244		
37.25	73.133		
37.50	73.413		
37.75	78.892		
38.00	70.208		
38.25	63.602		
38.50	62.216		
38.75	62.711		
39.00	61.599		
39.25	62.328		
39.50	61.646		
39.75	60.918		
40.00	65.651		
40.25	67.599		
40.50	65.472		
40.75	61.084		
41.00	61.365		
41.25	61.170		
41.50	60.296		
41.75	61.813		
42.00	62.596		
42.25	62.172		

Table V (H)

EXPERIMENTAL COUNT RATE FOR HELIUM 2

TWO THETA	P(2θ) (CPS)	TWO THETA	P(2θ) (CPS)	TWO THETA	P(2θ) (CPS)
0.50	2195.227	11.00	38.170	21.50	48.666
0.75	179.164	11.25	38.035	21.75	45.206
1.00	143.050	11.50	38.962	22.00	46.734
1.25	112.974	11.75	39.269	22.25	45.325
1.50	103.579	12.00	39.643	22.50	46.082
1.75	95.196	12.25	39.649	22.75	46.813
2.00	90.919	12.50	41.555	23.00	50.140
2.25	85.166	12.75	43.940	23.25	54.219
2.50	80.116	13.00	45.467	23.50	56.465
2.75	73.538	13.25	45.894	23.75	60.063
3.00	70.821	13.50	53.800	24.00	73.512
3.25	64.966	13.75	70.874	24.25	126.954
3.50	59.781	14.00	60.874	24.50	118.001
3.75	52.354	14.25	53.114	24.75	68.587
4.00	47.215	14.50	55.971	25.00	57.785
4.25	43.030	14.75	67.788	25.25	55.976
4.50	39.290	15.00	65.344	25.50	57.432
4.75	38.898	15.25	63.446	25.75	61.808
5.00	38.860	15.50	86.955	26.00	65.682
5.25	38.513	15.75	103.491	26.25	69.022
5.50	39.559	16.00	129.893	26.50	63.435
5.75	38.881	16.25	284.565	26.75	61.571
6.00	38.876	16.50	176.301	27.00	64.066
6.25	37.994	16.75	86.148	27.25	63.945
6.50	36.228	17.00	89.439	27.50	63.788
6.75	36.829	17.25	91.540	27.75	69.152
7.00	36.532	17.50	103.272	28.00	77.170
7.25	35.780	17.75	175.559	28.25	148.142
7.50	36.758	18.00	282.675	28.50	160.102
7.75	36.288	18.25	225.817	28.75	94.934
8.00	36.665	18.50	545.130	29.00	70.863
8.25	36.473	18.75	660.675	29.25	67.044
8.50	40.140	19.00	191.472	29.50	69.377
8.75	37.080	19.25	145.277	29.75	68.265
9.00	39.380	19.50	148.787	30.00	64.973
9.25	39.340	19.75	152.032	30.25	67.838
9.50	35.290	20.00	140.566	30.50	71.615
9.75	35.379	20.25	133.029	30.75	73.260
10.00	36.832	20.50	109.986	31.00	74.665
10.25	37.935	20.75	65.276	31.25	75.240
10.50	36.747	21.00	48.447	31.50	85.092
10.75	36.935	21.25	47.684	31.75	149.777

Table V (H) (cont.)

EXPERIMENTAL COUNT RATE FOR HELIUM 2

TWO THETA	P(2θ) (CPS)	TWO THETA	P(2θ) (CPS)
32.00	191.030	42.50	60.116
32.25	99.820	42.75	62.849
32.50	79.803	43.00	76.244
32.75	94.704	43.25	78.434
33.00	96.020	43.50	73.842
33.25	86.053	43.75	68.017
33.50	97.900	44.00	68.860
33.75	177.073	44.25	68.970
34.00	200.423	44.50	66.389
34.25	189.798	44.75	83.299
34.50	124.242	45.00	104.800
34.75	85.960		
35.00	82.408		
35.25	81.343		
35.50	76.659		
35.75	74.420		
36.00	76.605		
36.25	78.749		
36.50	80.529		
36.75	79.289		
37.00	75.115		
37.25	73.351		
37.50	75.777		
37.75	82.145		
38.00	72.013		
38.25	62.872		
38.50	59.425		
38.75	59.361		
39.00	59.781		
39.25	58.978		
39.50	59.844		
39.75	61.070		
40.00	66.409		
40.25	69.431		
40.50	65.980		
40.75	59.688		
41.00	59.299		
41.25	58.998		
41.50	59.854		
41.75	61.612		
42.00	62.072		
42.25	59.659		

Table VI

Ratio of Incident Intensity to Incident Intensity of
    State Helium 2

EXPERIMENT	$\dfrac{P^{o'}}{P^{o}}$
argon 1	.970
argon 2	.996
argon 3	.991
argon 1R	.991
argon 4	1.027
helium 1	.994
helium 2	1.000

Table VII

EMPTY CELL SCATTER DETERMINED FROM THE HELIUM 1 AND HELIUM 2 EXPERIMENTS

TWO THETA	HELIUM 1 $\frac{P^o}{P^o - P}_{cHe}(2\theta)$	HELIUM 1 $\frac{P^o}{P^o - P}_{c}(2\theta)$	HELIUM 2 $P_c(2\theta)$
0.50	2808.244	2809.800	2195.265
0.75	208.080	203.851	177.289
1.00	153.772	149.427	141.143
1.25	118.821	114.403	111.041
1.50	107.355	102.918	101.640
1.75	102.403	97.963	93.252
2.00	96.415	91.971	88.975
2.25	89.979	85.531	83.221
2.50	83.926	79.476	78.171
2.75	80.565	76.120	71.593
3.00	75.374	70.931	68.879
3.25	69.427	64.986	63.026
3.50	65.121	60.687	57.842
3.75	59.051	54.621	50.416
4.00	51.556	47.128	45.281
4.25	47.311	42.893	41.100
4.50	43.886	39.482	37.366
4.75	42.670	38.285	36.983
5.00	42.783	38.421	36.954
5.25	43.920	39.583	36.617
5.50	44.019	39.708	37.674
5.75	43.743	39.455	37.008
6.00	42.374	38.109	37.014
6.25	40.945	36.703	36.142
6.50	39.657	35.440	34.386
6.75	40.830	36.643	35.000
7.00	40.014	35.853	34.716
7.25	39.467	35.334	33.975
7.50	39.689	35.585	34.967
7.75	40.739	36.669	34.510
8.00	40.317	36.277	34.900
8.25	40.136	36.125	34.721
8.50	40.285	36.304	38.404
8.75	41.094	37.146	35.355
9.00	41.318	37.400	37.670
9.25	40.918	37.031	37.644
9.50	38.132	34.270	33.604
9.75	38.966	35.136	33.707
10.00	39.137	35.340	35.175
10.25	39.601	35.830	36.292
10.50	41.055	37.324	35.117

Table VII (contd.)

EMPTY CELL SCATTER DETERMINED FROM THE HELIUM 1 AND HELIUM 2 EXPERIMENTS

TWO THETA	HELIUM 1 $\frac{P^{o'}}{P^o} P_{cHe}(2\theta)$	HELIUM 1 $\frac{P^{o'}}{P^o} P_c(2\theta)$	HELIUM 2 $P_c(2\theta)$
10.75	40.705	37.004	35.318
11.00	40.350	36.679	36.567
11.25	40.709	37.069	36.446
11.50	41.034	37.425	37.387
11.75	42.272	38.697	37.708
12.00	41.745	38.199	38.095
12.25	42.611	39.095	38.114
12.50	43.429	39.945	40.035
12.75	47.260	43.814	42.434
13.00	47.611	44.195	43.975
13.25	49.431	46.047	44.415
13.50	55.807	52.464	52.340
13.75	73.037	69.758	69.442
14.00	63.360	60.089	59.445
14.25	56.349	53.091	51.690
14.50	59.619	56.395	54.561
14.75	69.969	66.794	66.401
15.00	67.857	64.704	63.966
15.25	65.194	62.060	62.078
15.50	89.630	86.572	85.619
15.75	106.059	103.062	102.180
16.00	136.009	133.090	128.616
16.25	287.864	285.282	283.432
16.50	187.359	184.599	175.085
16.75	92.054	89.127	84.866
17.00	92.184	89.281	88.170
17.25	95.966	93.095	90.283
17.50	106.079	103.249	102.034
17.75	185.246	182.599	174.394
18.00	271.181	268.727	281.611
18.25	221.558	219.028	224.714
18.50	568.130	566.314	544.308
18.75	654.433	652.809	659.961
19.00	205.113	202.612	190.367
19.25	149.468	146.877	144.142
19.50	153.885	151.322	147.663
19.75	154.950	152.410	150.920
20.00	144.773	142.231	139.452
20.25	133.290	130.745	131.918
20.50	113.943	111.378	108.863
20.75	65.544	62.902	64.123

Table VII (contd.)

EMPTY CELL SCATTER DETERMINED FROM THE HELIUM 1 AND
HELIUM 2 EXPERIMENTS

TWO THETA	HELIUM 1 $\frac{P^{o\prime}}{P^o} P_{cHe}(2\theta)$	HELIUM 1 $\frac{P^{o\prime}}{P^o} P_c(2\theta)$	HELIUM 2 $P_c(2\theta)$
21.00	52.079	49.428	47.286
21.25	49.842	47.204	46.532
21.50	47.698	45.074	47.523
21.75	49.305	46.702	44.067
22.00	49.764	47.179	45.604
22.25	49.124	46.554	44.201
22.50	47.953	45.398	44.966
22.75	49.001	46.464	45.704
23.00	50.467	47.948	49.042
23.25	55.059	52.560	53.131
23.50	58.462	55.991	55.385
23.75	63.421	60.975	58.993
24.00	76.382	73.975	72.460
24.25	130.317	126.032	125.952
24.50	118.215	115.920	116.999
24.75	70.127	67.752	67.550
25.00	60.053	57.672	56.745
25.25	60.301	57.934	54.943
25.50	62.381	60.055	56.403
25.75	61.653	59.315	60.788
26.00	67.237	64.925	64.672
26.25	69.134	66.839	68.020
26.50	65.084	62.793	62.434
26.75	61.904	59.619	60.574
27.00	63.527	61.257	63.076
27.25	68.089	65.840	62.961
27.50	66.114	63.874	62.808
27.75	72.087	69.870	68.182
28.00	75.582	73.383	76.211
28.25	139.226	137.162	147.247
28.50	164.790	162.787	159.223
28.75	98.560	96.439	94.005
29.00	70.666	68.503	69.919
29.25	68.037	65.879	66.101
29.50	66.951	64.800	68.441
29.75	68.715	66.580	67.333
30.00	67.165	65.037	64.042
30.25	68.569	66.453	66.914
30.50	73.292	71.196	70.699
30.75	73.063	70.970	72.350
31.00	73.075	70.997	73.759

Table VII (contd.)

EMPTY CELL SCATTER DETERMINED FROM THE HELIUM 1 AND
HELIUM 2 EXPERIMENTS

TWO THETA	HELIUM 1 $\frac{P^{o\prime}}{P^o}P_{cHe}(2\theta)$	HELIUM 1 $\frac{P^{o\prime}}{P^o}P_c(2\theta)$	HELIUM 2 $P_c(2\theta)$
31.25	74.287	72.221	74.340
31.50	85.920	83.887	84.204
31.75	148.836	146.933	148.946
32.00	180.173	178.341	190.237
32.25	98.809	96.829	98.956
32.50	78.403	76.393	78.926
32.75	92.856	90.882	93.844
33.00	95.116	93.156	95.165
33.25	87.369	85.403	85.194
33.50	94.521	92.577	97.054
33.75	168.676	166.884	176.295
34.00	195.132	193.399	199.668
34.25	178.175	176.418	189.039
34.50	128.195	126.350	123.432
34.75	85.136	83.267	85.123
35.00	82.465	80.549	81.572
35.25	78.183	76.267	80.509
35.50	75.319	73.405	75.825
35.75	74.946	73.040	73.588
36.00	75.420	73.523	75.778
36.25	78.768	76.886	77.928
36.50	80.668	78.798	79.713
36.75	78.125	76.258	78.475
37.00	73.752	71.885	74.301
37.25	73.224	71.363	72.538
37.50	75.726	73.876	74.970
37.75	80.136	78.303	81.347
38.00	70.060	68.215	71.210
38.25	61.709	59.857	62.064
38.50	58.922	57.072	58.618
38.75	59.462	57.620	58.557
39.00	59.146	57.311	58.981
39.25	58.160	56.331	58.181
39.50	59.110	57.290	59.051
39.75	59.587	57.775	60.281
40.00	66.181	64.388	65.627
40.25	70.709	68.932	68.655
40.50	64.839	63.060	65.204
40.75	57.745	55.958	58.910
41.00	56.769	54.988	58.524
41.25	59.422	57.653	58.226

Table VII (contd.)

EMPTY CELL SCATTER DETERMINED FROM THE HELIUM 1 AND
HELIUM 2 EXPERIMENTS

TWO THETA	HELIUM 1 $\frac{P^{o}{}'}{P^{o}}P_{cHe}(2\theta)$	HELIUM 1 $\frac{P^{o}{}'}{P^{o}}P_{c}(2\theta)$	HELIUM 2 $P_{c}(2\theta)$
41.50	60.290	58.530	59.085
41.75	58.965	57.208	60.848
42.00	58.884	57.134	61.311
42.25	59.105	57.362	58.899
42.50	59.246	57.510	59.360
42.75	60.105	58.379	62.097
43.00	74.820	73.129	75.506
43.25	78.899	77.222	77.702
43.50	72.300	70.617	73.108
43.75	68.803	67.120	67.281
44.00	70.061	68.386	68.129
44.25	68.067	66.397	68.241
44.50	65.665	63.996	65.661
44.75	80.146	78.511	82.588
45.00	102.407	100.821	104.109

Table VIII.

CORRECTION OF STATE 1R ARGON SCATTER FOR DOUBLE
SCATTERING AND DIVERGENCE

TWO THETA	P(2θ) (EQ. 35)	CORR. FOR DOUBLE SCATTER	CORR. FOR DIVERGENCE
0.50	2524.745	2522.202	2543.260
0.75	312.583	310.046	326.937
1.00	259.849	257.318	271.004
1.25	239.669	237.144	248.057
1.50	216.085	213.566	221.915
1.75	197.934	195.421	201.314
2.00	182.249	179.742	183.604
2.25	169.042	166.541	169.229
2.50	158.580	156.085	157.920
2.75	148.460	145.971	147.193
3.00	140.541	138.059	138.849
3.25	138.212	135.736	136.236
3.50	131.582	129.112	129.434
3.75	129.902	127.439	127.674
4.00	126.851	124.394	124.616
4.25	125.129	122.679	122.712
4.50	124.222	121.779	121.706
4.75	122.425	119.989	119.834
5.00	123.443	121.014	120.795
5.25	124.418	121.996	121.731
5.50	124.653	122.238	121.941
5.75	124.169	121.762	121.446
6.00	128.365	125.965	125.640
6.25	130.611	128.219	127.896
6.50	132.719	130.335	130.034
6.75	133.999	131.622	131.351
7.00	137.912	135.543	135.311
7.25	139.864	137.502	137.316
7.50	142.788	140.433	140.300
7.75	143.853	141.505	141.431
8.00	147.282	144.941	144.933
8.25	145.667	143.333	143.395
8.50	148.295	145.967	146.104
8.75	151.205	148.883	149.145
9.00	148.083	145.766	146.061
9.25	146.162	143.851	144.170
9.50	144.799	142.492	142.826
9.75	143.241	140.938	141.279
10.00	139.485	137.186	137.526
10.25	136.318	134.022	134.354
10.50	133.336	131.043	131.361

Table VIII (cont.)

CORRECTION OF STATE 1R ARGON SCATTER FOR DOUBLE
SCATTERING AND DIVERGENCE

TWO THETA	P(2θ) (EQ. 35)	CORR. FOR DOUBLE SCATTER	CORR. FOR DIVERGENCE
10.75	128.087	125.796	126.094
11.00	125.563	123.274	123.438
11.25	120.562	118.275	118.422
11.50	116.515	114.229	114.360
11.75	113.786	111.501	111.619
12.00	110.804	108.520	108.626
12.25	106.334	104.050	104.146
12.50	105.167	102.884	102.971
12.75	101.741	99.459	99.539
13.00	101.659	99.378	99.452
13.25	95.048	92.768	92.837
13.50	96.971	94.692	94.758
13.75	92.833	90.555	90.619
14.00	90.897	88.621	88.633
14.25	87.338	85.064	85.070
14.50	89.438	87.166	87.169
14.75	88.175	85.906	85.906
15.00	86.508	84.242	84.242
15.25	85.962	83.700	83.700
15.50	84.616	82.359	82.361
15.75	81.318	79.065	79.070
16.00	82.633	80.386	80.396
16.25	81.616	79.374	79.389
16.50	80.499	78.263	78.285
16.75	78.691	76.462	76.491
17.00	80.077	77.854	77.892
17.25	80.710	78.493	78.540
17.50	81.258	79.048	79.106
17.75	76.873	74.669	74.738
18.00	78.835	76.638	76.671
18.25	76.288	74.097	74.129
18.50	74.802	72.617	72.649
18.75	76.670	74.491	74.522
19.00	68.959	66.766	66.816
19.25	73.116	70.948	70.977
19.50	70.179	68.016	68.044
19.75	71.508	69.350	69.377
20.00	69.425	67.271	67.297
20.25	69.240	67.089	67.114
20.50	69.631	67.483	67.507
20.75	65.221	63.075	63.098

Table VIII (cont.)

CORRECTION OF STATE 1R ARGON SCATTER FOR DOUBLE
SCATTERING AND DIVERGENCE

TWO THETA	P(2θ) (EQ. 35)	CORR. FOR DOUBLE SCATTER	CORR. FOR DIVERGENCE
21.00	64.598	62.454	62.477
21.25	66.785	64.643	64.665
21.50	63.729	61.588	61.609
21.75	63.131	60.991	61.011
22.00	62.578	60.439	60.458
22.25	61.913	59.774	59.793
22.50	60.704	58.566	58.584
22.75	60.347	58.209	58.226
23.00	60.378	58.240	58.256
23.25	59.117	56.979	56.994
23.50	57.984	55.847	55.862
23.75	55.977	53.840	53.854
24.00	58.224	56.087	56.094
24.25	55.489	53.353	53.360
24.50	55.741	53.606	53.613
24.75	54.448	52.314	52.320
25.00	55.304	53.171	53.177
25.25	54.841	52.710	52.716
25.50	53.473	51.344	51.350
25.75	52.919	50.793	50.799
26.00	52.651	50.528	50.535
26.25	52.217	50.097	50.104
26.50	52.271	50.154	50.161
26.75	51.802	49.689	49.696
27.00	48.397	46.289	46.297
27.25	47.843	45.739	45.747
27.50	48.365	46.266	46.275
27.75	49.360	47.267	47.276
28.00	48.631	46.543	46.553
28.25	47.887	45.805	45.816
28.50	48.760	46.685	46.697
28.75	47.585	45.517	45.529
29.00	47.938	45.877	45.890
29.25	47.313	45.259	45.273
29.50	47.277	45.231	45.246
29.75	46.078	44.040	44.056
30.00	44.423	42.394	42.411
30.25	46.267	44.247	44.265
30.50	44.248	42.237	42.256
30.75	41.646	39.644	39.665
31.00	43.276	41.284	41.279

Table VIII (cont.)

CORRECTION OF STATE 1R ARGON SCATTER FOR DOUBLE
SCATTERING AND DIVERGENCE

TWO THETA	P(2θ) (EQ. 35)	CORR. FOR DOUBLE SCATTER	CORR. FOR DIVERGENCE
31.25	42.679	40.697	40.692
31.50	42.082	40.110	40.105
31.75	40.667	38.705	38.700
32.00	41.219	39.267	39.262
32.25	41.479	39.538	39.533
32.50	39.181	37.250	37.245
32.75	39.765	37.844	37.840
33.00	37.957	36.046	36.042
33.25	39.168	37.267	37.263
33.50	39.988	38.097	38.094
33.75	37.383	35.502	35.500
34.00	36.757	34.885	34.883
34.25	39.771	37.908	37.907
34.50	40.781	38.927	38.927
34.75	38.521	36.675	36.676
35.00	36.992	35.154	35.156
35.25	37.565	35.734	35.737
35.50	37.155	35.331	35.335
35.75	38.531	36.714	36.719
36.00	36.821	35.010	35.016
36.25	36.251	34.446	34.453
36.50	38.080	36.281	36.290
36.75	35.804	34.010	34.020
37.00	38.433	36.644	36.655
37.25	36.634	34.850	34.863
37.50	35.863	34.083	34.097
37.75	36.124	34.349	34.365
38.00	33.337	31.566	31.567
38.25	34.025	32.258	32.259
38.50	33.740	31.976	31.977
38.75	33.356	31.596	31.597
39.00	34.548	32.792	32.793
39.25	33.123	31.370	31.371
39.50	33.833	32.084	32.085
39.75	32.176	30.430	30.431
40.00	32.471	30.728	30.729
40.25	33.612	31.873	31.874
40.50	33.743	32.007	32.008
40.75	32.366	30.634	30.635
41.00	34.064	32.335	32.336
41.25	31.307	29.582	29.583

Table VIII (cont.)

CORRECTION OF STATE 1R ARGON SCATTER FOR DOUBLE
SCATTERING AND DIVERGENCE

TWO THETA	P(2θ) (EQ. 35)	CORR. FOR DOUBLE SCATTER	CORR. FOR DIVERGENCE
41.50	31.142	29.420	29.422
41.75	31.282	29.564	29.566
42.00	30.809	29.094	29.096
42.25	30.673	28.962	28.964
42.50	28.801	27.093	27.095
42.75	30.819	29.115	29.117
43.00	27.934	26.233	26.235
43.25	28.343	26.646	26.648
43.50	29.716	28.022	28.025
43.75	29.333	27.643	27.646
44.00	28.348	26.661	26.664
44.25	28.543	26.860	26.863
44.50	28.736	27.057	27.060
44.75	28.057	26.381	26.385
45.00	27.365	25.693	25.697

Table IX A

FULLY CORRECTED ARGON SCATTER FROM STATE ARGON 1

TWO THETA	Pa(2θ) (CPS)	TWO THETA	Pa(2θ) (CPS)	TWO THETA	Pa(2θ) (CPS)
0.50	1889.257	11.00	121.960	21.50	60.978
0.75	329.198	11.25	119.902	21.75	61.166
1.00	269.788	11.50	114.644	22.00	60.281
1.25	244.602	11.75	111.569	22.25	59.896
1.50	219.207	12.00	107.559	22.50	58.539
1.75	197.858	12.25	104.722	22.75	58.177
2.00	180.971	12.50	102.979	23.00	56.309
2.25	168.092	12.75	102.202	23.25	56.641
2.50	157.595	13.00	95.953	23.50	56.592
2.75	148.890	13.25	96.376	23.75	52.276
3.00	140.872	13.50	93.094	24.00	55.241
3.25	136.445	13.75	93.970	24.25	56.985
3.50	129.337	14.00	90.445	24.50	54.187
3.75	127.785	14.25	87.705	24.75	51.932
4.00	123.921	14.50	87.717	25.00	53.166
4.25	121.120	14.75	85.877	25.25	52.586
4.50	121.270	15.00	85.021	25.50	50.871
4.75	119.918	15.25	85.482	25.75	50.209
5.00	119.657	15.50	83.785	26.00	50.283
5.25	120.398	15.75	80.230	26.25	48.964
5.50	122.308	16.00	83.217	26.50	50.850
5.75	121.771	16.25	80.914	26.75	50.351
6.00	124.797	16.50	80.765	27.00	48.478
6.25	126.814	16.75	77.500	27.25	45.517
6.50	129.909	17.00	78.721	27.50	47.525
6.75	130.880	17.25	75.891	27.75	44.975
7.00	135.112	17.50	76.177	28.00	46.264
7.25	135.622	17.75	73.624	28.25	47.697
7.50	138.763	18.00	69.877	28.50	45.785
7.75	139.328	18.25	66.649	28.75	47.332
8.00	143.926	18.50	63.350	29.00	47.671
8.25	144.054	18.75	62.277	29.25	45.010
8.50	148.037	19.00	66.364	29.50	44.192
8.75	146.286	19.25	69.314	29.75	41.920
9.00	146.955	19.50	66.782	30.00	43.728
9.25	144.008	19.75	68.057	30.25	43.316
9.50	141.670	20.00	67.826	30.50	42.802
9.75	139.514	20.25	66.146	30.75	41.824
10.00	135.616	20.50	66.169	31.00	41.759
10.25	133.609	20.75	63.656	31.25	41.180
10.50	130.322	21.00	63.536	31.50	39.809
10.75	125.745	21.25	64.035	31.75	37.753

Table IX A (cont.)

FULLY CORRECTED ARGON SCATTER FROM STATE ARGON 1

TWO THETA	$P_a(2\theta)$ (CPS)	TWO THETA	$P_a(2\theta)$ (CPS)
32.00	37.393	42.50	29.410
32.25	42.730	42.75	29.104
32.50	36.883	43.00	29.425
32.75	37.757	43.25	27.210
33.00	37.671	43.50	27.310
33.25	38.032	43.75	26.063
33.50	39.071	44.00	28.197
33.75	34.644	44.25	26.385
34.00	36.609	44.50	27.269
34.25	38.042	44.75	24.316
34.50	39.723	45.00	27.014
34.75	37.578		
35.00	36.792		
35.25	37.851		
35.50	35.456		
35.75	36.501		
36.00	36.114		
36.25	34.933		
36.50	34.080		
36.75	34.812		
37.00	34.030		
37.25	35.742		
37.50	33.637		
37.75	33.618		
38.00	33.051		
38.25	33.225		
38.50	31.734		
38.75	30.992		
39.00	31.238		
39.25	31.724		
39.50	31.462		
39.75	30.944		
40.00	30.396		
40.25	32.477		
40.50	30.177		
40.75	29.168		
41.00	31.387		
41.25	30.913		
41.50	30.814		
41.75	28.812		
42.00	29.687		
42.25	29.342		

Table IX B

FULLY CORRECTED ARGON SCATTER FROM STATE ARGON 1R

TWO THETA	$P_a(2\theta)$ (CPS)	TWO THETA	$P_a(2\theta)$ (CPS)	TWO THETA	$P_a(2\theta)$ (CPS)
0.50	2543.260	11.00	123.438	21.50	61.609
0.75	326.937	11.25	118.422	21.75	61.011
1.00	271.004	11.50	114.360	22.00	60.458
1.25	248.057	11.75	111.619	22.25	59.793
1.50	221.915	12.00	108.626	22.50	58.584
1.75	201.314	12.25	104.146	22.75	58.226
2.00	183.604	12.50	102.971	23.00	58.256
2.25	169.229	12.75	99.539	23.25	56.994
2.50	157.920	13.00	99.452	23.50	55.862
2.75	147.193	13.25	92.837	23.75	53.854
3.00	138.849	13.50	94.758	24.00	56.094
3.25	130.236	13.75	90.619	24.25	53.360
3.50	129.434	14.00	88.633	24.50	53.613
3.75	127.074	14.25	85.070	24.75	52.320
4.00	124.616	14.50	87.169	25.00	53.177
4.25	122.712	14.75	85.906	25.25	52.716
4.50	121.706	15.00	84.242	25.50	51.350
4.75	119.834	15.25	83.700	25.75	50.799
5.00	120.795	15.50	82.361	26.00	50.535
5.25	121.731	15.75	79.070	26.25	50.104
5.50	121.941	16.00	80.396	26.50	50.161
5.75	121.446	16.25	79.389	26.75	49.696
6.00	125.640	16.50	78.285	27.00	46.297
6.25	127.896	16.75	76.491	27.25	45.747
6.50	130.034	17.00	77.892	27.50	46.275
6.75	131.351	17.25	78.540	27.75	47.276
7.00	135.311	17.50	79.106	28.00	46.553
7.25	137.316	17.75	74.738	28.25	45.816
7.50	140.300	18.00	76.671	28.50	46.697
7.75	141.431	18.25	74.129	28.75	45.529
8.00	144.933	18.50	72.649	29.00	45.890
8.25	143.395	18.75	74.522	29.25	45.273
8.50	146.104	19.00	66.816	29.50	45.246
8.75	149.145	19.25	70.977	29.75	44.056
9.00	146.061	19.50	68.044	30.00	42.411
9.25	144.170	19.75	69.377	30.25	44.265
9.50	142.826	20.00	67.297	30.50	42.256
9.75	141.279	20.25	67.114	30.75	39.665
10.00	137.526	20.50	67.507	31.00	41.279
10.25	134.354	20.75	63.098	31.25	40.692
10.50	131.361	21.00	62.477	31.50	40.105
10.75	126.094	21.25	64.065	31.75	38.700

Table IX B (cont.)

FULLY CORRECTED ARGON SCATTER FROM STATE ARGON 1R

TWO THETA	$P_a(2\theta)$ (CPS)	TWO THETA	$P_a(2\theta)$ (CPS)
32.00	39.262	42.50	27.095
32.25	39.533	42.75	29.117
32.50	37.245	43.00	26.235
32.75	37.840	43.25	26.648
33.00	36.042	43.50	28.025
33.25	37.263	43.75	27.646
33.50	38.094	44.00	26.664
33.75	35.500	44.25	26.863
34.00	34.883	44.50	27.060
34.25	37.907	44.75	26.385
34.50	38.927	45.00	25.697
34.75	36.676		
35.00	35.156		
35.25	35.737		
35.50	35.335		
35.75	36.719		
36.00	35.016		
36.25	34.453		
36.50	36.290		
36.75	34.020		
37.00	36.655		
37.25	34.863		
37.50	34.097		
37.75	34.365		
38.00	31.567		
38.25	32.259		
38.50	31.977		
38.75	31.597		
39.00	32.793		
39.25	31.371		
39.50	32.085		
39.75	30.431		
40.00	30.729		
40.25	31.874		
40.50	32.008		
40.75	30.635		
41.00	32.336		
41.25	29.583		
41.50	29.422		
41.75	29.566		
42.00	29.096		
42.25	28.964		

Table IX C

FULLY CORRECTED ARGON SCATTER FROM STATE ARGON 2

TWO THETA	Pa(2θ) (CPS)	TWO THETA	Pa(2θ) (CPS)	TWO THETA	Pa(2θ) (CPS)
0.50	1351.978	11.00	124.193	21.50	58.917
0.75	350.944	11.25	117.507	21.75	58.121
1.00	288.541	11.50	114.649	22.00	57.497
1.25	245.743	11.75	110.379	22.25	57.829
1.50	209.299	12.00	107.609	22.50	56.029
1.75	182.342	12.25	102.129	22.75	56.284
2.00	163.363	12.50	100.489	23.00	55.218
2.25	148.494	12.75	97.103	23.25	54.109
2.50	135.091	13.00	94.859	23.50	52.444
2.75	126.356	13.25	92.633	23.75	52.185
3.00	118.712	13.50	90.095	24.00	53.476
3.25	112.718	13.75	87.458	24.25	54.159
3.50	107.737	14.00	86.397	24.50	51.664
3.75	104.694	14.25	85.162	24.75	50.607
4.00	101.992	14.50	82.686	25.00	52.703
4.25	102.182	14.75	81.951	25.25	50.068
4.50	99.019	15.00	81.882	25.50	50.417
4.75	101.199	15.25	81.356	25.75	51.661
5.00	100.775	15.50	81.989	26.00	49.933
5.25	101.328	15.75	78.775	26.25	51.442
5.50	104.726	16.00	76.607	26.50	49.332
5.75	103.796	16.25	78.714	26.75	47.702
6.00	107.483	16.50	74.472	27.00	48.094
6.25	112.888	16.75	76.760	27.25	44.971
6.50	115.324	17.00	75.175	27.50	46.557
6.75	118.971	17.25	75.927	27.75	44.314
7.00	122.214	17.50	75.464	28.00	46.361
7.25	128.898	17.75	72.662	28.25	44.553
7.50	131.619	18.00	74.232	28.50	45.528
7.75	133.911	18.25	70.737	28.75	46.056
8.00	140.721	18.50	63.966	29.00	44.425
8.25	140.374	18.75	70.005	29.25	44.447
8.50	143.298	19.00	65.396	29.50	42.104
8.75	144.576	19.25	69.322	29.75	44.523
9.00	145.448	19.50	67.906	30.00	43.186
9.25	147.131	19.75	68.362	30.25	42.499
9.50	145.317	20.00	68.648	30.50	41.340
9.75	140.238	20.25	65.649	30.75	41.648
10.00	140.045	20.50	65.426	31.00	42.535
10.25	136.112	20.75	62.161	31.25	40.099
10.50	129.375	21.00	61.008	31.50	38.550
10.75	126.822	21.25	61.845	31.75	39.421

Table IX C (cont.)

FULLY CORRECTED ARGON SCATTER FROM STATE ARGON 2

TWO THETA	Pa(2θ) (CPS)	TWO THETA	Pa(2θ) (CPS)
32.00	38.517	42.50	27.979
32.25	40.963	42.75	27.892
32.50	37.519	43.00	28.148
32.75	38.359	43.25	27.633
33.00	37.231	43.50	27.973
33.25	36.921	43.75	26.861
33.50	37.167	44.00	26.967
33.75	35.191	44.25	26.654
34.00	33.479	44.50	26.372
34.25	37.531	44.75	24.859
34.50	38.259	45.00	26.295
34.75	35.089		
35.00	35.443		
35.25	37.768		
35.50	34.618		
35.75	34.888		
36.00	34.303		
36.25	33.583		
36.50	34.395		
36.75	33.990		
37.00	34.191		
37.25	34.618		
37.50	32.745		
37.75	32.492		
38.00	31.322		
38.25	31.984		
38.50	31.905		
38.75	32.235		
39.00	31.728		
39.25	31.121		
39.50	32.109		
39.75	30.153		
40.00	30.050		
40.25	30.534		
40.50	29.450		
40.75	31.322		
41.00	30.554		
41.25	29.606		
41.50	28.502		
41.75	28.572		
42.00	29.487		
42.25	27.969		

Table IX D

FULLY CORRECTED ARGON SCATTER FROM STATE ARGON 3

TWO THETA	$P_a(2\theta)$ (CPS)	TWO THETA	$P_a(2\theta)$ (CPS)	TWO THETA	$P_a(2\theta)$ (CPS)
0.50	2877.335	11.00	108.439	21.50	56.394
0.75	272.008	11.25	106.354	21.75	56.103
1.00	216.624	11.50	103.806	22.00	53.416
1.25	207.768	11.75	99.153	22.25	54.212
1.50	193.764	12.00	98.511	22.50	53.918
1.75	181.861	12.25	98.140	22.75	52.319
2.00	172.005	12.50	93.700	23.00	53.380
2.25	160.992	12.75	92.606	23.25	50.468
2.50	155.092	13.00	88.792	23.50	50.996
2.75	149.538	13.25	88.553	23.75	49.376
3.00	140.028	13.50	85.016	24.00	50.105
3.25	136.496	13.75	86.217	24.25	49.258
3.50	134.865	14.00	82.410	24.50	49.226
3.75	131.148	14.25	79.315	24.75	50.182
4.00	127.588	14.50	79.688	25.00	49.665
4.25	124.948	14.75	77.894	25.25	48.647
4.50	125.365	15.00	76.694	25.50	47.749
4.75	122.736	15.25	76.143	25.75	45.755
5.00	120.732	15.50	75.856	26.00	45.941
5.25	122.123	15.75	70.985	26.25	45.172
5.50	122.670	16.00	72.061	26.50	45.416
5.75	122.339	16.25	74.882	26.75	46.056
6.00	124.757	16.50	71.343	27.00	44.027
6.25	125.287	16.75	69.878	27.25	42.198
6.50	124.433	17.00	68.972	27.50	40.980
6.75	127.701	17.25	71.458	27.75	42.276
7.00	128.979	17.50	68.862	28.00	43.029
7.25	127.538	17.75	67.181	28.25	41.365
7.50	128.276	18.00	67.899	28.50	41.737
7.75	128.196	18.25	63.860	28.75	38.377
8.00	130.309	18.50	60.965	29.00	41.044
8.25	128.712	18.75	64.840	29.25	40.313
8.50	127.166	19.00	62.785	29.50	38.585
8.75	129.298	19.25	60.373	29.75	38.119
9.00	127.168	19.50	59.680	30.00	41.595
9.25	125.012	19.75	60.882	30.25	42.525
9.50	124.932	20.00	58.823	30.50	36.665
9.75	121.261	20.25	58.557	30.75	39.279
10.00	120.936	20.50	58.848	31.00	34.937
10.25	115.374	20.75	55.697	31.25	36.400
10.50	113.317	21.00	57.188	31.50	34.606
10.75	111.713	21.25	56.502	31.75	35.628

Table IX D (cont.)

FULLY CORRECTED ARGON SCATTER FROM STATE ARGON 3

TWO THETA	$P_a(2\theta)$ (CPS)	TWO THETA	$P_a(2\theta)$ (CPS)
32.00	37.118	42.50	26.719
32.25	34.720	42.75	25.150
32.50	34.124	43.00	26.317
32.75	34.535	43.25	24.061
33.00	32.996	43.50	25.958
33.25	35.628	43.75	24.306
33.50	34.733	44.00	26.708
33.75	32.662	44.25	25.688
34.00	31.696	44.50	24.207
34.25	34.692	44.75	24.192
34.50	35.647	45.00	22.100
34.75	33.490		
35.00	31.772		
35.25	33.047		
35.50	31.783		
35.75	32.287		
36.00	30.270		
36.25	31.746		
36.50	33.918		
36.75	30.510		
37.00	30.948		
37.25	30.504		
37.50	30.349		
37.75	30.477		
38.00	27.670		
38.25	29.415		
38.50	31.392		
38.75	29.524		
39.00	28.885		
39.25	29.899		
39.50	28.223		
39.75	28.929		
40.00	27.867		
40.25	28.828		
40.50	26.706		
40.75	28.687		
41.00	26.976		
41.25	26.058		
41.50	26.648		
41.75	27.983		
42.00	25.709		
42.25	27.400		

Table IX E

FULLY CORRECTED ARGON SCATTER FROM STATE ARGON 4

TWO THETA	$P_a(2\theta)$ (CPS)	TWO THETA	$P_a(2\theta)$ (CPS)	TWO THETA	$P_a(2\theta)$ (CPS)
0.50	2439.973	11.00	84.296	21.50	42.003
0.75	230.853	11.25	78.969	21.75	41.084
1.00	170.344	11.50	77.940	22.00	43.483
1.25	157.142	11.75	77.180	22.25	42.734
1.50	147.024	12.00	73.989	22.50	42.473
1.75	139.509	12.25	75.088	22.75	38.665
2.00	135.571	12.50	69.796	23.00	39.612
2.25	128.593	12.75	70.468	23.25	39.747
2.50	124.011	13.00	67.784	23.50	39.293
2.75	121.482	13.25	67.166	23.75	39.584
3.00	119.292	13.50	65.975	24.00	41.878
3.25	116.126	13.75	63.159	24.25	41.033
3.50	111.380	14.00	64.752	24.50	39.304
3.75	109.578	14.25	62.155	24.75	38.456
4.00	109.084	14.50	64.537	25.00	38.825
4.25	109.239	14.75	60.705	25.25	36.507
4.50	106.541	15.00	60.214	25.50	36.431
4.75	105.967	15.25	60.373	25.75	34.072
5.00	103.228	15.50	58.374	26.00	35.736
5.25	104.523	15.75	55.437	26.25	37.739
5.50	103.039	16.00	55.344	26.50	35.266
5.75	103.593	16.25	57.292	26.75	33.754
6.00	101.471	16.50	54.988	27.00	30.850
6.25	101.180	16.75	54.319	27.25	34.032
6.50	101.543	17.00	54.818	27.50	34.301
6.75	102.406	17.25	55.828	27.75	29.536
7.00	101.286	17.50	55.957	28.00	30.612
7.25	101.102	17.75	54.469	28.25	28.247
7.50	101.197	18.00	53.235	28.50	30.506
7.75	101.875	18.25	51.988	28.75	31.879
8.00	99.972	18.50	56.620	29.00	30.333
8.25	103.591	18.75	54.047	29.25	30.517
8.50	98.242	19.00	49.391	29.50	29.396
8.75	99.500	19.25	50.340	29.75	29.599
9.00	95.953	19.50	50.777	30.00	28.823
9.25	95.159	19.75	49.141	30.25	30.987
9.50	93.878	20.00	48.098	30.50	30.021
9.75	91.003	20.25	45.890	30.75	28.462
10.00	89.523	20.50	45.777	31.00	25.966
10.25	88.242	20.75	44.224	31.25	29.503
10.50	87.602	21.00	47.591	31.50	27.787
10.75	85.691	21.25	43.301	31.75	25.275

Table IX E (cont.)

FULLY CORRECTED ARGON SCATTER FROM STATE ARGON [4]

TWO THETA	$P_a(2\theta)$ (CPS)	TWO THETA	$P_a(2\theta)$ (CPS)
32.00	23.353	42.50	18.443
32.25	26.684	42.75	18.025
32.50	26.507	43.00	19.973
32.75	24.408	43.25	19.303
33.00	24.504	43.50	17.805
33.25	26.698	43.75	19.245
33.50	25.078	44.00	19.766
33.75	24.214	44.25	18.161
34.00	24.207	44.50	19.270
34.25	23.736	44.75	17.199
34.50	26.494	45.00	15.449
34.75	26.672		
35.00	25.873		
35.25	25.854		
35.50	22.409		
35.75	26.524		
36.00	23.556		
36.25	23.340		
36.50	25.559		
36.75	23.785		
37.00	25.327		
37.25	24.423		
37.50	22.836		
37.75	23.419		
38.00	20.735		
38.25	20.506		
38.50	21.650		
38.75	22.272		
39.00	20.904		
39.25	22.283		
39.50	21.056		
39.75	19.342		
40.00	20.310		
40.25	20.150		
40.50	20.415		
40.75	20.756		
41.00	21.411		
41.25	21.155		
41.50	19.739		
41.75	20.169		
42.00	20.001		
42.25	21.356		

Table X

Coherent Atomic Scattering Factors for Argon

$\sin\theta/\lambda$	$s(\text{Å}^{-1})$	$f^o(s)$ exptl. (Appen.C)	$f^o(s)$ Hartree-Foch	$f^2(s)$ exptl.	2θ for $\lambda=.5608\text{Å}$
.00	.0000	18.00	18.000	327.6	0.00
.05	.6283	17.54	17.535	311.2	3.21
.10	1.2566	16.32	16.294	269.6	6.43
.15	1.8850	14.87	14.640	224.1	9.65
.20	2.5132	13.34	12.938	180.6	12.88
.25	3.1416	11.80	11.428	141.6	16.12
.30	3.7699	10.80	10.202	118.8	19.37
.35	4.3982	9.90	9.258	100.0	22.64
.40	5.0265	9.23	8.544	87.1	25.93
.50	6.2832	7.96	7.563	65.0	32.57
.60	7.5398	7.30	6.862	54.8	39.33
.70	8.7965	6.63	6.238	45.3	46.23
.80	10.0531	(5.97)	5.623	(36.8)	
.90	11.3097	(5.33)	5.018	(29.5)	
1.00	12.5664	(4.71)	4.441	(23.1)	
1.10	13.8230		3.912		
1.20	15.0796		3.442		
1.30	16.3363		3.037		
1.40	17.5929		2.695		
1.50	18.8495		2.411		

$$f = f^o + \Delta f' + i\Delta f''$$

$$f^2(s) = (f^o + \Delta f')^2 - (\Delta f'')^2$$

$$\Delta f' = .101 \qquad \Delta f'' = .125$$

Table XI

Incoherent Scattering Factors for Argon

$\sin\theta/\lambda$	$s(\overset{\circ}{A})$	I_{inc}/R	$\Delta\lambda(A^{\circ})$	$\mathscr{I}_{inc}$	2θ for $\lambda=.5608\overset{\circ}{A}$
.000	.0000	.000	.00000	.000	.00
.005	.0628	.006	.00000	.006	.32
.010	.1257	.024	.00000	.024	.64
.050	.6283	.571	.00004	.571	3.20
.100	1.2566	1.956	.00015	1.955	6.43
.150	1.8850	3.558	.00034	3.554	9.65
.200	2.5132	5.033	.00061	5.022	12.88
.300	3.7699	7.377	.00137	7.341	19.37
.400	5.0265	8.998	.00187	8.938	22.64
.500	6.2832	10.106	.00244	10.019	25.93
.600	7.5398	10.967	.00382	10.819	32.57
.700	8.7965	11.726	.00549	11.500	39.33
.800	10.0531	12.424	.00748	12.099	46.23
.900	11.3097	13.061			
1.000	12.5664	13.629			
1.500	18.8495	15.489			
2.000	25.1328	16.324			
3.000	37.6992	17.132			
4.000	50.2656	17.573			
5.000	62.8320	17.800			
8.000	100.5312	17.978			

$$\Delta\lambda = \lambda' - \lambda = .02426A^{\circ}(1-\cos2\theta)$$

$$\mathscr{I}_{inc} = \frac{I_{inc}}{R}\left[\frac{\lambda}{\lambda'}\right]^{2}$$

Table XII

CORRECTION OF I(TWO THETA) FROM STATE 1R FOR
INCIDENT WAVELENGTH DISTRIBUTION

S(ANG.-1)	I(TWO THETA) EXPTL.	I(S) AG K ALPHA
0.19950	0.59546	0.61206
0.23828	0.46441	0.47418
0.27706	0.34885	0.35372
0.31584	0.25497	0.25735
0.35462	0.17111	0.17007
0.39340	0.09611	0.09221
0.43218	0.02998	0.02374
0.47096	-0.02727	-0.03537
0.50974	-0.07564	-0.08508
0.54853	-0.11512	-0.12540
0.58731	-0.14571	-0.15635
0.62609	-0.16739	-0.17757
0.66487	-0.18279	-0.19232
0.70365	-0.19573	-0.20554
0.74243	-0.20620	-0.21614
0.78121	-0.21419	-0.22405
0.81999	-0.21968	-0.22931
0.85877	-0.22263	-0.23190
0.89755	-0.22303	-0.23178
0.93633	-0.22085	-0.22894
0.97511	-0.21606	-0.22335
1.01389	-0.20860	-0.21489
1.05267	-0.19859	-0.20374
1.09145	-0.18625	-0.19017
1.13023	-0.17178	-0.17442
1.16902	-0.15541	-0.15671
1.20780	-0.13733	-0.13725
1.24658	-0.11778	-0.11629
1.28536	-0.09694	-0.09404
1.32414	-0.07505	-0.07071
1.36292	-0.05247	-0.04670
1.40170	-0.02954	-0.02246
1.44048	-0.00663	0.00165
1.47926	0.01592	0.02527
1.51804	0.03777	0.04804
1.55682	0.05856	0.06959
1.59560	0.07796	0.08955
1.63438	0.09561	0.10752
1.67316	0.11117	0.12327
1.71194	0.12424	0.13648
1.75072	0.13374	0.14537

Table XII (cont.)

CORRECTION OF I(TWO THETA) FROM STATE 1R FOR
INCIDENT WAVELENGTH DISTRIBUTION

S(ANG.-1)	I(TWO THETA) EXPTL.	I(S) AG K ALPHA
1.78951	0.13958	0.14992
1.82829	0.14201	0.15070
1.86707	0.14126	0.14817
1.90585	0.13758	0.14272
1.94463	0.13122	0.13462
1.98341	0.12243	0.12407
2.02219	0.11144	0.11135
2.06097	0.09850	0.09673
2.09975	0.08387	0.08022
2.13853	0.06777	0.06161
2.17731	0.05168	0.04326
2.21609	0.03703	0.02764
2.25487	0.02375	0.01424
2.29365	0.01175	0.00263
2.33243	0.00095	-0.00753
2.37121	-0.00873	-0.01658
2.40999	-0.01737	-0.02473
2.44878	-0.02506	-0.03204
2.48756	-0.03188	-0.03852
2.52634	-0.03790	-0.04423
2.56512	-0.04322	-0.04922
2.60390	-0.04792	-0.05352
2.64268	-0.05206	-0.05727
2.68146	-0.05575	-0.06077
2.72024	-0.05906	-0.06435
2.75902	-0.06162	-0.06736
2.79780	-0.06245	-0.06791
2.83658	-0.06171	-0.06631
2.87536	-0.05956	-0.06293
2.91414	-0.05620	-0.05811
2.95292	-0.05181	-0.05217
2.99170	-0.04659	-0.04542
3.03048	-0.04071	-0.03818
3.06927	-0.03437	-0.03069
3.10805	-0.02776	-0.02313
3.14683	-0.02105	-0.01565
3.18561	-0.01444	-0.00842
3.22439	-0.00812	-0.00164
3.26317	-0.00226	0.00454
3.30195	0.00294	0.00994
3.34073	0.00729	0.01442

Table XII (cont.)

CORRECTION OF I(TWO THETA) FROM STATE 1R FOR
INCIDENT WAVELENGTH DISTRIBUTION

S(ANG.-1)	I(TWO THETA) EXPTL.	I(S) AG K ALPHA
3.37951	0.01061	0.01774
3.41829	0.01271	0.01946
3.45707	0.01341	0.01911
3.49585	0.01251	0.01621
3.53463	0.01066	0.01196
3.57341	0.00900	0.00856
3.61219	0.00753	0.00594
3.65097	0.00622	0.00396
3.68976	0.00507	0.00252
3.72854	0.00405	0.00153
3.76732	0.00314	0.00090
3.80610	0.00234	0.00052
3.84488	0.00163	0.00026
3.88366	0.00098	0.00001
3.92244	0.00038	-0.00032
3.96122	-0.00019	-0.00073
4.00000	-0.00073	-0.00122

Table XIII

Isothermal Compressibility and Zero-Angle Structure Factor

STATE	$K_T = \frac{1}{n}\left(\frac{\partial n}{\partial P}\right)_T$	$i(0)$
argon 1, 1R	$.02794 \text{ atm}^{-1}$	1.075
argon 2	.02596	1.874
argon 3	.03347	.585

Table XIV

Conversion factors from Electron Units to Counts per

Second   (units of N_a are cps-atoms/cm)

state	$n(g/cm^3)$	$n(atoms/\overset{\circ}{A}{}^3)$	N_a: fit to $f^2(2)$ (eq. 45)	N_a: integral normalization (eq. 57)
1R	.2087	.003147	2.2730	2.2775
1	.2087	.003147	2.2856	2.2902
2	.3111	.004691	3.4361	3.5322
3	.1331	.002007	1.5036	1.4655

Table XV A

STRUCTURE FACTOR FOR ARGON STATE 1

S(ANG.-1)	I(S)	S(ANG.-1)	I(S)
0.0	1.075	1.82829	0.13413
0.19950	0.58999	1.86707	0.13024
0.23828	0.44779	1.90585	0.12380
0.27706	0.32403	1.94463	0.11510
0.31584	0.22649	1.98341	0.10451
0.35462	0.14206	2.02219	0.09238
0.39340	0.06973	2.06097	0.07907
0.43218	0.00827	2.09975	0.06490
0.47096	-0.04351	2.13853	0.05012
0.50974	-0.08677	2.17731	0.03568
0.54853	-0.12270	2.21609	0.02235
0.58731	-0.15249	2.25487	0.01002
0.62609	-0.17736	2.29365	-0.00139
0.66487	-0.19801	2.33243	-0.01189
0.70365	-0.21417	2.37121	-0.02148
0.74243	-0.22629	2.40999	-0.03014
0.78121	-0.23472	2.44878	-0.03779
0.81999	-0.23980	2.48756	-0.04431
0.85877	-0.24188	2.52634	-0.04964
0.89755	-0.24131	2.56512	-0.05370
0.93633	-0.23840	2.60390	-0.05647
0.97511	-0.23381	2.64268	-0.05784
1.01389	-0.22579	2.68146	-0.05760
1.05267	-0.21382	2.72024	-0.05549
1.09145	-0.19898	2.75902	-0.05192
1.13023	-0.18201	2.79780	-0.04838
1.16902	-0.16349	2.83658	-0.04489
1.20780	-0.14399	2.87536	-0.04146
1.24658	-0.12410	2.91414	-0.03806
1.28536	-0.10455	2.95292	-0.03467
1.32414	-0.08639	2.99170	-0.03129
1.36292	-0.06536	3.03048	-0.02788
1.40170	-0.04143	3.06927	-0.02444
1.44048	-0.01600	3.10805	-0.02104
1.47926	0.00969	3.14683	-0.01774
1.51804	0.03482	3.18561	-0.01460
1.55682	0.05869	3.22439	-0.01168
1.59560	0.08057	3.23520	0.00629
1.63438	0.09974	3.33630	0.01771
1.67316	0.11532	3.43740	0.02522
1.71194	0.12633	3.53850	0.02814
1.75072	0.13269	3.63960	0.02693
1.78951	0.13509	3.74070	0.02229

Table XV A (cont.)

STRUCTURE FACTOR FOR ARGON STATE 1

S(ANG.-1)	I(S)	S(ANG.-1)	I(S)
3.84180	0.01553	8.18910	-0.00031
3.94290	0.00794	8.29020	-0.00025
4.04400	0.00062	8.39130	-0.00018
4.14510	-0.00546	8.49240	-0.00015
4.24620	-0.00990	8.59350	-0.00014
4.34730	-0.01237	8.69460	-0.00015
4.44840	-0.01304	8.79570	-0.00016
4.54950	-0.01213	8.89680	-0.00015
4.65060	-0.01001	8.99790	-0.00013
4.75170	-0.00715	9.09900	-0.00008
4.85280	-0.00391	9.20010	-0.00003
4.95390	-0.00078	9.30120	0.00002
5.05500	0.00203	9.40230	0.00007
5.15610	0.00421	9.50340	0.00009
5.25720	0.00564	9.60450	0.00011
5.35830	0.00632	9.70560	0.00009
5.45940	0.00623	9.80670	0.00008
5.56050	0.00552	9.90780	0.00007
5.66160	0.00428	10.00890	0.00006
5.76270	0.00277	10.11000	0.00007
5.86380	0.00110	10.21110	0.00008
5.96490	-0.00051	10.31220	0.00010
6.06600	-0.00188	10.41330	0.00010
6.16710	-0.00291	10.51440	0.00010
6.26820	-0.00346	10.61550	0.00007
6.36930	-0.00356	10.71660	0.00003
6.47040	-0.00320	10.81770	-0.00002
6.57150	-0.00250	10.91880	-0.00008
6.67260	-0.00159	11.01990	-0.00013
6.77370	-0.00059	11.12100	-0.00017
6.87480	0.00030	11.22210	-0.00018
6.97590	0.00103	11.32320	-0.00017
7.07700	0.00149	11.42430	-0.00014
7.17810	0.00167	11.52540	-0.00009
7.27920	0.00161	11.62650	-0.00003
7.38030	0.00134	11.72760	0.00003
7.48140	0.00097	11.82870	0.00008
7.58250	0.00054	11.92980	0.00012
7.68360	0.00017	12.03090	0.00014
7.78470	-0.00013	12.13200	0.00014
7.88580	-0.00031	12.23310	0.00013
7.98690	-0.00038	12.33420	0.00009
8.08800	-0.00038	12.43530	0.00006

Table XV A (cont.)

STRUCTURE FACTOR FOR ARGON STATE   1

S(ANG.-1)	I(S)
12.53640	0.00002
12.63750	-0.00002
12.73860	-0.00005
12.83970	-0.00007
12.94080	-0.00008
13.04190	-0.00008
13.14300	-0.00007
13.24410	-0.00006
13.34520	-0.00004
13.44630	-0.00002
13.54740	0.0
13.64850	0.00002
13.74960	0.00003
13.85070	0.00004
13.95180	0.00004
14.05290	0.00004
14.15400	0.00004
14.25510	0.00002
14.35620	0.00001
14.45730	0.0
14.55840	-0.00001
14.65950	-0.00002
14.76060	-0.00002
14.86170	-0.00002
14.96280	-0.00002
15.06390	-0.00002
15.16500	-0.00001
15.26610	0.0
15.36720	0.0
15.46830	0.00001
15.56940	0.00001
15.67050	0.00001
15.77160	0.00001
15.87270	0.00001
15.97380	0.00001
16.07489	0.0
16.17599	0.0
16.27710	0.0
16.37819	0.0
16.47929	0.0
16.58040	0.0
16.68149	0.0
16.78259	0.0

Table XV B

STRUCTURE FACTOR FOR ARGON STATE 1R

S(ANG.-1)	I(S)	S(ANG.-1)	I(S)
0.0	1.075	1.82829	0.14831
0.19950	0.60872	1.86707	0.14579
0.23828	0.47112	1.90585	0.14035
0.27706	0.35091	1.94463	0.13227
0.31584	0.25474	1.98341	0.12174
0.35462	0.16764	2.02219	0.10904
0.39340	0.08994	2.06097	0.09445
0.43218	0.02162	2.09975	0.07798
0.47096	-0.03737	2.13853	0.05941
0.50974	-0.08698	2.17731	0.04110
0.54853	-0.12721	2.21609	0.02551
0.58731	-0.15810	2.25487	0.01214
0.62609	-0.17928	2.29365	0.00055
0.66487	-0.19400	2.33243	-0.00959
0.70365	-0.20719	2.37121	-0.01862
0.74243	-0.21777	2.40999	-0.02675
0.78121	-0.22566	2.44878	-0.03405
0.81999	-0.23091	2.48756	-0.04051
0.85877	-0.23349	2.52634	-0.04621
0.89755	-0.23337	2.56512	-0.05119
0.93633	-0.23054	2.60390	-0.05548
0.97511	-0.22496	2.64268	-0.05923
1.01389	-0.21652	2.68146	-0.06272
1.05267	-0.20539	2.72024	-0.06629
1.09145	-0.19185	2.75902	-0.06930
1.13023	-0.17613	2.79780	-0.06984
1.16902	-0.15846	2.83658	-0.06825
1.20780	-0.13904	2.87536	-0.06487
1.24658	-0.11812	2.91414	-0.06006
1.28536	-0.09592	2.95292	-0.05414
1.32414	-0.07264	2.99170	-0.04740
1.36292	-0.04868	3.03048	-0.04018
1.40170	-0.02449	3.06927	-0.03270
1.44048	-0.00043	3.10805	-0.02516
1.47926	0.02314	3.14683	-0.01769
1.51804	0.04587	3.17440	-0.00148
1.55682	0.06737	3.27360	0.01103
1.59560	0.08729	3.37280	0.02036
1.63438	0.10522	3.47200	0.02578
1.67316	0.12094	3.57120	0.02709
1.71194	0.13412	3.67040	0.02470
1.75072	0.14299	3.76960	0.01962
1.78951	0.14753	3.86880	0.01284

Table XV B (cont.)

STRUCTURE FACTOR FOR ARGON STATE 1R

S(ANG.-1)	I(S)	S(ANG.-1)	I(S)
3.96800	0.00568	8.23360	-0.00046
4.06720	-0.00105	8.33280	-0.00029
4.16640	-0.00651	8.43200	-0.00015
4.26560	-0.01035	8.53120	-0.00002
4.36480	-0.01242	8.63040	0.00004
4.46400	-0.01277	8.72960	0.00009
4.56320	-0.01172	8.82880	0.00009
4.66240	-0.00953	8.92800	0.00008
4.76160	-0.00669	9.02720	0.00006
4.86080	-0.00351	9.12640	0.00003
4.96000	-0.00042	9.22560	0.00001
5.05920	0.00232	9.32480	-0.00003
5.15840	0.00446	9.42400	-0.00004
5.25760	0.00583	9.52320	-0.00006
5.35680	0.00649	9.62240	-0.00006
5.45600	0.00637	9.72160	-0.00005
5.55520	0.00562	9.82080	-0.00003
5.65440	0.00435	9.92000	0.00001
5.75360	0.00279	10.01920	0.00005
5.85280	0.00108	10.11840	0.00010
5.95200	-0.00059	10.21760	0.00014
6.05120	-0.00201	10.31680	0.00018
6.15040	-0.00308	10.41600	0.00018
6.24960	-0.00367	10.51520	0.00016
6.34880	-0.00380	10.61440	0.00012
6.44800	-0.00344	10.71360	0.00005
6.54720	-0.00272	10.81280	-0.00002
6.64640	-0.00176	10.91200	-0.00010
6.74560	-0.00070	11.01120	-0.00016
6.84480	0.00030	11.11040	-0.00020
6.94400	0.00113	11.20960	-0.00021
7.04320	0.00167	11.30880	-0.00020
7.14240	0.00194	11.40800	-0.00016
7.24160	0.00190	11.50720	-0.00010
7.34080	0.00164	11.60640	-0.00004
7.44000	0.00121	11.70560	0.00004
7.53920	0.00070	11.80480	0.00009
7.63840	0.00021	11.90400	0.00013
7.73760	-0.00021	12.00320	0.00015
7.83680	-0.00050	12.10240	0.00015
7.93600	-0.00066	12.20160	0.00013
8.03520	-0.00067	12.30080	0.00010
8.13440	-0.00059	12.40000	0.00006

Table XV B (cont.)

STRUCTURE FACTOR FOR ARGON STATE 1R

S(ANG.-1)	I(S)
12.49920	0.00002
12.59840	-0.00002
12.69760	-0.00005
12.79680	-0.00007
12.89600	-0.00008
12.99520	-0.00008
13.09440	-0.00007
13.19360	-0.00006
13.29280	-0.00004
13.39200	-0.00002
13.49120	0.0
13.59040	0.00002
13.68960	0.00003
13.78880	0.00004
13.88800	0.00004
13.98720	0.00004
14.08640	0.00004
14.18560	0.00003
14.28480	0.00002
14.38400	0.0
14.48320	-0.00001
14.58240	-0.00002
14.68160	-0.00002
14.78080	-0.00002
14.88000	-0.00002
14.97920	-0.00002
15.07840	-0.00001
15.17760	-0.00001
15.27680	0.0
15.37600	0.00001
15.47520	0.00001
15.57440	0.00001
15.67360	0.00001
15.77280	0.00001
15.87200	0.00001
15.97120	0.0
16.07039	0.0
16.16959	0.0
16.26880	0.0
16.36800	0.0
16.46719	0.0
16.56639	0.0
16.66559	0.0

Table XV C

STRUCTURE FACTOR FOR ARGON STATE 2

S(ANG.-1)	I(S)	S(ANG.-1)	I(S)
0.0	1.874	1.82829	0.19126
0.19950	0.80433	1.86707	0.18875
0.23828	0.54265	1.90585	0.18200
0.27706	0.34415	1.94463	0.17170
0.31584	0.21998	1.98341	0.15837
0.35462	0.11209	2.02219	0.14259
0.39340	0.01996	2.06097	0.12496
0.43218	-0.05786	2.09975	0.10608
0.47096	-0.12278	2.13853	0.08659
0.50974	-0.17612	2.17731	0.06748
0.54853	-0.21924	2.21609	0.04922
0.58731	-0.25352	2.25487	0.03179
0.62609	-0.28028	2.29365	0.01517
0.66487	-0.30117	2.33243	-0.00054
0.70365	-0.31725	2.37121	-0.01530
0.74243	-0.32878	2.40999	-0.02895
0.78121	-0.33615	2.44878	-0.04135
0.81999	-0.33980	2.48756	-0.05235
0.85877	-0.34012	2.52634	-0.06178
0.89755	-0.33752	2.56512	-0.06955
0.93633	-0.33239	2.60390	-0.07554
0.97511	-0.32533	2.64268	-0.07960
1.01389	-0.31567	2.68146	-0.08136
1.05267	-0.30283	2.72024	-0.08040
1.09145	-0.28701	2.75902	-0.07725
1.13023	-0.26826	2.79780	-0.07401
1.16902	-0.24660	2.83658	-0.07073
1.20780	-0.22203	2.87536	-0.06737
1.24658	-0.19461	2.91414	-0.06391
1.28536	-0.16428	2.95292	-0.06030
1.32414	-0.13070	2.99170	-0.05655
1.36292	-0.09722	3.03048	-0.05256
1.40170	-0.06465	3.06927	-0.04838
1.44048	-0.03283	3.10805	-0.04404
1.47926	-0.00167	3.14683	-0.03962
1.51804	0.02867	3.18561	-0.03520
1.55682	0.05796	3.22439	-0.03083
1.59560	0.08597	3.24160	0.00540
1.63438	0.11240	3.34290	0.02535
1.67316	0.13760	3.44420	0.03931
1.71194	0.16191	3.54550	0.04573
1.75072	0.17914	3.64680	0.04489
1.78951	0.18846	3.74810	0.03780

Table XV C (cont.)

STRUCTURE FACTOR FOR ARGON STATE 2

S(ANG.-1)	I(S)	S(ANG.-1)	I(S)
3.84940	0.02672	8.20530	-0.00010
3.95070	0.01387	8.30660	-0.00007
4.05200	0.00143	8.40790	-0.00009
4.15330	-0.00892	8.50920	-0.00021
4.25460	-0.01632	8.61050	-0.00034
4.35590	-0.02025	8.71180	-0.00051
4.45720	-0.02107	8.81310	-0.00061
4.55850	-0.01920	8.91440	-0.00065
4.65980	-0.01547	9.01570	-0.00059
4.76110	-0.01064	9.11700	-0.00042
4.86240	-0.00544	9.21830	-0.00022
4.96370	-0.00062	9.31960	0.00002
5.06500	0.00349	9.42090	0.00022
5.16630	0.00647	9.52220	0.00037
5.26760	0.00828	9.62350	0.00043
5.36890	0.00895	9.72480	0.00041
5.47020	0.00865	9.82610	0.00035
5.57150	0.00758	9.92740	0.00024
5.67280	0.00590	10.02870	0.00015
5.77410	0.00397	10.13000	0.00007
5.87540	0.00185	10.23130	0.00003
5.97670	-0.00020	10.33260	0.00002
6.07800	-0.00203	10.43390	0.00003
6.17930	-0.00347	10.53520	0.00005
6.28060	-0.00437	10.63650	0.00004
6.38190	-0.00473	10.73780	0.00002
6.48320	-0.00446	10.83910	-0.00003
6.58450	-0.00374	10.94040	-0.00009
6.68580	-0.00263	11.04170	-0.00015
6.78710	-0.00136	11.14300	-0.00020
6.88840	-0.00013	11.24430	-0.00023
6.98970	0.00094	11.34560	-0.00023
7.09100	0.00167	11.44690	-0.00019
7.19230	0.00206	11.54820	-0.00014
7.29360	0.00208	11.64950	-0.00006
7.39490	0.00184	11.75080	0.00002
7.49620	0.00140	11.85210	0.00010
7.59750	0.00091	11.95340	0.00016
7.69880	0.00046	12.05470	0.00018
7.80010	0.00010	12.15600	0.00020
7.90140	-0.00010	12.25730	0.00018
8.00270	-0.00018	12.35860	0.00014
8.10400	-0.00015	12.45990	0.00010

Table XV C (cont.)

STRUCTURE FACTOR FOR ARGON STATE 2

S(ANG.-1)	I(S)
12.56120	0.00004
12.66250	0.0
12.76380	-0.00005
12.86510	-0.00007
12.96640	-0.00010
13.06770	-0.00011
13.16900	-0.00011
13.27030	-0.00010
13.37160	-0.00007
13.47290	-0.00005
13.57420	-0.00002
13.67550	0.00001
13.77680	0.00004
13.87810	0.00005
13.97940	0.00006
14.08070	0.00007
14.18200	0.00006
14.28330	0.00005
14.38460	0.00003
14.48590	0.00001
14.58720	-0.00001
14.68850	-0.00002
14.78980	-0.00003
14.89110	-0.00004
14.99240	-0.00004
15.09370	-0.00003
15.19500	-0.00002
15.29630	-0.00001
15.39760	0.0
15.49890	0.00001
15.60020	0.00001
15.70150	0.00002
15.80280	0.00001
15.90410	0.00001
16.00539	0.00001
16.10669	0.0
16.20799	0.0
16.30930	0.0
16.41060	0.0
16.51189	-0.00001
16.61319	0.0
16.71449	0.0
16.81580	0.0

Table XV D

STRUCTURE FACTOR FOR ARGON STATE 3

S(ANG.-1)	I(S)	S(ANG.-1)	I(S)
0.0	.585	1.82829	0.09266
0.19950	0.39369	1.86707	0.08910
0.23828	0.32251	1.90585	0.08371
0.27706	0.25830	1.94463	0.07693
0.31584	0.20401	1.98341	0.06902
0.35462	0.15195	2.02219	0.06028
0.39340	0.10301	2.06097	0.05108
0.43218	0.05776	2.09975	0.04175
0.47096	0.01682	2.13853	0.03270
0.50974	-0.01921	2.17731	0.02452
0.54853	-0.04972	2.21609	0.01733
0.58731	-0.07413	2.25487	0.01091
0.62609	-0.09151	2.29365	0.00510
0.66487	-0.10425	2.33243	-0.00024
0.70365	-0.11657	2.37121	-0.00521
0.74243	-0.12725	2.40999	-0.00988
0.78121	-0.13601	2.44878	-0.01429
0.81999	-0.14274	2.48756	-0.01846
0.85877	-0.14721	2.52634	-0.02247
0.89755	-0.14919	2.56512	-0.02634
0.93633	-0.14848	2.60390	-0.03011
0.97511	-0.14485	2.64268	-0.03386
1.01389	-0.13814	2.68146	-0.03793
1.05267	-0.12886	2.72024	-0.04265
1.09145	-0.11746	2.75902	-0.04717
1.13023	-0.10438	2.79780	-0.04908
1.16902	-0.09001	2.83658	-0.04873
1.20780	-0.07477	2.87536	-0.04655
1.24658	-0.05909	2.91414	-0.04293
1.28536	-0.04336	2.95292	-0.03825
1.32414	-0.02801	2.99170	-0.03286
1.36292	-0.01381	3.03048	-0.02713
1.40170	-0.00068	3.06927	-0.02133
1.44048	0.01163	3.10805	-0.01563
1.47926	0.02330	3.14683	-0.01018
1.51804	0.03437	3.18561	-0.00515
1.55682	0.04496	3.19360	-0.00249
1.59560	0.05510	3.29340	0.00528
1.63438	0.06482	3.39320	0.01126
1.67316	0.07455	3.49300	0.01505
1.71194	0.08473	3.59280	0.01638
1.75072	0.09131	3.69260	0.01550
1.78951	0.09367	3.79240	0.01284

Table XV D (cont.)

STRUCTURE FACTOR FOR ARGON STATE 3

S(ANG.-1)	I(S)	S(ANG.-1)	I(S)
3.89220	0.00901	8.18360	-0.00043
3.99200	0.00471	8.28340	-0.00036
4.09180	0.00048	8.38320	-0.00027
4.19160	-0.00311	8.48300	-0.00016
4.29140	-0.00584	8.58280	-0.00006
4.39120	-0.00746	8.68260	0.00001
4.49100	-0.00802	8.78240	0.00007
4.59080	-0.00762	8.88220	0.00009
4.69060	-0.00643	8.98200	0.00010
4.79040	-0.00472	9.08180	0.00008
4.89020	-0.00273	9.16160	0.00006
4.99000	-0.00074	9.28140	0.00002
5.08980	0.00109	9.38120	-0.00001
5.18960	0.00254	9.48100	-0.00004
5.28940	0.00353	9.58080	-0.00006
5.38920	0.00403	9.68060	-0.00006
5.48900	0.00405	9.78040	-0.00006
5.58880	0.00365	9.88020	-0.00004
5.68860	0.00289	9.98000	-0.00002
5.78840	0.00195	10.07980	0.00002
5.88820	0.00089	10.17960	0.00006
5.98800	-0.00014	10.27940	0.00009
6.08780	-0.00105	10.37920	0.00011
6.18760	-0.00173	10.47900	0.00012
6.28740	-0.00215	10.57880	0.00012
6.38720	-0.00229	10.67860	0.00009
6.48700	-0.00214	10.77840	0.00006
6.58680	-0.00178	10.87820	0.00001
6.68660	-0.00124	10.97800	-0.00004
6.78640	-0.00064	11.07780	-0.00008
6.88620	-0.00003	11.17760	-0.00011
6.98600	0.00049	11.27740	-0.00013
7.08580	0.00088	11.37720	-0.00013
7.18560	0.00111	11.47700	-0.00011
7.28540	0.00116	11.57680	-0.00008
7.38520	0.00107	11.67660	-0.00005
7.48500	0.00086	11.77640	-0.00001
7.58480	0.00058	11.87620	0.00003
7.68460	0.00028	11.97600	0.00006
7.78440	0.0	12.07580	0.00008
7.88420	-0.00022	12.17560	0.00009
7.98400	-0.00037	12.27540	0.00009
8.08380	-0.00043	12.37520	0.00008

Table XV D (cont.)

STRUCTURE FACTOR FOR ARGON STATE 3

S(ANG.-1)	I(S)
12.47500	0.00006
12.57480	0.00003
12.67460	0.00001
12.77440	-0.00001
12.87420	-0.00003
12.97400	-0.00005
13.07380	-0.00005
13.17360	-0.00005
13.27340	-0.00004
13.37320	-0.00004
13.47300	-0.00002
13.57280	-0.00001
13.67260	0.0
13.77240	0.00001
13.87220	0.00002
13.97200	0.00003
14.07180	0.00003
14.17160	0.00003
14.27140	0.00002
14.37120	0.00002
14.47100	0.00001
14.57080	0.0
14.67060	0.0
14.77040	-0.00001
14.87020	-0.00001
14.97000	-0.00001
15.06980	-0.00001
15.16960	-0.00001
15.26940	-0.00001
15.36920	0.0
15.46900	0.0
15.56880	0.0
15.66860	0.0
15.76840	0.00001
15.86820	0.0
15.96800	0.0
16.06779	0.0
16.16759	0.0
16.26740	0.0
16.36719	0.0
16.46700	0.0
16.56679	0.0
16.66660	0.0

Table XVI (A)

DISTRIBUTION FUNCTIONS AND PERCUS-YEVICK EFFECTIVE
POTENTIAL FOR ARGON STATE 1

R(ANG.)	G(R)	C(R)	U EFF. PY (DEG.K)
0.05	-0.1365	-2.3391	
0.10	-0.1194	-2.3159	
0.15	-0.0925	-2.2788	
0.20	-0.0580	-2.2304	
0.25	-0.0185	-2.1733	
0.30	0.0233	-2.1107	
0.35	0.0648	-2.0453	
0.40	0.1041	-1.9793	
0.45	0.1402	-1.9144	
0.50	0.1724	-1.8511	
0.55	0.2014	-1.7897	
0.60	0.2278	-1.7295	
0.65	0.2531	-1.6695	
0.70	0.2784	-1.6090	
0.75	0.3046	-1.5472	
0.80	0.3323	-1.4839	
0.85	0.3614	-1.4194	
0.90	0.3911	-1.3547	
0.95	0.4203	-1.2912	
1.00	0.4473	-1.2304	
1.05	0.4707	-1.1741	
1.10	0.4891	-1.1239	
1.15	0.5013	-1.0807	
1.20	0.5071	-1.0451	
1.25	0.5064	-1.0170	
1.30	0.5000	-0.9958	
1.35	0.4890	-0.9804	
1.40	0.4744	-0.9697	
1.45	0.4576	-0.9624	
1.50	0.4394	-0.9576	
1.55	0.4203	-0.9548	
1.60	0.4005	-0.9539	
1.65	0.3795	-0.9552	
1.70	0.3567	-0.9593	
1.75	0.3313	-0.9669	
1.80	0.3028	-0.9787	
1.85	0.2706	-0.9950	
1.90	0.2351	-1.0155	
1.95	0.1968	-1.0396	
2.00	0.1571	-1.0659	
2.05	0.1174	-1.0927	
2.10	0.0796	-1.1184	

Table XVI (A) (cont.)

DISTRIBUTION FUNCTIONS AND PERCUS-YEVICK EFFECTIVE
POTENTIAL FOR ARGON STATE   1

R(ANG.)	G(R)	C(R)	U EFF. PY (DEG.K)
2.15	0.0454	-1.1412	
2.20	0.0159	-1.1597	
2.25	-0.0080	-1.1733	
2.30	-0.0266	-1.1820	
2.35	-0.0407	-1.1867	
2.40	-0.0519	-1.1889	
2.45	-0.0622	-1.1907	
2.50	-0.0738	-1.1942	
2.55	-0.0888	-1.2014	
2.60	-0.1083	-1.2136	
2.65	-0.1327	-1.2310	
2.70	-0.1612	-1.2526	
2.75	-0.1913	-1.2763	
2.80	-0.2195	-1.2984	
2.85	-0.2413	-1.3143	
2.90	-0.2512	-1.3186	
2.95	-0.2438	-1.3059	
3.00	-0.2139	-1.2708	
3.05	-0.1573	-1.2093	
3.10	-0.0709	-1.1183	
3.15	0.0461	-0.9967	
3.20	0.1931	-0.8454	291.2705
3.25	0.3672	-0.6672	179.3376
3.30	0.5635	-0.4670	104.5110
3.35	0.7758	-0.2509	48.5235
3.40	0.9966	-0.0266	4.5590
3.45	1.2177	0.1980	-30.7253
3.50	1.4311	0.4147	-59.2495
3.55	1.6293	0.6160	-82.2418
3.60	1.8057	0.7954	-100.5553
3.65	1.9552	0.9476	-114.8243
3.70	2.0745	1.0698	-125.5495
3.75	2.1619	1.1599	-133.1491
3.80	2.2177	1.2181	-137.9901
3.85	2.2435	1.2463	-140.4097
3.90	2.2424	1.2476	-140.7285
3.95	2.2186	1.2259	-139.2594
4.00	2.1765	1.1859	-136.3109
4.05	2.1210	1.1324	-132.1868
4.10	2.0565	1.0699	-127.1815
4.15	1.9872	1.0024	-121.5721
4.20	1.9164	0.9335	-115.6079

Table XVI (A) (cont.)

DISTRIBUTION FUNCTIONS AND PERCUS-YEVICK EFFECTIVE
POTENTIAL FOR ARGON STATE   1

R(ANG.)	G(R)	C(R)	U EFF. PY (DEG.K)
4.25	1.8468	0.8655	-109.4988
4.30	1.7799	0.8003	-103.4065
4.35	1.7168	0.7388	-97.4388
4.40	1.6576	0.6813	-91.6507
4.45	1.6026	0.6276	-86.0508
4.50	1.5508	0.5772	-80.6146
4.55	1.5019	0.5296	-75.3007
4.60	1.4552	0.4842	-70.0662
4.65	1.4105	0.4408	-64.8838
4.70	1.3676	0.3991	-59.7517
4.75	1.3267	0.3593	-54.6997
4.80	1.2882	0.3219	-49.7895
4.85	1.2525	0.2872	-45.1076
4.90	1.2202	0.2559	-40.7547
4.95	1.1917	0.2283	-36.8301
5.00	1.1674	0.2049	-33.4151
5.05	1.1475	0.1856	-30.5588
5.10	1.1316	0.1704	-28.2679
5.15	1.1194	0.1589	-26.5038
5.20	1.1104	0.1503	-25.1864
5.25	1.1036	0.1440	-24.2054
5.30	1.0984	0.1390	-23.4339
5.35	1.0938	0.1346	-22.7449
5.40	1.0891	0.1301	-22.0245
5.45	1.0838	0.1248	-21.1836
5.50	1.0776	0.1184	-20.1636
5.55	1.0703	0.1109	-18.9391
5.60	1.0620	0.1022	-17.5162
5.65	1.0529	0.0925	-15.9273
5.70	1.0433	0.0823	-14.2235
5.75	1.0336	0.0718	-12.4666
5.80	1.0243	0.0615	-10.7203
5.85	1.0156	0.0517	-9.0420
5.90	1.0077	0.0426	-7.4778
5.95	1.0010	0.0344	-6.0588
6.00	0.9954	0.0272	-4.8012
6.05	0.9909	0.0210	-3.7084
6.10	0.9876	0.0157	-2.7745
6.15	0.9853	0.0112	-1.9892
6.20	0.9839	0.0076	-1.3417
6.25	0.9835	0.0047	-0.8244
6.30	0.9840	0.0025	-0.4337

Table XVI (A) (cont.)

DISTRIBUTION FUNCTIONS AND PERCUS-YEVICK EFFECTIVE
POTENTIAL FOR ARGON STATE   1

R(ANG.)	G(R)	C(R)	U EFF. PY (DEG.K)
6.35	0.9854	0.0010	-0.1704
6.40	0.9877	0.0002	-0.0381
6.45	0.9910	0.0002	-0.0406
6.50	0.9952	0.0010	-0.1794
6.55	1.0003	0.0026	-0.4511
6.60	1.0063	0.0049	-0.8461
6.65	1.0130	0.0079	-1.3482
6.70	1.0203	0.0113	-1.9358
6.75	1.0281	0.0152	-2.5831
6.80	1.0361	0.0193	-3.2628
6.85	1.0442	0.0235	-3.9484
6.90	1.0521	0.0277	-4.6159
6.95	1.0597	0.0316	-5.2456
7.00	1.0669	0.0353	-5.8227
7.05	1.0735	0.0386	-6.3365
7.10	1.0795	0.0414	-6.7807
7.15	1.0847	0.0439	-7.1511
7.20	1.0893	0.0458	-7.4455
7.25	1.0930	0.0473	-7.6620
7.30	1.0960	0.0483	-7.7983
7.35	1.0981	0.0487	-7.8518
7.40	1.0993	0.0485	-7.8198
7.45	1.0996	0.0478	-7.6997
7.50	1.0990	0.0465	-7.4903
7.55	1.0976	0.0447	-7.1922
7.60	1.0954	0.0422	-6.8090
7.65	1.0924	0.0393	-6.3471
7.70	1.0887	0.0360	-5.8165
7.75	1.0844	0.0323	-5.2298
7.80	1.0797	0.0283	-4.6019
7.85	1.0747	0.0242	-3.9492
7.90	1.0695	0.0201	-3.2884
7.95	1.0642	0.0161	-2.6356
8.00	1.0590	0.0122	-2.0058
8.05	1.0539	0.0086	-1.4120
8.10	1.0491	0.0052	-0.8652
8.15	1.0445	0.0023	-0.3744
8.20	1.0403	-0.0003	0.0536
8.25	1.0366	-0.0025	0.4134
8.30	1.0332	-0.0042	0.7012
8.35	1.0303	-0.0055	0.9145
8.40	1.0279	-0.0063	1.0520

Table XVI (A) (cont.)

DISTRIBUTION FUNCTIONS AND PERCUS-YEVICK EFFECTIVE
POTENTIAL FOR ARGON STATE 1

R(ANG.)	G(R)	C(R)	U EFF. PY (DEG.K)
8.45	1.0260	-0.0066	1.1137
8.50	1.0246	-0.0065	1.1012
8.55	1.0236	-0.0060	1.0177
8.60	1.0230	-0.0051	0.8682
8.65	1.0229	-0.0039	0.6595
8.70	1.0231	-0.0024	0.4002
8.75	1.0236	-0.0008	0.1003
8.80	1.0244	0.0014	-0.2292
8.85	1.0253	0.0034	-0.5767
8.90	1.0263	0.0055	-0.9305
8.95	1.0274	0.0076	-1.2790
9.00	1.0284	0.0095	-1.6115
9.05	1.0294	0.0113	-1.9182
9.10	1.0302	0.0129	-2.1904
9.15	1.0308	0.0143	-2.4206
9.20	1.0311	0.0154	-2.6025
9.25	1.0313	0.0161	-2.7310
9.30	1.0311	0.0165	-2.8022
9.35	1.0307	0.0166	-2.8135
9.40	1.0299	0.0163	-2.7638
9.45	1.0288	0.0156	-2.6534
9.50	1.0275	0.0146	-2.4841
9.55	1.0259	0.0133	-2.2593
9.60	1.0240	0.0117	-1.9839
9.65	1.0219	0.0098	-1.6645
9.70	1.0196	0.0077	-1.3089
9.75	1.0173	0.0054	-0.9257
9.80	1.0148	0.0031	-0.5247
9.85	1.0124	0.0007	-0.1158
9.90	1.0100	-0.0017	0.2908
9.95	1.0077	-0.0040	0.6853
10.00	1.0056	-0.0062	1.0581

Table XVI (B)

DISTRIBUTION FUNCTIONS AND PERCUS-YEVICK EFFECTIVE POTENTIAL FOR ARGON STATE 1R

R(ANG.)	G(R)	C(R)	U EFF. PY (DEG.K)
0.05	-0.1423	-2.4744	
0.10	-0.1249	-2.4496	
0.15	-0.0969	-2.4094	
0.20	-0.0597	-2.3554	
0.25	-0.0151	-2.2897	
0.30	0.0349	-2.2144	
0.35	0.0887	-2.1317	
0.40	0.1444	-2.0438	
0.45	0.2008	-1.9523	
0.50	0.2571	-1.8585	
0.55	0.3127	-1.7634	
0.60	0.3674	-1.6676	
0.65	0.4213	-1.5713	
0.70	0.4745	-1.4751	
0.75	0.5270	-1.3791	
0.80	0.5785	-1.2840	
0.85	0.6286	-1.1905	
0.90	0.6765	-1.0997	
0.95	0.7210	-1.0130	
1.00	0.7610	-0.9318	
1.05	0.7951	-0.8576	
1.10	0.8222	-0.7916	
1.15	0.8412	-0.7351	
1.20	0.8516	-0.6887	
1.25	0.8532	-0.6527	
1.30	0.8462	-0.6270	
1.35	0.8310	-0.6111	
1.40	0.8086	-0.6042	
1.45	0.7797	-0.6054	
1.50	0.7454	-0.6139	
1.55	0.7064	-0.6288	
1.60	0.6631	-0.6495	
1.65	0.6161	-0.6756	
1.70	0.5654	-0.7070	
1.75	0.5112	-0.7435	
1.80	0.4533	-0.7849	
1.85	0.3921	-0.8310	
1.90	0.3280	-0.8812	
1.95	0.2619	-0.9347	
2.00	0.1948	-0.9902	
2.05	0.1283	-1.0460	
2.10	0.0639	-1.1005	

Table XVI (B) (cont.)

DISTRIBUTION FUNCTIONS AND PERCUS-YEVICK EFFECTIVE POTENTIAL FOR ARGON STATE 1R

R(ANG.)	G(R)	C(R)	U EFF. PY (DEG.K)
2.15	0.0034	-1.1520	
2.20	-0.0517	-1.1988	
2.25	-0.1004	-1.2397	
2.30	-0.1420	-1.2741	
2.35	-0.1767	-1.3021	
2.40	-0.2052	-1.3242	
2.45	-0.2288	-1.3417	
2.50	-0.2490	-1.3561	
2.55	-0.2675	-1.3691	
2.60	-0.2857	-1.3820	
2.65	-0.3043	-1.3955	
2.70	-0.3233	-1.4095	
2.75	-0.3414	-1.4227	
2.80	-0.3562	-1.4326	
2.85	-0.3641	-1.4358	
2.90	-0.3607	-1.4278	
2.95	-0.3412	-1.4038	
3.00	-0.3006	-1.3587	
3.05	-0.2344	-1.2882	
3.10	-0.1394	-1.1889	
3.15	-0.0137	-1.0591	
3.20	0.1424	-0.8989	344.4697
3.25	0.3270	-0.7104	199.9220
3.30	0.5357	-0.4981	113.8375
3.35	0.7623	-0.2679	52.1454
3.40	0.9993	-0.0275	4.7026
3.45	1.2380	0.2144	-32.9375
3.50	1.4697	0.4491	-63.1503
3.55	1.6857	0.6680	-87.3776
3.60	1.8786	0.8635	-106.5829
3.65	2.0424	1.0296	-121.4616
3.70	2.1727	1.1622	-132.5532
3.75	2.2677	1.2591	-140.3038
3.80	2.3272	1.3205	-145.1045
3.85	2.3533	1.3482	-147.3163
3.90	2.3494	1.3458	-147.2852
3.95	2.3203	1.3180	-145.3509
4.00	2.2711	1.2700	-141.8503
4.05	2.2074	1.2074	-137.1145
4.10	2.1344	1.1354	-131.4624
4.15	2.0566	1.0585	-125.1890
4.20	1.9775	0.9803	-118.5521

Table XVI (B) (cont.)

DISTRIBUTION FUNCTIONS AND PERCUS-YEVICK EFFECTIVE
POTENTIAL FOR ARGON STATE 1R

R(ANG.)	G(R)	C(R)	U EFF. PY (DEG.K)
4.25	1.8998	0.9035	-111.7598
4.30	1.8251	0.8296	-104.9610
4.35	1.7541	0.7595	-98.2430
4.40	1.6869	0.6932	-91.6360
4.45	1.6231	0.6303	-85.1264
4.50	1.5621	0.5704	-78.6744
4.55	1.5034	0.5128	-72.2351
4.60	1.4466	0.4572	-65.7778
4.65	1.3917	0.4036	-59.3026
4.70	1.3389	0.3522	-52.8505
4.75	1.2888	0.3035	-46.5065
4.80	1.2421	0.2584	-40.3952
4.85	1.1996	0.2177	-34.6684
4.90	1.1622	0.1820	-29.4872
4.95	1.1303	0.1519	-24.9991
5.00	1.1044	0.1279	-21.3161
5.05	1.0844	0.1099	-18.4966
5.10	1.0700	0.0974	-16.5359
5.15	1.0607	0.0901	-15.3673
5.20	1.0556	0.0869	-14.8724
5.25	1.0537	0.0869	-14.8991
5.30	1.0541	0.0890	-15.2824
5.35	1.0558	0.0924	-15.8628
5.40	1.0580	0.0962	-16.5022
5.45	1.0601	0.0996	-17.0923
5.50	1.0616	0.1024	-17.5590
5.55	1.0624	0.1041	-17.8609
5.60	1.0623	0.1048	-17.9844
5.65	1.0614	0.1044	-17.9369
5.70	1.0600	0.1032	-17.7385
5.75	1.0580	0.1012	-17.4145
5.80	1.0558	0.0987	-16.9888
5.85	1.0534	0.0956	-16.4797
5.90	1.0509	0.0922	-15.8976
5.95	1.0484	0.0883	-15.2449
6.00	1.0457	0.0841	-14.5186
6.05	1.0430	0.0794	-13.7127
6.10	1.0400	0.0742	-12.8225
6.15	1.0369	0.0686	-11.8471
6.20	1.0336	0.0625	-10.7926
6.25	1.0303	0.0560	-9.6723
6.30	1.0270	0.0492	-8.5072

Table XVI (B) (cont.)

DISTRIBUTION FUNCTIONS AND PERCUS-YEVICK EFFECTIVE
POTENTIAL FOR ARGON STATE 1R

R(ANG.)	G(R)	C(R)	U EFF. PY (DEG.K)
6.35	1.0238	0.0424	-7.3238
6.40	1.0210	0.0356	-6.1521
6.45	1.0186	0.0291	-5.0224
6.50	1.0168	0.0230	-3.9630
6.55	1.0157	0.0174	-2.9973
6.60	1.0153	0.0125	-2.1428
6.65	1.0157	0.0082	-1.4104
6.70	1.0168	0.0047	-0.8053
6.75	1.0187	0.0019	-0.3276
6.80	1.0212	-0.0001	0.0253
6.85	1.0243	-0.0015	0.2580
6.90	1.0279	-0.0022	0.3749
6.95	1.0320	-0.0023	0.3802
7.00	1.0364	-0.0017	0.2771
7.05	1.0412	-0.0004	0.0691
7.10	1.0463	0.0014	-0.2401
7.15	1.0516	0.0039	-0.6445
7.20	1.0571	0.0069	-1.1358
7.25	1.0627	0.0104	-1.7022
7.30	1.0683	0.0143	-2.3282
7.35	1.0737	0.0184	-2.9953
7.40	1.0789	0.0227	-3.6828
7.45	1.0837	0.0270	-4.3686
7.50	1.0880	0.0312	-5.0311
7.55	1.0917	0.0350	-5.6504
7.60	1.0947	0.0386	-6.2089
7.65	1.0969	0.0416	-6.6930
7.70	1.0984	0.0441	-7.0926
7.75	1.0990	0.0460	-7.4014
7.80	1.0989	0.0473	-7.6165
7.85	1.0980	0.0480	-7.7375
7.90	1.0963	0.0481	-7.7660
7.95	1.0940	0.0476	-7.7044
8.00	1.0911	0.0466	-7.5555
8.05	1.0877	0.0450	-7.3225
8.10	1.0837	0.0430	-7.0083
8.15	1.0792	0.0405	-6.6161
8.20	1.0744	0.0375	-6.1500
8.25	1.0692	0.0341	-5.6149
8.30	1.0637	0.0304	-5.0176
8.35	1.0580	0.0263	-4.3671
8.40	1.0521	0.0221	-3.6743

Table XVI (B) (cont.)

DISTRIBUTION FUNCTIONS AND PERCUS-YEVICK EFFECTIVE
PUTENTIAL FOR ARGON STATE 1R

R (ANG.)	G(R)	C(R)	U EFF. PY (DEG.K)
8.45	1.0462	0.0177	-2.9523
8.50	1.0403	0.0132	-2.2160
8.55	1.0346	0.0088	-1.4810
8.60	1.0291	0.0045	-0.7635
8.65	1.0240	0.0005	-0.0786
8.70	1.0192	-0.0033	0.5595
8.75	1.0149	-0.0067	1.1390
8.80	1.0111	-0.0097	1.6505
8.85	1.0078	-0.0122	2.0868
8.90	1.0050	-0.0143	2.4435
8.95	1.0028	-0.0159	2.7179
9.00	1.0012	-0.0170	2.9095
9.05	1.0000	-0.0176	3.0185
9.10	0.9994	-0.0177	3.0467
9.15	0.9992	-0.0174	2.9964
9.20	0.9995	-0.0167	2.8708
9.25	1.0002	-0.0156	2.6739
9.30	1.0014	-0.0140	2.4108
9.35	1.0029	-0.0122	2.0880
9.40	1.0047	-0.0100	1.7132
9.45	1.0068	-0.0076	1.2955
9.50	1.0090	-0.0049	0.8454
9.55	1.0115	-0.0022	0.3740
9.60	1.0140	0.0006	-0.1069
9.65	1.0165	0.0034	-0.5855
9.70	1.0189	0.0062	-1.0507
9.75	1.0212	0.0088	-1.4925
9.80	1.0234	0.0112	-1.9024
9.85	1.0254	0.0134	-2.2733
9.90	1.0271	0.0153	-2.6002
9.95	1.0286	0.0170	-2.8795
10.00	1.0298	0.0183	-3.1091

Table. XVI (C)

DISTRIBUTION FUNCTIONS AND PERCUS-YEVICK EFFECTIVE
POTENTIAL FOR ARGON STATE 2

R(ANG.)	G(R)	C(R)	U EFF. PY (DEG.K)
0.05	0.0449	-2.7416	
0.10	0.0720	-2.7051	
0.15	0.1137	-2.6478	
0.20	0.1655	-2.5746	
0.25	0.2220	-2.4911	
0.30	0.2777	-2.4035	
0.35	0.3276	-2.3169	
0.40	0.3683	-2.2354	
0.45	0.3979	-2.1616	
0.50	0.4163	-2.0960	
0.55	0.4252	-2.0375	
0.60	0.4273	-1.9841	
0.65	0.4260	-1.9327	
0.70	0.4248	-1.8805	
0.75	0.4264	-1.8252	
0.80	0.4326	-1.7650	
0.85	0.4435	-1.7017	
0.90	0.4583	-1.6348	
0.95	0.4749	-1.5672	
1.00	0.4905	-1.5020	
1.05	0.5024	-1.4421	
1.10	0.5080	-1.3901	
1.15	0.5059	-1.3477	
1.20	0.4954	-1.3155	
1.25	0.4771	-1.2929	
1.30	0.4526	-1.2785	
1.35	0.4241	-1.2699	
1.40	0.3940	-1.2648	
1.45	0.3645	-1.2609	
1.50	0.3370	-1.2567	
1.55	0.3122	-1.2513	
1.60	0.2899	-1.2451	
1.65	0.2689	-1.2390	
1.70	0.2477	-1.2346	
1.75	0.2244	-1.2334	
1.80	0.1977	-1.2369	
1.85	0.1667	-1.2457	
1.90	0.1316	-1.2598	
1.95	0.0933	-1.2779	
2.00	0.0537	-1.2981	
2.05	0.0154	-1.3179	
2.10	-0.0193	-1.3348	

Table XVI (C) (cont.)

DISTRIBUTION FUNCTIONS AND PERCUS-YEVICK EFFECTIVE
POTENTIAL FOR ARGON STATE 2

R(ANG.)	G(R)	C(R)	U EFF. PY (DEG.K)
2.15	-0.0480	-1.3464	
2.20	-0.0693	-1.3512	
2.25	-0.0828	-1.3489	
2.30	-0.0893	-1.3401	
2.35	-0.0909	-1.3269	
2.40	-0.0901	-1.3119	
2.45	-0.0903	-1.2984	
2.50	-0.0945	-1.2893	
2.55	-0.1050	-1.2871	
2.60	-0.1230	-1.2929	
2.65	-0.1482	-1.3063	
2.70	-0.1785	-1.3252	
2.75	-0.2101	-1.3460	
2.80	-0.2381	-1.3636	
2.85	-0.2565	-1.3720	
2.90	-0.2592	-1.3651	
2.95	-0.2404	-1.3371	
3.00	-0.1951	-1.2831	
3.05	-0.1203	-1.1998	
3.10	-0.0143	-1.0858	
3.15	0.1222	-0.9417	
3.20	0.2867	-0.7700	225.8859
3.25	0.4746	-0.5751	137.4550
3.30	0.6801	-0.3630	74.0682
3.35	0.8962	-0.1406	25.2424
3.40	1.1153	0.0845	-13.6485
3.45	1.3301	0.3050	-45.0971
3.50	1.5332	0.5135	-70.6250
3.55	1.7183	0.7038	-91.2461
3.60	1.8801	0.8706	-107.6820
3.65	2.0148	1.0100	-120.4740
3.70	2.1197	1.1195	-130.0476
3.75	2.1939	1.1979	-136.7519
3.80	2.2375	1.2457	-140.8862
3.85	2.2522	1.2644	-142.7186
3.90	2.2406	1.2567	-142.4999
3.95	2.2062	1.2260	-140.4741
4.00	2.1531	1.1764	-136.8862
4.05	2.0856	1.1124	-131.9866
4.10	2.0081	1.0383	-126.0322
4.15	1.9249	0.9583	-119.2843
4.20	1.8395	0.8761	-112.0016

Table XVI (C) (cont.)

DISTRIBUTION FUNCTIONS AND PERCUS-YEVICK EFFECTIVE
POTENTIAL FOR ARGON STATE 2

R(ANG.)	G(R)	C(R)	U EFF. PY (DEG.K)
4.25	1.7552	0.7949	-104.4303
4.30	1.6742	0.7169	-96.7916
4.35	1.5982	0.6438	-89.2694
4.40	1.5279	0.5764	-82.0010
4.45	1.4638	0.5149	-75.0734
4.50	1.4055	0.4594	-68.5275
4.55	1.3528	0.4091	-62.3690
4.60	1.3049	0.3636	-56.5851
4.65	1.2616	0.3227	-51.1631
4.70	1.2223	0.2857	-46.1065
4.75	1.1872	0.2527	-41.4463
4.80	1.1563	0.2238	-37.2433
4.85	1.1299	0.1992	-33.5809
4.90	1.1083	0.1793	-30.5505
4.95	1.0918	0.1642	-28.2297
5.00	1.0804	0.1542	-26.6605
5.05	1.0739	0.1488	-25.8316
5.10	1.0718	0.1477	-25.6694
5.15	1.0732	0.1498	-26.0416
5.20	1.0771	0.1543	-26.7704
5.25	1.0823	0.1597	-27.6542
5.30	1.0874	0.1650	-28.4913
5.35	1.0914	0.1688	-29.1018
5.40	1.0933	0.1704	-29.3448
5.45	1.0927	0.1692	-29.1287
5.50	1.0892	0.1648	-28.4157
5.55	1.0829	0.1575	-27.2193
5.60	1.0743	0.1476	-25.5977
5.65	1.0641	0.1358	-23.6423
5.70	1.0528	0.1227	-21.4645
5.75	1.0412	0.1092	-19.1803
5.80	1.0301	0.0958	-16.8969
5.85	1.0198	0.0830	-14.7012
5.90	1.0107	0.0712	-12.6529
5.95	1.0030	0.0605	-10.7829
6.00	0.9966	0.0510	-9.0971
6.05	0.9915	0.0425	-7.5836
6.10	0.9875	0.0348	-6.2219
6.15	0.9845	0.0280	-4.9923
6.20	0.9825	0.0218	-3.8824
6.25	0.9813	0.0162	-2.8913
6.30	0.9810	0.0114	-2.0294

Table XVI (C) (cont.)

DISTRIBUTION FUNCTIONS AND PERCUS-YEVICK EFFECTIVE
POTENTIAL FOR ARGON STATE 2

R(ANG.)	G(R)	C(R)	U EFF. PY (DEG.K)
6.35	0.9818	0.0074	-1.3154
6.40	0.9838	0.0044	-0.7713
6.45	0.9869	0.0024	-0.4160
6.50	0.9914	0.0015	-0.2599
6.55	0.9971	0.0017	-0.3014
6.60	1.0040	0.0030	-0.5257
6.65	1.0119	0.0053	-0.9060
6.70	1.0205	0.0083	-1.4072
6.75	1.0296	0.0118	-1.9903
6.80	1.0390	0.0156	-2.6170
6.85	1.0483	0.0195	-3.2537
6.90	1.0573	0.0234	-3.8737
6.95	1.0659	0.0271	-4.4583
7.00	1.0740	0.0305	-4.9960
7.05	1.0814	0.0337	-5.4804
7.10	1.0881	0.0365	-5.9082
7.15	1.0940	0.0389	-6.2766
7.20	1.0990	0.0410	-6.5818
7.25	1.1032	0.0426	-6.8175
7.30	1.1063	0.0437	-6.9755
7.35	1.1084	0.0442	-7.0462
7.40	1.1095	0.0441	-7.0206
7.45	1.1093	0.0433	-6.8913
7.50	1.1081	0.0418	-6.6547
7.55	1.1058	0.0396	-6.3122
7.60	1.1024	0.0367	-5.8700
7.65	1.0982	0.0333	-5.3396
7.70	1.0932	0.0295	-4.7363
7.75	1.0876	0.0253	-4.0784
7.80	1.0816	0.0209	-3.3849
7.85	1.0754	0.0165	-2.6751
7.90	1.0690	0.0121	-1.9664
7.95	1.0627	0.0078	-1.2746
8.00	1.0565	0.0037	-0.6132
8.05	1.0506	-0.0000	0.0060
8.10	1.0450	-0.0035	0.5728
8.15	1.0398	-0.0065	1.0776
8.20	1.0351	-0.0091	1.5113
8.25	1.0309	-0.0112	1.8656
8.30	1.0273	-0.0127	2.1327
8.35	1.0244	-0.0137	2.3067
8.40	1.0221	-0.0142	2.3838

Table XVI (C) (cont.)

DISTRIBUTION FUNCTIONS AND PERCUS-YEVICK EFFECTIVE
POTENTIAL FOR ARGON STATE 2

R(ANG.)	G(R)	C(R)	U EFF. PY (DEG.K)
8.45	1.0205	-0.0140	2.3633
8.50	1.0195	-0.0133	2.2480
8.55	1.0192	-0.0121	2.0438
8.60	1.0193	-0.0104	1.7600
8.65	1.0200	-0.0083	1.4081
8.70	1.0211	-0.0059	1.0013
8.75	1.0225	-0.0033	0.5528
8.80	1.0242	-0.0004	0.0760
8.85	1.0260	0.0025	-0.4168
8.90	1.0279	0.0054	-0.9142
8.95	1.0299	0.0083	-1.4055
9.00	1.0318	0.0111	-1.8806
9.05	1.0337	0.0136	-2.3295
9.10	1.0354	0.0165	-2.7420
9.15	1.0368	0.0184	-3.1075
9.20	1.0380	0.0203	-3.4160
9.25	1.0389	0.0217	-3.6577
9.30	1.0393	0.0227	-3.8244
9.35	1.0394	0.0232	-3.9102
9.40	1.0390	0.0232	-3.9121
9.45	1.0381	0.0227	-3.8304
9.50	1.0369	0.0217	-3.6688
9.55	1.0353	0.0203	-3.4342
9.60	1.0334	0.0185	-3.1359
9.65	1.0312	0.0164	-2.7847
9.70	1.0288	0.0141	-2.3921
9.75	1.0264	0.0116	-1.9693
9.80	1.0238	0.0090	-1.5267
9.85	1.0213	0.0063	-1.0737
9.90	1.0188	0.0036	-0.6188
9.95	1.0163	0.0010	-0.1701
10.00	1.0140	-0.0015	0.2644

Table XVI (D)

DISTRIBUTION FUNCTIONS AND PERCUS-YEVICK EFFECTIVE
POTENTIAL FOR ARGON STATE 3

R(ANG.)	G(R)	C(R)	U EFF. PY (DEG.K)
0.05	0.1054	-1.6708	
0.10	0.1242	-1.6474	
0.15	0.1543	-1.6097	
0.20	0.1939	-1.5598	
0.25	0.2407	-1.4998	
0.30	0.2926	-1.4323	
0.35	0.3473	-1.3598	
0.40	0.4028	-1.2844	
0.45	0.4578	-1.2078	
0.50	0.5114	-1.1311	
0.55	0.5633	-1.0550	
0.60	0.6135	-0.9797	
0.65	0.6624	-0.9049	
0.70	0.7105	-0.8306	
0.75	0.7581	-0.7566	
0.80	0.8052	-0.6831	
0.85	0.8515	-0.6107	
0.90	0.8963	-0.5401	
0.95	0.9383	-0.4729	
1.00	0.9762	-0.4103	
1.05	1.0086	-0.3542	
1.10	1.0339	-0.3059	
1.15	1.0512	-0.2668	
1.20	1.0595	-0.2372	
1.25	1.0587	-0.2180	
1.30	1.0490	-0.2088	
1.35	1.0309	-0.2091	
1.40	1.0053	-0.2179	
1.45	0.9733	-0.2344	
1.50	0.9357	-0.2574	
1.55	0.8934	-0.2863	
1.60	0.8468	-0.3204	
1.65	0.7964	-0.3595	
1.70	0.7420	-0.4034	
1.75	0.6837	-0.4522	
1.80	0.6214	-0.5058	
1.85	0.5552	-0.5641	
1.90	0.4856	-0.6268	
1.95	0.4134	-0.6923	
2.00	0.3398	-0.7600	
2.05	0.2665	-0.8280	
2.10	0.1951	-0.8946	

Table XVI (D) (cont.)

DISTRIBUTION FUNCTIONS AND PERCUS-YEVICK EFFECTIVE
POTENTIAL FOR ARGON STATE 3

R(ANG.)	G(R)	C(R)	U EFF. PY (DEG.K)
2.15	0.1274	-0.9578	
2.20	0.0649	-1.0163	
2.25	0.0036	-1.0688	
2.30	-0.0410	-1.1150	
2.35	-0.0843	-1.1550	
2.40	-0.1220	-1.1897	
2.45	-0.1557	-1.2205	
2.50	-0.1870	-1.2489	
2.55	-0.2173	-1.2765	
2.60	-0.2477	-1.3045	
2.65	-0.2785	-1.3325	
2.70	-0.3089	-1.3602	
2.75	-0.3367	-1.3854	
2.80	-0.3586	-1.4048	
2.85	-0.3704	-1.4141	
2.90	-0.3669	-1.4081	
2.95	-0.3430	-1.3816	
3.00	-0.2936	-1.3297	
3.05	-0.2148	-1.2484	
3.10	-0.1040	-1.1353	
3.15	0.0392	-0.9897	
3.20	0.2134	-0.8132	272.0000
3.25	0.4147	-0.6098	156.5905
3.30	0.6373	-0.3851	81.8535
3.35	0.8735	-0.1470	26.9268
3.40	1.1147	0.0960	-15.5962
3.45	1.3515	0.3345	-49.2459
3.50	1.5750	0.5596	-76.0120
3.55	1.7771	0.7631	-97.1527
3.60	1.9511	0.9383	-113.5386
3.65	2.0922	1.0805	-125.8206
3.70	2.1930	1.1872	-134.5201
3.75	2.2679	1.2580	-140.0826
3.80	2.3038	1.2945	-142.9095
3.85	2.3088	1.3001	-143.3790
3.90	2.2877	1.2793	-141.8570
3.95	2.2457	1.2377	-138.7023
4.00	2.1885	1.1806	-134.2646
4.05	2.1212	1.1134	-128.8786
4.10	2.0484	1.0408	-122.8516
4.15	1.9740	0.9664	-116.4517
4.20	1.9008	0.8930	-109.8945

Table XVI (D) (cont.)

DISTRIBUTION FUNCTIONS AND PERCUS-YEVICK EFFECTIVE
POTENTIAL FOR ARGON STATE 3

R(ANG.)	G(R)	C(R)	U EFF. PY (DEG.K)
4.25	1.8299	0.8224	-103.3348
4.30	1.7627	0.7552	-96.8648
4.35	1.6991	0.6917	-90.5202
4.40	1.6389	0.6316	-84.2937
4.45	1.5815	0.5744	-78.1539
4.50	1.5264	0.5196	-72.0655
4.55	1.4733	0.4670	-66.0084
4.60	1.4223	0.4165	-59.9916
4.65	1.3736	0.3684	-54.0621
4.70	1.3277	0.3232	-48.3043
4.75	1.2853	0.2817	-42.8343
4.80	1.2472	0.2445	-37.7853
4.85	1.2139	0.2123	-33.2901
4.90	1.1859	0.1855	-29.4606
4.95	1.1634	0.1643	-26.3706
5.00	1.1463	0.1486	-24.0435
5.05	1.1342	0.1379	-22.4487
5.10	1.1263	0.1315	-21.5073
5.15	1.1219	0.1287	-21.1041
5.20	1.1202	0.1285	-21.1049
5.25	1.1201	0.1301	-21.3732
5.30	1.1210	0.1325	-21.7852
5.35	1.1223	0.1353	-22.2389
5.40	1.1234	0.1376	-22.6602
5.45	1.1240	0.1398	-23.0021
5.50	1.1242	0.1412	-23.2415
5.55	1.1238	0.1419	-23.3727
5.60	1.1228	0.1419	-23.4008
5.65	1.1215	0.1414	-23.3339
5.70	1.1198	0.1403	-23.1781
5.75	1.1178	0.1386	-22.9333
5.80	1.1154	0.1364	-22.5918
5.85	1.1125	0.1335	-22.1396
5.90	1.1090	0.1298	-21.5583
5.95	1.1049	0.1252	-20.8296
6.00	1.1001	0.1196	-19.9384
6.05	1.0945	0.1130	-18.8770
6.10	1.0881	0.1054	-17.6468
6.15	1.0810	0.0969	-16.2594
6.20	1.0734	0.0876	-14.7365
6.25	1.0654	0.0777	-13.1074
6.30	1.0572	0.0674	-11.4070

Table XVI (D) (cont.)

DISTRIBUTION FUNCTIONS AND PERCUS-YEVICK EFFECTIVE
POTENTIAL FOR ARGON STATE 3

R(ANG.)	G(R)	C(R)	U EFF. PY (DEG.K)
6.35	1.0491	0.0570	-9.6719
6.40	1.0413	0.0467	-7.9379
6.45	1.0339	0.0366	-6.2373
6.50	1.0270	0.0269	-4.5973
6.55	1.0208	0.0178	-3.0395
6.60	1.0152	0.0092	-1.5807
6.65	1.0104	0.0014	-0.2342
6.70	1.0063	-0.0058	0.9887
6.75	1.0029	-0.0121	2.0771
6.80	1.0004	-0.0176	3.0191
6.85	0.9986	-0.0222	3.8017
6.90	0.9978	-0.0257	4.4115
6.95	0.9978	-0.0283	4.8358
7.00	0.9988	-0.0296	5.0643
7.05	1.0008	-0.0299	5.0912
7.10	1.0037	-0.0289	4.9170
7.15	1.0074	-0.0268	4.5491
7.20	1.0120	-0.0237	4.0025
7.25	1.0173	-0.0196	3.2988
7.30	1.0231	-0.0147	2.4649
7.35	1.0293	-0.0091	1.5310
7.40	1.0357	-0.0032	0.5284
7.45	1.0421	0.0031	-0.5123
7.50	1.0484	0.0094	-1.5632
7.55	1.0544	0.0157	-2.5998
7.60	1.0601	0.0218	-3.6015
7.65	1.0653	0.0276	-4.5515
7.70	1.0700	0.0331	-5.4360
7.75	1.0742	0.0380	-6.2434
7.80	1.0777	0.0425	-6.9632
7.85	1.0805	0.0463	-7.5853
7.90	1.0826	0.0495	-8.0998
7.95	1.0839	0.0519	-8.4966
8.00	1.0844	0.0535	-8.7661
8.05	1.0841	0.0543	-8.8997
8.10	1.0828	0.0542	-8.8906
8.15	1.0807	0.0532	-8.7350
8.20	1.0777	0.0512	-8.4327
8.25	1.0739	0.0484	-7.9875
8.30	1.0693	0.0448	-7.4077
8.35	1.0640	0.0404	-6.7054
8.40	1.0581	0.0354	-5.8963

Table XVI (D) (cont.)

DISTRIBUTION FUNCTIONS AND PERCUS-YEVICK EFFECTIVE
POTENTIAL FOR ARGON STATE 3

R(ANG.)	G(R)	C(R)	U EFF. PY (DEG.K)
8.45	1.0518	0.0299	-4.9987
8.50	1.0452	0.0241	-4.0324
8.55	1.0383	0.0179	-3.0176
8.60	1.0314	0.0117	-1.9744
8.65	1.0246	0.0054	-0.9218
8.70	1.0178	-0.0007	0.1224
8.75	1.0113	-0.0067	1.1420
8.80	1.0051	-0.0124	2.1218
8.85	0.9995	-0.0177	3.0476
8.90	0.9939	-0.0227	3.9055
8.95	0.9890	-0.0271	4.6823
9.00	0.9847	-0.0310	5.3648
9.05	0.9810	-0.0342	5.9406
9.10	0.9780	-0.0368	6.3984
9.15	0.9757	-0.0387	6.7287
9.20	0.9742	-0.0397	6.9245
9.25	0.9734	-0.0400	6.9823
9.30	0.9734	-0.0396	6.9022
9.35	0.9741	-0.0384	6.6883
9.40	0.9756	-0.0364	6.3487
9.45	0.9777	-0.0339	5.8948
9.50	0.9803	-0.0307	5.3405
9.55	0.9835	-0.0271	4.7016
9.60	0.9870	-0.0230	3.9949
9.65	0.9909	-0.0187	3.2368
9.70	0.9949	-0.0141	2.4433
9.75	0.9992	-0.0094	1.6293
9.80	1.0035	-0.0047	0.8085
9.85	1.0078	0.0000	-0.0066
9.90	1.0120	0.0047	-0.8045
9.95	1.0161	0.0092	-1.5744
10.00	1.0201	0.0135	-2.3059

Table XVII

PAIR POTENTIAL U(R) AS DETERMINED BY EACH OF THE FOUR
ARGON STATES (UNITS ARE DEGREES KELVIN)

R(ANG.)	STATE 1	STATE 1R	STATE 2	STATE 3
3.20	286.9756	340.1746	219.3322	269.1958
3.25	175.2202	195.8046	131.1770	153.9045
3.30	100.5678	109.8942	68.0601	79.2830
3.35	44.7503	48.3721	19.4971	24.4687
3.40	0.9510	1.0945	-19.1567	-17.9528
3.45	-34.2000	-36.4122	-50.4029	-51.5159
3.50	-62.5954	-66.4962	-75.7300	-78.1961
3.55	-85.4604	-90.5964	-96.1534	-99.2522
3.60	-103.6488	-109.6764	-112.3953	-115.5551
3.65	-117.7954	-124.4327	-124.9981	-127.7561
3.70	-128.4013	-135.4050	-134.3876	-136.3769
3.75	-135.8862	-143.0409	-140.9286	-141.8695
3.80	-140.6305	-147.7450	-144.9126	-144.6322
3.85	-142.9549	-149.8616	-146.5974	-145.0384
3.90	-143.1804	-149.7370	-146.2341	-143.4546
3.95	-141.6200	-147.7115	-144.0674	-140.2396
4.00	-138.5825	-144.1219	-140.3424	-135.7433
4.05	-134.3719	-139.2997	-135.3097	-130.3003
4.10	-129.2849	-133.5659	-129.2366	-124.2225
4.15	-123.6018	-127.2187	-122.3747	-117.7739
4.20	-117.5655	-120.5098	-114.9808	-111.1692
4.25	-111.3863	-113.6473	-107.3014	-104.5631
4.30	-105.2257	-106.7802	-99.5577	-98.0482
4.35	-99.1918	-99.9959	-91.9337	-91.6600
4.40	-93.3394	-93.3248	-84.5670	-85.3915
4.45	-87.6788	-86.7543	-77.5486	-79.2129
4.50	-82.1853	-80.2450	-70.9146	-73.0868
4.55	-76.8156	-73.7500	-64.6707	-66.9931
4.60	-71.5272	-67.2388	-58.8041	-60.9410
4.65	-66.2926	-60.7114	-53.3021	-54.9772
4.70	-61.1101	-54.2089	-48.1683	-49.1864
4.75	-56.0094	-47.8162	-43.4336	-43.6845
4.80	-51.0520	-41.6577	-39.1585	-38.6047
4.85	-46.3247	-35.8856	-35.4268	-34.0798
4.90	-41.9281	-30.6606	-32.3295	-30.2217
4.95	-37.9613	-26.1302	-29.9443	-27.1042
5.00	-34.5056	-22.4066	-28.3131	-24.7505
5.05	-31.6102	-19.5480	-27.4245	-23.1303
5.10	-29.2816	-17.5497	-27.2034	-22.1636
5.15	-27.4798	-16.3433	-27.5178	-21.7357
5.20	-26.1259	-15.8119	-28.1911	-21.7127
5.25	-25.1099	-15.8037	-29.0219	-21.9584

Table XVII (cont.)

PAIR POTENTIAL U(R) AS DETERMINED BY EACH OF THE FOUR
ARGON STATES (UNITS ARE DEGREES KELVIN)

R(ANG.)	STATE 1	STATE 1R	STATE 2	STATE 3
5.30	-24.3049	-16.1534	-29.8081	-22.3485
5.35	-23.5837	-16.7017	-30.3699	-22.7814
5.40	-22.8326	-17.3102	-30.5661	-23.1828
5.45	-21.9621	-17.8708	-30.3017	-23.5040
5.50	-20.9108	-18.3062	-29.5415	-23.7232
5.55	-19.6566	-18.5783	-28.3003	-23.8352
5.60	-18.2054	-18.6735	-26.6359	-23.8449
5.65	-16.5894	-18.5990	-24.6398	-23.7606
5.70	-14.8598	-18.3740	-22.4230	-23.5882
5.75	-13.0783	-18.0262	-20.1016	-23.3274
5.80	-11.3078	-17.5763	-17.7774	-22.9685
5.85	-9.6037	-17.0414	-15.5430	-22.4997
5.90	-8.0150	-16.4347	-13.4579	-21.9027
5.95	-6.5727	-15.7589	-11.5532	-21.1591
6.00	-5.2932	-15.0105	-9.8344	-20.2539
6.05	-4.1794	-14.1837	-8.2895	-19.1790
6.10	-3.2257	-13.2736	-6.8966	-17.9354
6.15	-2.4200	-12.2779	-5.6329	-16.5334
6.20	-1.7510	-11.2018	-4.4909	-14.9968
6.25	-1.2133	-10.0612	-3.4696	-13.3548
6.30	-0.8033	-8.8769	-2.5791	-11.6421
6.35	-0.5219	-7.6754	-1.8382	-9.8955
6.40	-0.3725	-6.4865	-1.2686	-8.1507
6.45	-0.3589	-5.3407	-0.8867	-6.4387
6.50	-0.4805	-4.2641	-0.7030	-4.7868
6.55	-0.7347	-3.2808	-0.7185	-3.2179
6.60	-1.1131	-2.4098	-0.9184	-1.7488
6.65	-1.5998	-1.6620	-1.2758	-0.3925
6.70	-2.1728	-1.0423	-1.7555	0.8397
6.75	-2.8064	-0.5509	-2.3184	1.9367
6.80	-3.4733	-0.1851	-2.9249	2.8873
6.85	-4.1459	0.0605	-3.5422	3.6782
6.90	-4.8011	0.1897	-4.1440	4.2959
6.95	-5.4192	0.2066	-4.7116	4.7274
7.00	-5.9854	0.1144	-5.2332	4.9628
7.05	-6.4890	-0.0834	-5.7025	4.9962
7.10	-6.9235	-0.3829	-6.1162	4.8280
7.15	-7.2849	-0.7783	-6.4724	4.4653
7.20	-7.5715	-1.2618	-6.7662	3.9236
7.25	-7.7807	-1.8209	-6.9911	3.2245
7.30	-7.9101	-2.4400	-7.1389	2.3950
7.35	-7.9571	-3.1006	-7.2001	1.4652

Table XVII (cont.)

PAIR POTENTIAL U(R) AS DETERMINED BY EACH OF THE FOUR
ARGON STATES   (UNITS ARE DEGREES KELVIN)

R(ANG.)	STATE 1	STATE 1R	STATE 2	STATE 3
7.40	-7.9190	-3.7819	-7.1654	0.4665
7.45	-7.7931	-4.4620	-7.0278	-0.5707
7.50	-7.5783	-5.1192	-6.7845	-1.6187
7.55	-7.2759	-5.7341	-6.4355	-2.6525
7.60	-6.8885	-6.2885	-5.9872	-3.6516
7.65	-6.4228	-6.7687	-5.4510	-4.5992
7.70	-5.8884	-7.1645	-4.8423	-5.4814
7.75	-5.2982	-7.4698	-4.1791	-6.2865
7.80	-4.6670	-7.6816	-3.4810	-7.0043
7.85	-4.0112	-7.7996	-2.7671	-7.6246
7.90	-3.3478	-7.8254	-2.0545	-8.1375
7.95	-2.6925	-7.7613	-1.3590	-8.5327
8.00	-2.0603	-7.6101	-0.6941	-8.8007
8.05	-1.4643	-7.3748	-0.0715	-8.9329
8.10	-0.9153	-7.0584	0.4985	-8.9224
8.15	-0.4224	-6.6642	1.0062	-8.7656
8.20	0.0074	-6.1962	1.4426	-8.4621
8.25	0.3690	-5.6593	1.7994	-8.0158
8.30	0.6584	-5.0605	2.0690	-7.4350
8.35	0.8733	-4.4083	2.2453	-6.7317
8.40	1.0123	-3.7140	2.3247	-5.9216
8.45	1.0755	-2.9906	2.3064	-5.0231
8.50	1.0644	-2.2528	2.1931	-4.0558
8.55	0.9822	-1.5166	1.9908	-3.0402
8.60	0.8339	-0.7978	1.7088	-1.9963
8.65	0.6264	-0.1118	1.3588	-0.9430
8.70	0.3683	0.5275	0.9536	0.1020
8.75	0.0694	1.1081	0.5068	1.1223
8.80	-0.2591	1.6206	0.0315	2.1028
8.85	-0.6056	2.0580	-0.4598	3.0292
8.90	-0.9584	2.4156	-0.9557	3.8877
8.95	-1.3059	2.6910	-1.4457	4.6651
9.00	-1.6376	2.8834	-1.9195	5.3481
9.05	-1.9434	2.9933	-2.3671	5.9245
9.10	-2.2148	3.0223	-2.7784	6.3828
9.15	-2.4443	2.9728	-3.1428	6.7136
9.20	-2.6254	2.8479	-3.4501	6.9099
9.25	-2.7531	2.6517	-3.6907	6.9682
9.30	-2.8236	2.3894	-3.8564	6.8885
9.35	-2.8343	2.0672	-3.9412	6.6751
9.40	-2.7840	1.6931	-3.9421	6.3359
9.45	-2.6729	1.2760	-3.8594	5.8823

Table XVII (cont.)

PAIR POTENTIAL U(R) AS DETERMINED BY EACH OF THE FOUR
ARGON STATES   (UNITS ARE DEGREES KELVIN)

R(ANG.)	STATE 1	STATE 1R	STATE 2	STATE 3
9.50	-2.5030	0.8265	-3.6970	5.3284
9.55	-2.2776	0.3557	-3.4615	4.6899
9.60	-2.0017	-0.1246	-3.1624	3.9835
9.65	-1.6817	-0.6027	-2.8104	3.2258
9.70	-1.3255	-1.0674	-2.4170	2.4327
9.75	-0.9419	-1.5087	-1.9934	1.6190
9.80	-0.5404	-1.9181	-1.5501	0.7985
9.85	-0.1311	-2.2886	-1.0964	-0.0163
9.90	0.2760	-2.6150	-0.6408	-0.8139
9.95	0.6710	-2.8939	-0.1915	-1.5835
10.00	1.0442	-3.1230	0.2437	-2.3148

Table XVIII

Experimental Pair Potential Characteristics for Each State

STATE	$n(g/cm^3)$	$\varsigma(A^\circ)$	$\epsilon(^\circ K)$	$r_{min}(A^\circ)$
1	.2087	3.401 ± .038	143.2 ± 10.2	3.89 ± .09
2	.3111	3.375 ± .023	146.6 ± 6.8	3.87 ± .05
3	.1331	3.379 ± .050	145.1 ± 16.0	3.83 ± .13
1R	.2087	3.402 ± .035	149.9 ± 10.2	3.87 ± .07

Table XIX

COMPARISON OF EFFECTIVE POTENTIALS FROM PINGS TREATMENT
AND FROM THE PERCUS-YEVICK EQUATION   for state 2

R(ANG.)	U EFF. (PY)	U EFF. (PINGS)
3.20	225.89	224.40
3.25	137.46	136.03
3.30	74.07	72.71
3.35	25.24	23.96
3.40	-13.65	-14.85
3.45	-45.10	-46.21
3.50	-70.62	-71.64
3.55	-91.25	-92.17
3.60	-107.68	-108.52
3.65	-120.47	-121.21
3.70	-130.05	-130.70
3.75	-136.75	-137.32
3.80	-140.89	-141.39
3.85	-142.72	-143.16
3.90	-142.50	-142.87
3.95	-140.47	-140.78
4.00	-136.89	-137.12
4.05	-131.99	-132.16
4.10	-126.03	-126.17
4.15	-119.28	-119.41
4.20	-112.00	-112.10
4.25	-104.43	-104.50
4.30	-96.79	-96.84
4.35	-89.27	-89.29
4.40	-82.00	-82.00
4.45	-75.07	-75.09
4.50	-68.53	-68.57
4.55	-62.37	-62.42
4.60	-56.59	-56.66
4.65	-51.16	-51.25
4.70	-46.11	-46.20
4.75	-41.45	-41.56
4.80	-37.24	-37.41
4.85	-33.58	-33.79
4.90	-30.55	-30.80
4.95	-28.23	-28.52
5.00	-26.66	-26.99
5.05	-25.83	-26.21
5.10	-25.67	-26.09
5.15	-26.04	-26.52
5.20	-26.77	-27.31
5.25	-27.65	-28.25

Table XIX (cont.)

COMPARISON OF EFFECTIVE POTENTIALS FROM PINGS TREATMENT
AND FROM THE PERCUS-YEVICK EQUATION   FOR STATE2

R(ANG.)	U EFF. (PY)	U EFF. (PINGS)
5.30	-28.49	-29.14
5.35	-29.10	-29.81
5.40	-29.34	-30.11
5.45	-29.13	-29.94
5.50	-28.42	-29.27
5.55	-27.22	-28.12
5.60	-25.60	-26.54
5.65	-23.64	-24.63
5.70	-21.46	-22.50
5.75	-19.18	-20.26
5.80	-16.90	-17.98
5.85	-14.70	-15.78
5.90	-12.65	-13.74
5.95	-10.78	-11.87
6.00	-9.10	-10.19
6.05	-7.58	-8.69
6.10	-6.22	-7.32
6.15	-4.99	-6.04
6.20	-3.88	-4.89
6.25	-2.89	-3.85
6.30	-2.03	-2.94
6.35	-1.32	-2.19
6.40	-0.77	-1.60
6.45	-0.42	-1.18
6.50	-0.26	-0.96
6.55	-0.30	-0.94
6.60	-0.53	-1.09
6.65	-0.91	-1.40
6.70	-1.41	-1.82
6.75	-1.99	-2.33
6.80	-2.62	-2.90
6.85	-3.25	-3.49
6.90	-3.87	-4.07
6.95	-4.46	-4.61
7.00	-5.00	-5.10
7.05	-5.48	-5.53
7.10	-5.91	-5.91
7.15	-6.28	-6.24
7.20	-6.58	-6.50
7.25	-6.82	-6.70
7.30	-6.98	-6.82
7.35	-7.05	-6.86

Table XIX (cont.)

COMPARISON OF EFFECTIVE POTENTIALS FROM PINGS TREATMENT
AND FROM THE PERCUS-YEVICK EQUATION   FOR STATE 2

R(ANG.)	U EFF. (PY)	U EFF. (PINGS)
7.40	-7.02	-6.81
7.45	-6.89	-6.67
7.50	-6.65	-6.43
7.55	-6.31	-6.08
7.60	-5.87	-5.65
7.65	-5.34	-5.12
7.70	-4.74	-4.53
7.75	-4.08	-3.89
7.80	-3.38	-3.21
7.85	-2.68	-2.52
7.90	-1.97	-1.82
7.95	-1.27	-1.15
8.00	-0.61	-0.51
8.05	0.01	0.09
8.10	0.57	0.64
8.15	1.08	1.14
8.20	1.51	1.56
8.25	1.87	1.90
8.30	2.13	2.16
8.35	2.31	2.33
8.40	2.38	2.40
8.45	2.36	2.37
8.50	2.25	2.25
8.55	2.04	2.04
8.60	1.76	1.76
8.65	1.41	1.40
8.70	1.00	0.99
8.75	0.55	0.54
8.80	0.08	0.06
8.85	-0.42	-0.43
8.90	-0.91	-0.93
8.95	-1.41	-1.42
9.00	-1.88	-1.89
9.05	-2.33	-2.34
9.10	-2.74	-2.76
9.15	-3.11	-3.12
9.20	-3.42	-3.43
9.25	-3.66	-3.67
9.30	-3.82	-3.83
9.35	-3.91	-3.92
9.40	-3.91	-3.92
9.45	-3.83	-3.84

Table XIX (cont.)

COMPARISON OF EFFECTIVE POTENTIALS FROM PINGS TREATMENT
AND FROM THE PERCUS-YEVICK EQUATION FOR STATE 2

R(ANG.)	U EFF. (PY)	U EFF. (PINGS)
9.50	-3.67	-3.67
9.55	-3.43	-3.44
9.60	-3.14	-3.14
9.65	-2.78	-2.79
9.70	-2.39	-2.39
9.75	-1.97	-1.97
9.80	-1.53	-1.52
9.85	-1.07	-1.07
9.90	-0.62	-0.61
9.95	-0.17	-0.16
10.00	0.26	0.27

Table XX

EXPERIMENTAL INTERMOLECULAR PAIR POTENTIAL FOR ARGON

R(ANG.)	U(R)(DEG. K)	R(ANG.)	U(R)(DEG. K)
3.20	272.6904	5.35	-24.2430
3.25	161.0105	5.40	-24.3413
3.30	87.8011	5.45	-24.2204
3.35	33.3762	5.50	-23.8307
3.40	-9.1948	5.55	-23.1619
3.45	-43.2612	5.60	-22.2340
3.50	-70.6928	5.65	-21.0907
3.55	-92.6959	5.70	-19.7904
3.60	-110.1062	5.75	-18.3960
3.65	-123.5424	5.80	-16.9635
3.70	-133.4913	5.85	-15.5420
3.75	-140.3641	5.90	-14.1651
3.80	-144.5181	5.95	-12.8494
3.85	-146.2648	6.00	-11.5978
3.90	-145.9134	6.05	-10.4039
3.95	-143.7659	6.10	-9.2573
4.00	-140.1210	6.15	-8.1482
4.05	-135.2751	6.20	-7.0757
4.10	-129.5223	6.25	-6.0467
4.15	-123.1345	6.30	-5.0745
4.20	-116.3572	6.35	-4.1780
4.25	-109.4049	6.40	-3.3786
4.30	-102.4468	6.45	-2.6954
4.35	-95.6023	6.50	-2.1426
4.40	-88.9405	6.55	-1.7292
4.45	-82.4893	6.60	-1.4551
4.50	-76.2402	6.65	-1.3114
4.55	-70.1704	6.70	-1.2829
4.60	-64.2590	6.75	-1.3512
4.65	-58.5022	6.80	-1.4962
4.70	-52.9235	6.85	-1.7004
4.75	-47.5800	6.90	-1.9496
4.80	-42.5592	6.95	-2.2335
4.85	-37.9695	7.00	-2.5450
4.90	-33.9246	7.05	-2.8792
4.95	-30.5236	7.10	-3.2323
5.00	-27.8320	7.15	-3.6003
5.05	-25.8671	7.20	-3.9766
5.10	-24.5899	7.25	-4.3519
5.15	-23.9086	7.30	-4.7147
5.20	-23.6915	7.35	-5.0519
5.25	-23.7813	7.40	-5.3494
5.30	-24.0152	7.45	-5.5942

Table XX (cont.)

EXPERIMENTAL INTERMOLECULAR PAIR POTENTIAL FOR ARGON

R(ANG.)	U(R)(DEG. K)	R(ANG.)	U(R)(DEG. K)
7.50	-5.7754	9.65	-1.0698
7.55	-5.8848	9.70	-1.0765
7.60	-5.9177	9.75	-1.0633
7.65	-5.8740	9.80	-1.0318
7.70	-5.7569	9.85	-0.9845
7.75	-5.5728	9.90	-0.9237
7.80	-5.3300	9.95	-0.8522
7.85	-5.0378	10.00	-0.7731
7.90	-4.7053		
7.95	-4.3410		
8.00	-3.9526		
8.05	-3.5468		
8.10	-3.1298		
8.15	-2.7073		
8.20	-2.2854		
8.25	-1.8700		
8.30	-1.4678		
8.35	-1.0854		
8.40	-0.7298		
8.45	-0.4071		
8.50	-0.1226		
8.55	0.1197		
8.60	0.3174		
8.65	0.4696		
8.70	0.5770		
8.75	0.6416		
8.80	0.6660		
8.85	0.6537		
8.90	0.6085		
8.95	0.5341		
9.00	0.4349		
9.05	0.3148		
9.10	0.1784		
9.15	0.0304		
9.20	-0.1244		
9.25	-0.2807		
9.30	-0.4335		
9.35	-0.5777		
9.40	-0.7089		
9.45	-0.8232		
9.50	-0.9178		
9.55	-0.9909		
9.60	-1.0415		

Table XXI

Error Limits on the Structure Factor for Each of the Four
Argon States due to Statistical Imprecision of the
Scattering Data

	error limits			
$s(\overset{\circ}{A}^{-1})$	state 1	state 1R	state 2	state 3
.15	.0200	.0200	.0300	.0300
.46	.0090	.0080	.0100	.0108
.80	.0064	.0072	.0064	.0090
1.14	.0064	.0072	.0082	.0082
1.51	.0074	.0082	.0082	.0082
1.92	.0076	.0068	.0084	.0092
2.44	.0076	.0070	.0070	.0084
3.12	.0082	.0082	.0070	.0086
4.08	.0094	.0076	.0076	.0096
5.32	.0088	.0092	.0088	.0116
6.64	.0120	.0124	.0108	.0148
7.94	.0130	.0126	.0118	.0172

Table XXII

Total Error Limits on the Structure Factor for Each of the
Four Argon States

feature	$s(A^{\circ -1})$	state 1	state 1R	state 2	state 3
approach to s=0	.22	.0268	.0268	.0298	.0298
first crossover	.45	.0218	.0220	.0226	.0226
first valley	.80	.0210	.0212	.0208	.0220
second crossover	1.40	.0216	.0216	.0216	.0218
first peak	1.80	.0214	.0214	.0218	.0218
third crossover	2.30	.0214	.0214	.0212	.0218
second valley	2.80	.0214	.0214	.0212	.0218
fourth crossover	3.41	.0222	.0228	.0214	.0232

Table XXIII

Error Limits on the Pair Potential as Determined from Each
of the Four Argon States

	± error limits (°K)		
r(A°)	state 1 and state 1R	state 2	state 3
3.20	91.4	60.6	133.6
3.25	31.2	20.7	45.6
3.40	13.3	8.7	21.2
3.50	9.2	6.1	14.6
3.75	6.0	4.0	9.7
3.85	5.1	3.4	8.0
4.00	4.6	3.1	7.4
4.25	4.8	3.1	7.7
4.50	6.1	4.0	9.8
4.75	7.5	5.0	11.9
5.00	7.1	4.8	11.4
5.25	5.9	3.9	9.4
5.50	5.9	3.9	9.4
5.75	5.7	3.8	9.1
6.00	5.1	3.4	8.0
6.25	4.1	3.7	7.5
6.50	4.1	2.7	6.7
6.75	3.3	1.9	5.5
7.00	3.9	2.7	5.1
7.25	4.4	3.0	6.0
7.50	4.8	3.3	7.7
7.75	4.5	2.9	6.9
8.00	3.2	2.2	5.1
8.25	2.8	1.9	4.5
8.50	3.7	2.4	5.7
8.75	3.8	2.5	6.1
9.00	3.2	2,1	5.0
9.25	2.1	1.4	3.3
9.50	2.8	1.9	4.5
9.75	3.6	2.1	5.0
10.00	2.8	1.8	4.3

Table XXIV

Error Limits on the Average Pair Potential

r(A°)	± error limits (°K)
3.20	86.7
3.25	29.6
3.40	12.9
3.50	8.9
3.75	5.9
3.85	4.9
4.00	4.5
4.25	4.7
4.50	5.9
4.75	7.3
5.00	6.9
5.25	5.7
5.50	5.7
5.75	5.5
6.00	4.9
6.25	4.6
6.50	4.0
6.75	3.1
7.00	3.7
7.25	4.2
7.50	4.6
7.75	4.3
8.00	3.1
8.25	2.7
8.50	3.5
8.75	3.6
9.00	3.1
9.25	2.0
9.50	2.7
9.75	3.3
10.00	2.7

Table XXV

Average Pair Potential Characteristics

sigma-   3.389 A$^\circ$ $\pm$ .015 A$^\circ$

epsilon- 146.3 $^\circ$K $\pm$ 4.9 $^\circ$K

r_{min}- 3.86 A$^\circ$ $\pm$ .05 A$^\circ$

Table XXVI

Values Used for the High Energy Repulsive Region to
Calculate the Second Virial Coefficient

$r(\overset{\circ}{A})$	$u(r)$ (°K)
2.70	6000
2.80	3400
2.90	2200
3.00	1300
3.10	700

Table XXVII

Comparison of Calculated and Experimental Second Virial Coefficients

T(°K)	exptl.B(T) (cm³/mole)	error	u(r)[I] calc.	u(r)[I] exptl.-calc.	u(r)[II] calc.	u(r)[II] exptl.-calc.
81	-284	5	-269.26	-14.74	-277.44	-6.56
85	-256	3	-244.79	-11.21	-252.47	-3.53
90	-228	3	-218.98	-9.02	-226.11	-1.89
95	-204.5	2	-197.31	-7.19	-203.98	-0.52
100	-185.5	1	-178.89	-6.61	-185.15	-0.35
110	-156.0	1	-149.31	-6.69	-154.88	-1.12
125	-123.5	1	-117.17	-6.33	-121.95	-1.55
150	-84.7	1	-82.24	-2.46	-86.10	+1.40
200	-47.6	1	-44.48	-3.12	-47.27	-0.33
250	-28.0	1	-24.57	-3.43	-26.76	-1.24
300	-15.6	.5	-12.39	-3.21	-14.18	-1.42
400	-0.9	.5	1.65	-2.55	0.33	-1.23
500	7.3	.5	9.35	-2.05	8.31	-1.01
600	12.5	.5	12.73	-0.23	11.86	+0.64
101.202	-176.03	1.30	-174.87	-1.16	-181.03	+5.00
116.421	-138.28	.10	-134.11	-4.17	-139.31	+1.03
138.224	-101.05	.18	-96.58	-4.47	-100.82	-0.23

The first group (81 °K to 600 °K) is for the data compiled by Dymond and Smith.[47]

The second group (101.202 °K to 138.224 °K) is the data of Pope and co-workers.[48]

Table XXVIII

Experimental and Calculated Vibrational Transition Energies

CALCULATED EIGENVALUES (cm^{-1})

# of nodes	u(r)[I]	u(r)[II]
0	87.76	87.76
1	60.48	60.50
2	37.57	38.04
3	19.45	21.78
4	11.23	11.22
5	3.62	4.79
6	1.83	1.46
7	—	.17

$\Delta G_{v+1/2}$ TERM VALUES (cm^{-1})

v + 1/2	expt. 50	error limits	u(r)[I]	u(r)[II]
1/2	26.36	±.88	27.28	27.26
3/2	20.45	±.88	22.91	22.46
5/2	15.86	±.81	18.12	16.26
7/2	10.22	±1.03	8.22	10.56
9/2	6.81	±1.05	7.61	6.43
11/2			1.83	3.33
13/2			—	1.29

Table XXIX

Summary of Argon Potential Parameters from Various Sources

Potential	year	ϵ(°K)	σ(A°)	r_{min}(A°)
Lennard-Jones	1954	119.8	3.405	3.382
Guggenheim-McGlashen	1960	137.5		3.812
Kihara	1964	142.9	3.363	
exponant-6	1964	152	3.644	
Munn-Smith	1965	153	3.31	3.64
Dymond-Rigby-Smith	1965	147	3.28	
18-6	1966	160.3	3.277	
Barker-Pompe	1968	147.7	3.341	3.76
Dymond-Alder	1969	138.2	3.280	3.81
Klein-Hanley	1970	153	3.290	3.67
Barker-Bobetic	1970	140.2	3.367	3.76
Barker-Fisher-Watts	1971	142.1	3.361	3.76
Maitland-Smith	1971	142.5	3.355	3.75
Parson-Siska-Lee	1972	140.7	3.345	3.715
this work	1973	146.3	3.389	3.86

APPENDIX A   INCIDENT INTENSITY RATIOS
AND ABSORPTION COEFFICIENTS

In order to correctly subtract the cell scatter $P_c(2\theta)$ from the cell + sample scatter $P_{ca}(2\theta)$ using equation (35), it is necessary to calculate the quantities $P^{O'}/P^O$ and $A_c(2\theta)/A_c'(2\theta)$ for each experiment.

Determination of $\dfrac{P^{O'}}{P^O}$

The amount of variation in the incident intensity between the empty cell experiment (incident count rate = $P^{O'}$) and the cell + sample experiment (incident count rate = P^O) must be determined in order to use equation (35).

The method used to determine $P^{O'}/P^O$ is as follows: $H(2\theta)$ is the count rate at 2θ from the coherent scattering of a beryllium peak, and is determined as the count rate above the smoothly varying background in the diffraction pattern. The measured $H(2\theta)$ was corrected for absorption and the ratios $H_c(2\theta)/H_{ca}(2\theta)$, the relative heights of the beryllium peak in the empty cell and the cell + sample experiments, were calculated. The average value of these ratios was taken to be the ratio of incident intensities for the two experiments:

$$\frac{P^{O'}}{P^O} = \frac{\sum_{i=1}^{9}\left\{\frac{H_c(2\theta)}{H_{ca}(2\theta)}\right\}_i}{9} \tag{A1}$$

where the ratio is evaluated for 9 values of 2θ located on four of the beryllium peaks.

This method of determining $P^{O'}/P^O$ has the following favorable characteristics:

1) The crystal peak intensities from the cell scattering could be easily determined as sharp peaks above a slowly varying background, even in the presence of argon scatter.

2) The sharp peaks correspond to scattering of the characteristic $\overline{K\alpha}$ wavelength of the incident intensity. Therefore, the absorption coefficient is precisely known and the absorption correction of $H(2\theta)$ is straightforward.

3) By choosing for each peak at least one point on each side of the maximum, the effect of shifting of the peaks in angle space is minimized. For example, if a peak shifts to higher angles, the $H(2\theta)$ values on the high 2θ side of the maximum will increase, the $H(2\theta)$ values on the low 2θ side will decrease, and the average will remain more constant than either measurement alone.

4) If there is an error in μ, the absorption coefficient for argon, it will be compensated to first order by this method. Suppose the value used for μ is erroneously large so that the absorption corrected $H_{ca}(2\theta)$ values are, say, 2% too large. The value of $P^{O'}/P^O$ determined from equation (A1) will be 2% too small, but the ratio $A_c(2\theta)/A_c'(2\theta)$ used in equation (35) will also be 2% too small, and $P_a(2\theta)$ from equation (35) will be in error by a constant factor of $.98$ which will be absorbed in the integral normalization (see Chapter V).

The ratio of incident intensities for the argon 1R and argon 1 states was found by this method to be $P^O(1R)/P^O(1) = .982$. By adding up the total diffracted intensity of the 12 scans for each state this ratio was found to be $P^O(1R)/P^O(1) = .979$. This agreement is within the estimated 1% accuracy of the method described.

Table AI presents the details of the evaluation of the ratio $P^{O'}/P^O$ for state 1R. The values of $P^{O'}/P^O$ for all the states are presented in Table VI.

Decomposition of $P_c(2\theta)$

There are three types of scatter present in the diffraction pattern from the empty cell: The coherent scatter from the cell, $P_{c(c)}(2\theta)$, the incoherent scatter from the cell, $P_{c(i)}(2\theta)$, and the scattering from the empty cryostat, $P_{c(e)}(2\theta)$. Each of these types of scattering has a different value for the ratio of absorption coefficients and must be treated separately. Thus the quantity subtracted in equation (35) is rewritten

$$P_c(2\theta)\frac{A_c(2\theta)}{A'_c(2\theta)} = P_{c(c)}(2\theta)\frac{A_{c(c)}(2\theta)}{A'_{c(c)}(2\theta)} + P_{c(i)}(2\theta)\frac{A_{c(i)}(2\theta)}{A'_{c(i)}(2\theta)}$$

$$+ P_{c(e)}(2\theta)\frac{A_{c(e)}(2\theta)}{A'_{c(e)}(2\theta)} \tag{A2}$$

These components of the cell scatter are determined in the following manner:

The empty cryostat scatter, $P_{c(e)}(2\theta)$ is known from previous studies of the empty cryostat and is shown in Figure 7. $P_{c(e)}(2\theta)$ is

corrected for absorption by the cell and subtracted from $P_c(2\theta)$, leaving $P_{c(c)}(2\theta)$ and $P_{c(i)}(2\theta)$. Then the amount of incoherent scatter is calculated in electron units from theory (see Appendix C) and corrected for polarization and absorption by the cell. N_{Be}, the normalization constant for the cell scatter, is determined by fitting the calculated incoherent cell scatter to the remaining cell scattering in the interval $2\theta = 9.00^\circ$ to $2\theta = 12.00^\circ$. Thus $P_{c(i)}(2\theta)$ in counts per second is known and subtracted from the cell scatter leaving the coherent scatter $P_{c(c)}(2\theta)$. As a simplifying assumption with negligible effect on equation (35), the cell scatter with the incoherent scatter subtracted is treated as empty cryostat scatter from 0 to 12° and coherent cell scatter from 12.25° to 45°. The **value obtained for** N_{Be} is 66.99 counts per second/cm. if this value is used with the crystal density of 1.85 g/cm^3 in equation (40) a value for $P^\circ\Omega$ is obtained, $P^{\circ\prime}\Omega = 6826$ cps, as compared with $P^{\circ\prime}\Omega = 9241$ cps determined from the argon scatter at high s.

Evaluation of the Absorption Coefficients for the Cell Scatter

Coherent Scatter - For monochromatic incident radiation of wavelength λ, equation (29) may be evaluated analytically to obtain

$$A'_{c(c)}(2\theta,\lambda) = \frac{e^{-\mu_c(\lambda)2t/\cos(2\theta-45^\circ)} - e^{-\mu_c(\lambda)2t/\cos45^\circ}}{\lambda_c(\lambda)\left(1 - \dfrac{\cos45^\circ}{\cos(2\theta-45^\circ)}\right)} \tag{A3}$$

and

$$A_{c(c)}(2\theta, \lambda) = \frac{\left[e^{-\mu_c(\lambda)t/\cos(2\theta-45^o)} - e^{-\mu_c(\lambda)t/\cos 45^o}\right]\left[e^{-\frac{\mu_c(\lambda)t+\mu_a(\lambda)P}{\cos(2\theta-45^o)}} + e^{-\frac{\mu_c(\lambda)t+\mu_a(\lambda)P}{\cos 45^o}}\right]}{\mu_c(\lambda)\left(1 - \frac{\cos 45^o}{\cos(2\theta-45^o)}\right)}$$

(A4)

and the ratio

$$\frac{A_{c(c)}(2\theta, \lambda)}{A'_{c(c)}(2\theta, \lambda)} = \frac{e^{-\frac{\mu_c(\lambda)t+\mu_a(\lambda)P}{\cos(2\theta-45^o)}} + e^{-\frac{\mu_c(\lambda)t+\mu_a(\lambda)P}{\cos 45^o}}}{e^{-\mu_c(\lambda)t/\cos(2\theta-45^o)} + e^{-\mu_c(\lambda)t/\cos 45^o}}$$

(A5)

where p is the width of the cell cavity and t is the thickness of one beryllium window. The subscripts a and c refer to the linear absorption coefficients in argon and in the cell. $\mu_a(\lambda)$ and $\mu_c(\lambda)$ were taken from the International Tables for X-Ray Crystallography.[43]

The coherent cell scattering may be written as the sum of the contributions from the individual plane spacings. If the incident beam was monochromatic and there was no divergence, the coherent scattering distribution would (neglecting thermal motion of the beryllium atoms) consist of delta functions:

$$P_{c(c)}(2\theta) = \sum_i H_i \delta(2\theta - (2\theta_o)_i)$$

(A6)

where $(2\theta_o)_i$ is the angle at which the ith peak occurs. Because of the distribution of the incident radiation and divergence of the incident and diffracted beams, these peaks are experimentally

observed as $H_i(2\theta)$, which are continuous functions of 2θ. Each $H_i(2\theta)$ consists of a large sharp peak of half-width $\sim .5^{\circ}$ (because of divergence) above a small background from the continuous incident radiation. The range of this background, which is on the order of a few degrees, is determined from equation (2) and the absorption edges for rhodium ($\lambda = .6198$ A$^{\circ}$) and molybdenum ($\lambda = .5338$ A$^{\circ}$). The value of $\dfrac{A_{c(c)}(2\theta)}{A'_{c(c)}(2\theta)}$ is determined by summing the contributions from each peak distribution to the total coherent scattering at the angle 2θ:

$$\frac{A_{c(c)}(2\theta)}{A'_{c(c)}(2\theta)} = \frac{\sum\limits_{i} \int P^{\circ}(\lambda) H_i(2\theta,\lambda) A_{c(c)}(2\theta,\lambda)\ d\lambda}{\sum\limits_{i} \int P^{\circ}(\lambda) H_i(2\theta,\lambda) A'_{c(c)}(2\theta,\lambda)\ d\lambda} \tag{A7}$$

where $A'_{c(c)}(2\theta, \lambda)$ and $A_{c(c)}(2\theta, \lambda)$ are determined from equations (A4) and (A5), and $H_i(2\theta, \lambda)$ is determined from the peak height at $2\theta = 2\theta_o$ and the incident wavelength distribution. The features of the $H_i(2\theta, \lambda)$ used to reduce the 1R state data are presented in Table AII. The coherent absorption coefficient ratios from (A5) ($\lambda = .5608$A$^{\circ}$) and from (A7) are present for the 1R state in Table AIII and Figure A1.

Incoherent Scatter - For incident radiation of wavelength λ, equation (29) is integrated analytically to obtain

$$A'_{c(i)}(2\theta,\lambda) = \frac{e^{-\dfrac{2\mu_{c(i)}(2\theta,\lambda)t}{\cos(2\theta-45^{\circ})} } - e^{-\dfrac{2\mu_c(\lambda)t}{\cos45^{\circ}} }}{\dfrac{\mu_c(\lambda)}{\cos45^{\circ}} - \dfrac{\mu_{c(i)}(2\theta,\lambda)}{\cos(2\theta-45^{\circ})}} \tag{A8}$$

and

$$A'_{c(i)}(2\theta, \lambda) = \frac{\left[e^{-\frac{\mu_{c(i)}(2\theta, \lambda)t}{\cos(2\theta-45°)}} - e^{-\frac{\mu_c(\lambda)t}{\cos(45°)}} \right] \times \left[e^{-\frac{\mu_{c(i)}(2\theta, \lambda)t + \mu_{a(i)}(2\theta, \lambda)p}{\cos(2\theta-45°)}} + e^{-\frac{\mu_c(\lambda)t - \mu_a(\lambda)p}{\cos 45°}} \right]}{\dfrac{\mu_c}{\cos 45°} - \dfrac{\mu_{c(i)}(2\theta)}{\cos(2\theta-45°)}} \quad \text{(A9)}$$

$\mu_{c(i)}$ and $\mu_{a(i)}$ are the absorption coefficients for absorption of the incoherent scattering by the cell and sample. They are functions of λ and 2θ because λ', the wavelength of the incoherently scattered radiation, is a function of λ and 2θ as shown by equation (48).

From (A8) and (A9) we have, for monochromatic radiation

$$\frac{A_{c(i)}(2\theta, \lambda)}{A'_{c(i)}(2\theta, \lambda)} = \frac{e^{-\frac{\mu_{c(i)}(\lambda, 2\theta)t + \mu_{a(i)}(\lambda, 2\theta)p}{\cos(2\theta-45°)}} + e^{-\frac{\mu_c(\lambda)t + \mu_a(\lambda)p}{\cos 45°}}}{e^{-\mu_{c(i)}(2\theta, \lambda)t/\cos(2\theta-45°)} + e^{-\mu_c(\lambda)t/\cos 45°}} \quad \text{(A10)}$$

For an incident wavelength λ, the incoherent cell scatter as absorbed by the cell is given by

$$P_{c(i)}(2\theta, \lambda)A'_{c(i)}(2\theta, \lambda) = $$
$$N_{Be}Pol(2\theta)\mathscr{I}_{inc}(2\theta, \lambda) A'_{c(i)}(2\theta, \lambda) \quad \text{(A11)}$$

with $A'_{c(i)}$ given by (A8).

The incoherent cell scatter as absorbed by the cell and sample is given by

$$P_{c(i)}(2\theta, \lambda) A_{c(i)}(2\theta, \lambda) = $$
$$N_{Be}Pol(2\theta)\mathscr{I}_{inc}(2\theta, \lambda)A_{c(i)}(2\theta, \lambda) \quad \text{(A12)}$$

with $A_{c(i)}(2\theta, \lambda)$ given by equation (A9).

To find the absorption coefficient ratio for the actual incident radiation, (A11) and (A12) are integrated over λ and the results are divided to obtain

$$\frac{A_{c(i)}(2\theta)}{A'_{c(i)}(2\theta)} = \frac{\int_\lambda P^o(\lambda)\mathscr{I}_{inc}(2\theta, \lambda) A_{c(i)}(2\theta, \lambda)\, d\lambda}{\int_\lambda P^o(\lambda)\mathscr{I}_{inc}(2\theta, \lambda) A'_{c(i)}(2\theta, \lambda)\, d\lambda} \qquad (A13)$$

The ratio $\dfrac{A_{c(i)}(2\theta)}{A'_{c(i)}(2\theta)}$ for state 1R is shown in Figure A2 and Table AIV for the monochromatic $\mathrm{K}\overline{\alpha}$ radiation (equation (A10)) and for the actual incident distribution (Equation (A13)).

Empty Cryostat Scatter - 33% of the radiation scattered by the cryostat is estimated to come from the incident side of the cell and pass through the cell and sample at an angle of $(2\theta-45^o)$ relative to the cell's long axis. 67% is estimated to originate from the diffraction side of the cell, the incident beam having passed through the cell at 45° relative to the cell's long axis. For a monochromatic source, then,

$$\frac{A_{c(e)}(2\theta, \lambda)}{A'_{c(e)}(2\theta, \lambda)} = \frac{\frac{1}{3} e^{-\frac{\mu_a(\lambda) + 2\mu_c(\lambda)t}{\cos(2\theta-45^o)}} + \frac{2}{3} e^{-\frac{\mu_a(\lambda)p + 2\mu_c(\lambda)t}{\cos 45^o}}}{\frac{1}{3} e^{-\frac{2\mu_c(\lambda)t}{\cos(2\theta-45^o)}} + \frac{2}{3} e^{-\frac{2\mu_c(\lambda)t}{\cos 45^o}}} \qquad (A14)$$

For the actual distribution of incident radiation:

$$\frac{A_{c(e)}(2\theta)}{A'_{c(e)}(2\ )} = \int_{\lambda} P^{o}(\lambda) \frac{A_{c(e)}(2\theta, \lambda)}{A'_{c(e)}(2\theta, \lambda)} \ d\lambda \tag{A15}$$

where $\dfrac{A_{c(e)}(2\theta, \lambda)}{A'_{c(e)}(2\theta, \lambda)}$ is given by equation (A14).

These absorption coefficients for the $K\overline{\alpha}$ radiation (equation (A14)) and for the actual incident intensity (equation (A15)) are listed in Table AV for the 1R state.

In order to illustrate the comparative size of the absorption coefficients for the four densities studied, the ratio of coherent cell scattering absorption coefficients for the $AgK\overline{\alpha}$ radiation (equation (AV)) is presented in Table AVI for all four densities at selected angles.

Absorption Coefficients for Argon Scatter

The absorption coefficients for absorption of argon scatter by the cell and sample as used in equations (44) and (45) can be calculated analytically, with the results:

$$A_{a(c)}(2\theta, \lambda) = \frac{1}{\mu_a(\lambda)\left(1 - \frac{\cos 45^\circ}{\cos(2\theta-45^\circ)}\right)} \left[e^{-\frac{\mu_a(\lambda)p}{\cos(2\theta-45^\circ)}} - e^{-\frac{\mu_a(\lambda)p}{\cos 45^\circ}} \right]$$

$$\times \ e^{-\mu_c(\lambda)\left(\frac{t}{\cos(2\theta-45^\circ)} + \frac{t}{\cos 45^\circ}\right)} \tag{A16}$$

and

$$A_{a(i)}(2\theta, \lambda) = \frac{1}{\mu_a(\lambda) - \mu_{a(i)}(\lambda, 2\theta) \frac{\cos 45^\circ}{\cos(2\theta - 45^\circ)}} \left[e^{\frac{-\mu_{a(i)}(\lambda, 2\theta)p}{\cos(2\theta - 45^\circ)}} \right.$$

$$\left. - e^{\frac{-\mu_a(\lambda)p}{\cos 45^\circ}} \right] \times e^{\frac{-\mu_{c(i)}(\lambda, 2\theta)t}{\cos(2\theta - 45^\circ)}} - \frac{\mu_c(\lambda)t}{\cos 45^\circ}$$

(A17)

Selected values for $A_{a(c)}(2\theta)$ and $A_{a(i)}(2\theta)$ with Ag K$\bar{\alpha}$ radiation are presented, for the four densities studied, in Tables AVII and VIII.

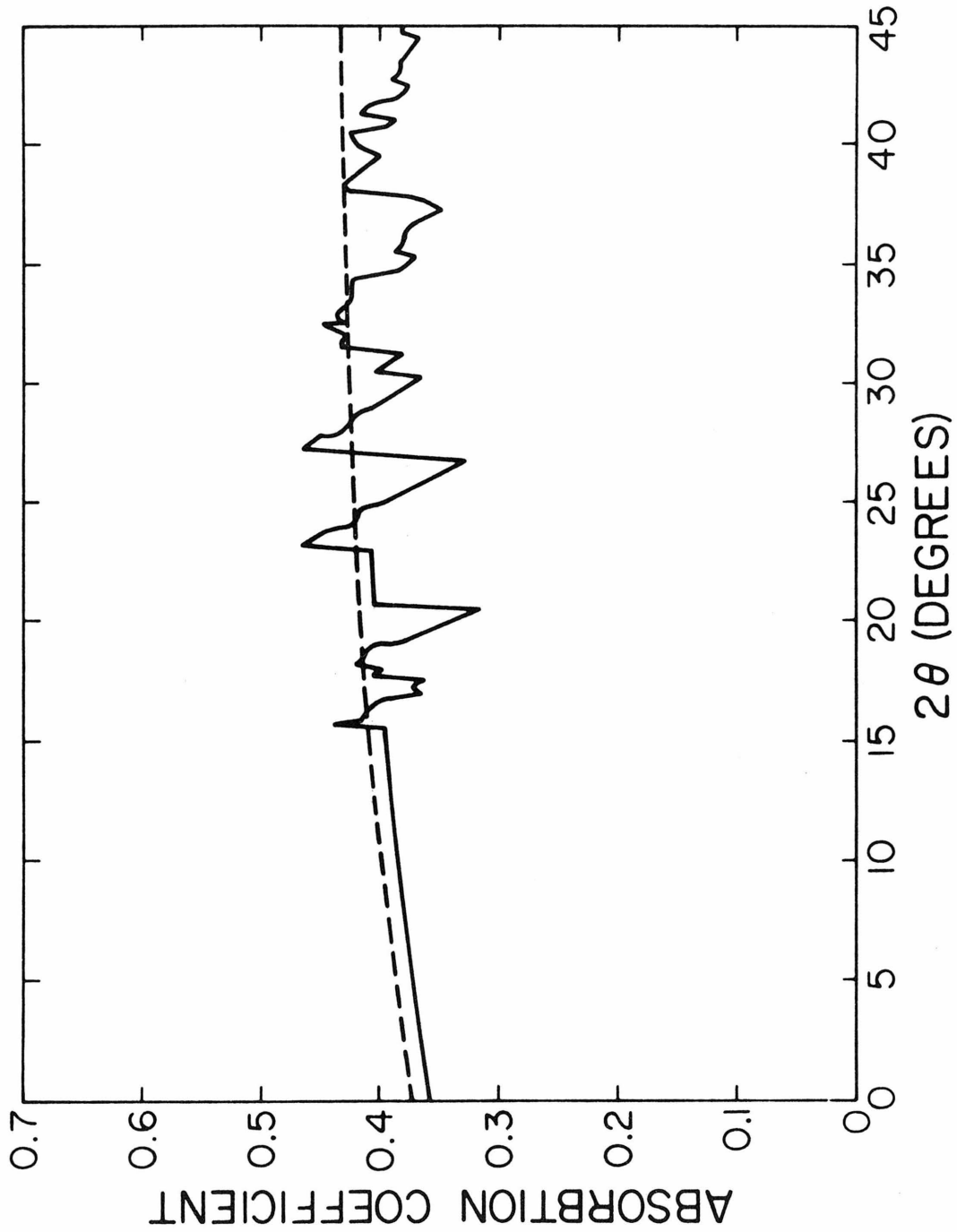Figure Al. Absorbtion Factors for Coherent Cell Scatter from State lR. --- monochro-
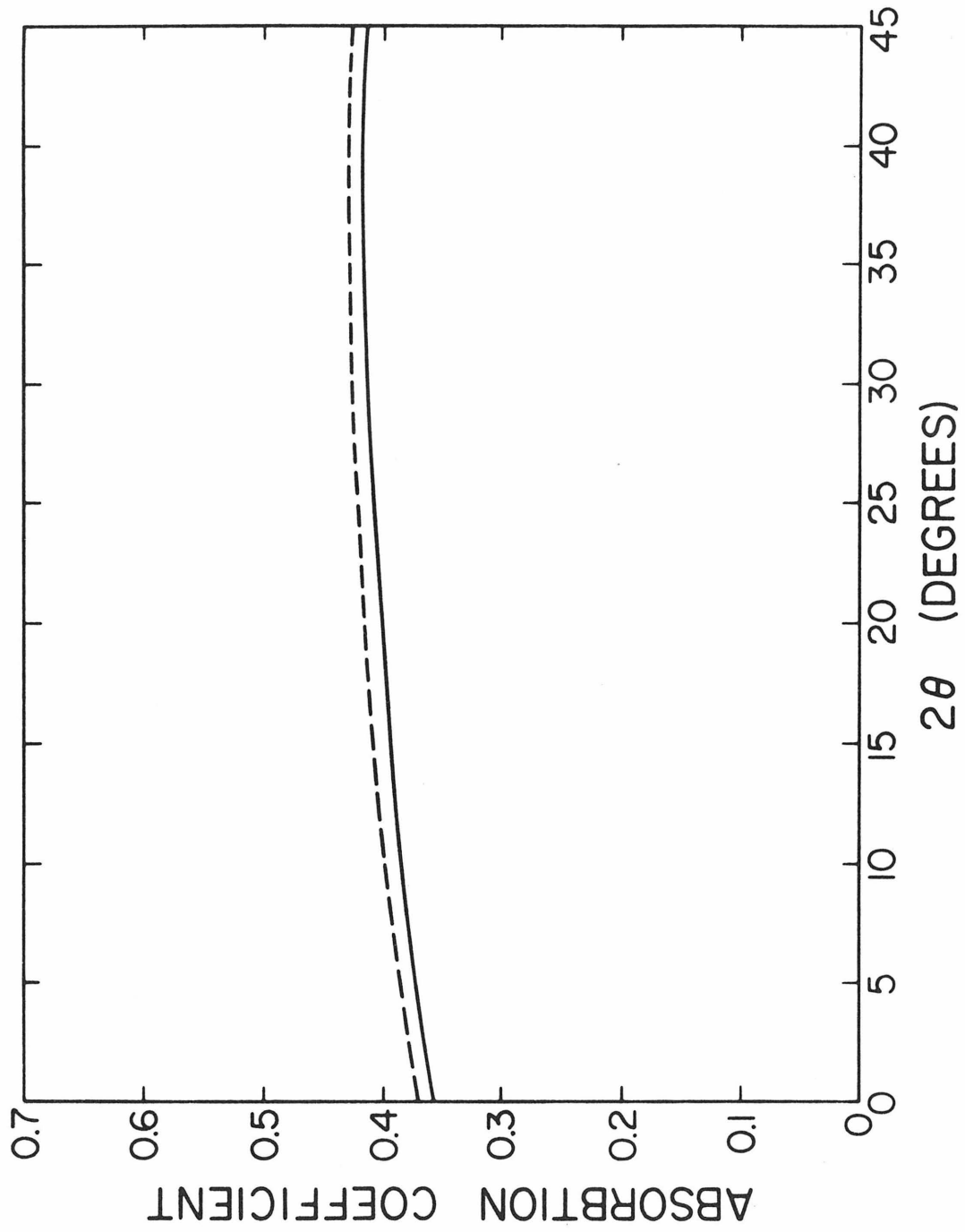matic Kα radiation. —— actual wavelength distribution of incident intensity.

Figure A2. Absorbtion Factors for Incoherent Cell Scatter from State 1R. --- monochromatic Kα radiation. —— actual wavelength distribution of incident intensity.

Table A I
Evaluation of $P^{o'}/P^o$ for state 1R

2θ	$H_{ca}(2\theta)$	$H_c(2\theta)$	$\dfrac{H_c(2\theta)}{H_{ca}(2\theta)}$	$\sigma\left(\dfrac{H_c(2\theta)}{H_{ca}(2\theta)}\right)$
24.25	74.89	74.89	1.000	.049
24.50	64.11	63.09	.984	.059
28.25	82.79	82.10	.992	.047
28.50	110.12	106.36	.966	.031
31.75	81.10	79.95	.986	.047
32.00	119.38	115.94	.971	.032
33.75	89.37	92.28	1.033	.045
34.00	116.97	120.84	1.033	.034
34.25	108.10	104.16	.964	.037

$$\frac{P^{o'}}{P^o} = \frac{\displaystyle\sum \frac{\frac{H_c(2\theta)}{H_{ca}(2\theta)}}{\sigma}}{\displaystyle\sum \frac{1}{\sigma}} = .991$$

Table A II

Beryllium Peak Heights in the State Helium 1 Cell
Scattering

2d spacing (angstroms)	$\{2\theta_0\}_i$ $\lambda = K\overline{\alpha}$ .5608 A°	2θ =rhod.edge .5338 A°	2θ =moly.edge .6198 A°	H_i (cps)
3.958	16.29	15.50	18.02	224.4
3.583	18.01	17.14	19.92	75.7
3.465	18.63	17.72	20.61	566.4
2.657	24.37	23.18	26.98	77.6
2.285	28.41	27.02	31.48	106.5
2.045	31.83	30.26	35.29	112.8
1.979	32.92	31.30	36.50	11.8
1.918*	34.01*	32.32	37.71	165.4
1.792	36.48	34.66	40.47	7.2
1.733	37.77	35.88	41.91	14.4
1.632	40.19	38.18	44.64	13.5
1.524	43.18	41.01	47.99	15.4
1.496	44.02	41.81	48.95	2.5
1.465	45.02	42.74	50.06	41.1

All angles are in degrees.

The peak at 34.01 degrees is actually the sum of
two peaks which are indistinguishable in this
experiment: ($2\theta_0 = 33.84$ and $2\theta_0 = 34.19$)

Table A III

State 1R Absorbtion Coefficients for Coherent Cell
Scatter, $A_{c(c)}(2\theta)/A'_{c(c)}(2\theta)$

2θ	for $P^\circ(\lambda)$	for Ag K$\bar{\alpha}$
1.00	.3603	.3736
2.00	.3633	.3767
3.00	.3663	.3796
4.00	.3691	.3825
5.00	.3718	.3852
6.00	.3745	.3879
7.00	.3770	.3904
8.00	.3795	.3929
9.00	.3819	.3953
10.00	.3841	.3975
11.00	.3863	.3997
12.00	.3885	.4018
13.00	.3905	.4039
14.00	.3924	.4058
15.00	.3943	.4077
16.00	.4158	.4095
17.00	.3669	.4112
18.00	.3980	.4129
19.00	.4035	.4144
20.00	.3423	.4160
21.00	.4040	.4174
22.00	.4054	.4188
23.00	.4067	.4201
24.00	.4263	.4213
25.00	.3963	.4225
26.00	.3571	.4236
27.00	.4113	.4246
28.00	.4308	.4256
29.00	.4058	.5265
30.00	.3722	.4274
31.00	.3874	.4282
32.00	.4286	.4289
33.00	.4316	.4296
34.00	.4244	.4303
35.00	.3770	.4308
36.00	.3792	.4313
37.00	.3542	.4318
38.00	.4259	.4322
39.00	.4107	.4326
40.00	.4193	.4329
41.00	.3845	.4331
42.00	.4349	.4333
43.00	.4362	.4334
44.00	.4252	.4335
45.00	.4316	.4335

Table A IV

State 1R Absorbtion Coefficients for Incoherent Cell
Scatter, $A_{c(i)}(2\theta)/A'_{c(i)}(2\theta)$

2θ	for $P°(\lambda)$	for Ag $K\bar{a}$
1.00	.3625	.3736
2.00	.3654	.3767
3.00	.3681	.3796
4.00	.3708	.3824
5.00	.3733	.3851
6.00	.3757	.3877
7.00	.3780	.3902
8.00	.3801	.3927
9.00	.3823	.3950
10.00	.3844	.3972
11.00	.3864	.3993
12.00	.3883	.4014
13.00	.3902	.4033
14.00	.3921	.4052
15.00	.3939	.4069
16.00	.3956	.4086
17.00	.3972	.4102
18.00	.3987	.4118
19.00	.4002	.4132
20.00	.4016	.4146
21.00	.4029	.4159
22.00	.4042	.4171
23.00	.4054	.4183
24.00	.4065	.4194
25.00	.4075	.4204
26.00	.4085	.4213
27.00	.4094	.4222
28.00	.4102	.4230
29.00	.4109	.4238
30.00	.4116	.4244
31.00	.4122	.4251
32.00	.4128	.4256
33.00	.4133	.4261
34.00	.4137	.4265
35.00	.4141	.4269
36.00	.4144	.4272
37.00	.4146	.4274
38.00	.4148	.4276
39.00	.4149	.4277
40.00	.4149	.4278
41.00	.4149	.4278
42.00	.4149	.4277
43.00	.4147	.4276
44.00	.4146	.4274
45.00	.4143	.4272

State 1R Absorbtion Coefficients for Empty Cryostat
Scatter, $A_{c(e)}(2\theta)/A'_{c(e)}(2\theta)$

2θ	for P°(λ)	for Ag K$\bar{\alpha}$
1.00	.3611	.3744
2.00	.3651	.3785
3.00	.3690	.3824
4.00	.3728	.3862
5.00	.3765	.3898
6.00	.3800	.3934
7.00	.3834	.3968
8.00	.3867	.4001
9.00	.3898	.4032
10.00	.3929	.4063
11.00	.3958	.4092
12.00	.3986	.4120
13.00	.4014	.4148
14.00	.4040	.4174
15.00	.4065	.4199
16.00	.4089	.4223
17.00	.4112	.4246
18.00	.4134	.4268
19.00	.4155	.4289
20.00	.4175	.4309
21.00	.4195	.4328
22.00	.4213	.4346
23.00	.4231	.4364
24.00	.4247	.4380
25.00	.4263	.4396
26.00	.4278	.4411
27.00	.4292	.4425
28.00	.4305	.4438
29.00	.4317	.4450
30.00	.4329	.4462
31.00	.4340	.4473
32.00	.4350	.4483
33.00	.4359	.4492
34.00	.4368	.4500
35.00	.4375	.4508
36.00	.4382	.4515
37.00	.4389	.4521
38.00	.4394	.4526
39.00	.4399	.4531
40.00	.4403	.4535
41.00	.4406	.4538
42.00	.4409	.4541
43.00	.4410	.4543
44.00	.4412	.4544
45.00	.4412	.4544

Table A VI

Monochromatic Absorbtion Coefficients for Coherent Cell Scatter for the Four Densities, $A_{c(c)}(2\theta)/A'_{c(c)}(2\theta)$ for Ag Kα radiation

2θ	$.3111 g/cm^3$	$.2087 g/cm^3$	$.1331 g/cm^3$	$.0824 g/cm^3$
2.50	.2346	.3782	.5380	.6815
5.00	.2413	.3852	.5443	.6864
7.50	.2474	.3917	.5500	.6908
10.00	.2531	.3975	.5551	.6947
12.50	.2584	.4029	.5597	.6982
15.00	.2632	.4077	.5639	.7013
17.50	.2676	.4121	.5676	.7041
20.00	.2715	.4160	.5709	.7066
22.50	.2751	.4194	.5738	.7088
25.00	.2782	.4225	.5764	.7107
27.50	.2810	.4251	.5786	.7123
30.00	.2833	.4274	.5805	.7137
32.50	.2853	.4293	.5821	.7149
35.00	.2869	.4308	.5833	.7158
37.50	.2882	.4320	.5843	.7165
40.00	.2891	.4329	.5850	.7171
42.50	.2896	.4334	.5854	.7174
45.00	.2898	.4335	.5856	.7175

Table A VII
Monochromatic Absorbtion Coefficients for Coherent Argon
Scatter at the Four Densities, $A_{a(c)}(2\theta)/2p$
for Ag Kα radiation

2θ	$.3111g/cm^3$	$.2087g/cm^3$	$.1331g/cm^3$	$.0824g/cm^3$
2.50	.2113	.3406	.4846	.6138
5.00	.2175	.3475	.4911	.6183
7.50	.2232	.3537	.4970	.6243
10.00	.2283	.3593	.5022	.6287
12.50	.2330	.3643	.5069	.6327
15.00	.2373	.3689	.5111	.6362
17.50	.2411	.3729	.5148	.6393
20.00	.2445	.3765	.5181	.6420
22.50	.2476	.3797	.5210	.6444
25.00	.2503	.3825	.5236	.6465
27.50	.2526	.3849	.5258	.6483
30.00	.2546	.3870	.5276	.6498
32.50	.2563	.3887	.5292	.6511
35.00	.2576	.3901	.5304	.6522
37.50	.2587	.3912	.5314	.6529
40.00	.2594	.3920	.5321	.6535
42.50	.2599	.3924	.5325	.6538
45.00	.2600	.3926	.5326	.6540

Table A VIII

Monochromatic Absorbtion Coefficients for Incoherent Argon
Scatter at the Four Densities, $A_{a(i)}(2\theta)/2\rho$
for Ag K$\bar{\alpha}$ radiation

2θ	$.3111 g/cm^3$	$.2087 g/cm^3$	$.1331 g/cm^3$	$.0824 g/cm^3$
2.50	.2113	.3406	.4846	.6138
5.00	.2174	.3474	.4910	.6183
7.50	.2230	.3535	.4968	.6242
10.00	.2280	.3590	.5019	.6285
12.50	.2326	.3639	.5065	.6323
15.00	.2366	.3682	.5105	.6357
17.50	.2402	.3720	.5140	.6386
20.00	.2434	.3753	.5171	.6412
22.50	.2462	.3782	.5197	.6434
25.00	.2485	.3807	.5220	.6453
27.50	.2505	.3828	.5239	.6469
30.00	.2521	.3845	.5254	.6481
32.50	.2534	.3858	.5266	.6491
35.00	.2543	.3867	.5275	.6499
37.50	.2549	.3873	.5281	.6504
40.00	.2551	.3876	.5283	.6506
42.50	.2550	.3875	.5283	.6506
45.00	.2546	.3871	.5279	.6503

APPENDIX B

CALCULATION OF DOUBLE SCATTERING

As was demonstrated by Strong and Kaplow,[B1] the intensity of doubly-scattered radiation is sensitive to the geometry of the system under consideration, the wavelength of the incident radiation, and the atomic number of the scatterer. Accordingly, it was necessary to calculate the amount of double scatter for the specific conditions of this experiment.

The calculation involves integration of the expression for the doubly scattered intensity

$$dI(2) = I° \left(\frac{e^4}{m^2 c^4}\right)^2 \frac{n_1 n_2}{R^2} \frac{J_1(2\theta_1) J_2(2\theta_2)}{r_{12}^2}$$

$$\times \quad Pol_2(2\theta) A^*(2) dv_1 dv_2 \tag{B1}$$

over the volumes of the irradiated (v_1) and detected (v_2) scattering regions. In equation (B1) the subscripts 1 and 2 refer to the first and second scattering processes. Thus, for example, in sample-cell double scattering, $J_1(2\theta_1)$ is the single scatter diffraction from argon in units of electron units per atom where $2\theta_1$ is the scattering angle for the first scattering process. $A^*(2)$ expresses the absorption of the incident beam to the first scattering at $\vec{r}_1$, absorption of the scattered beam from $\vec{r}_1$ to $\vec{r}_2$, and absorption of the twice scattered beam from $\vec{r}_2$ out to the counter. r_{12} is the separation of the two scattering elements:

$$r_{12} = \left| \vec{r}_1 - \vec{r}_2 \right| \tag{B2}$$

The Polarization term for a double scattering is given by

$$Pol_2(2\theta, 2\theta_1, 2\theta_2) = [\cos^2 2\theta_1 + \cos^2 2\theta_2$$

$$+ (\cos 2\theta - \cos 2\theta_1 \cos 2\theta_2)^2]/2 \tag{B3}$$

Equation (B1) results from using the intensity of singly diffracted radiation (equation (25)) as an incident intensity for the second scattering process. Calculation of the intensity of double scatter involves evaluating the integral

$$\iint_{V_1 V_2} \frac{J_1 J_2}{r_{12}^2} Pol_2 A^*(2)\, dv_1 dv_2 = \iint_{V_1 V_2} F\ (2\theta, \vec{r}_1, \vec{r}_2)\, dv_1 dv_2 \tag{B4}$$

where J_2, Pol_2, $A^*(2)$ are functions of 2θ, x_1, x_2, y_1, y_2, z_1, and z_2, and J_1, r_{12} are functions of x_1, x_2, y_1, y_2, z_1 and z_2.

After examining (and rejecting) the possibility of evaluating expression (B4) by a direct numerical method, I decided to use Monte Carlo techniques (as did Strong and Kaplow[B1]) to evaluate the double integral.

Monte Carlo Calculations

The techniques for using the Monte Carlo method to evaluate integrals are explained in texts by Lowry[B2] and Hammersley.[B3] Basically, the method estimates the average value of a function by evaluating the function for a large number of randomly selected values of the independent coordinates of integration. The integral is then obtained from the average value of F by

$$\int F(x_1 \cdots x_N) \ dx_1 \cdots dx_n = \langle F(x_1 \cdots x_N) \rangle \times V \tag{B5}$$

where V is the volume of the n dimensional coordinate space. In the case of equation (B4), $n = 6$ and $N = 7$. The standard deviation of the estimated $\langle F \rangle$ after N_T evaluations is given by

$$\sigma = \sqrt{\frac{1}{N_T} \frac{1}{N_T - 1} \sum_{i=1}^{N_T} (F_i - \langle F \rangle)^2} \tag{B6}$$

where F_i is the value of F for the ith random evaluation, and $\langle F \rangle$ is the average after N_T evaluations.

Evaluation of (B4) by a straightforward application of Monte Carlo sampling produces an estimate of $\langle F \rangle$ which converges very slowly because of the singularity at $r_{12} = 0$. In order to improve the convergence of the estimate, this singularity was removed as follows:

1) For the argon-argon and cell-cell double scatter a spherical volume of radius .02 cm was defined about the location $\vec{r}_1$ of the first scattering. Within this volume, (B4) was integrated analytically. The Monte Carlo sampling was then restricted to the exterior of this defined volume. The integrals over the two volumes were combined to produce a rapidly convergent evaluation of the total integral.

2) For the argon-to-cell and the cell-to-argon scatter the singularity was removed by defining a thin slab of excluded volume at the cell-sample interface and proceeding as above.

Stratified sampling[B2,B3] was used in the evaluation of each type of double scattering (cell-cell, argon-argon, cell-argon,

argon-cell) to further improve convergence. The estimates were continued until σ from equation (B6) was less than or equal to 5% of $\langle F \rangle$.

The method described above was also used to estimate the value of a $1/r_{12}^2$ calibration function:

$$In = \iint_{V_1 \, V_2} \frac{1}{r_{12}^2} \, d\vec{r}_1 d\vec{r}_2 \tag{B7}$$

The exact value of In was determined and compared with the Monte Carlo estimate. Figure C1 shows the convergence of the Monte Carlo estimate to the exact $1/r_{12}^2$ solution as a function of the number of evaluations made. The error bars indicate the 95% confidence limits on In as calculated from expression (B6).

Results

The results of these calculations are presented in Tables BI to BV. Table BI is the count rate of double scatter from the empty cell. Tables BII to BV give the count rate of the cell-cell, cell-argon, argon-cell, and argon-argon double scatter for the four densities studied. Figure B2 shows the ratio I(2)/I(1) for the argon scatter. I(1) is the singly scattered radiation from argon. I(2) includes the double scattering not present in the empty cell: cell-sample, sample-cell, and sample-sample. The intensity ratio I(2)/I(1) equals the count-rate ratio P(2)/P(1).

References for Appendix B

B1. S. L. Strong and R. Kaplow, Acta. Cryst. $\underline{23}$, 38(1967)

B2. G. C. Lowry (ed.), Markov Chains and Monte Carlo Calculations in Polymer Science (Marcel Dekker Inc., New York, 1970)

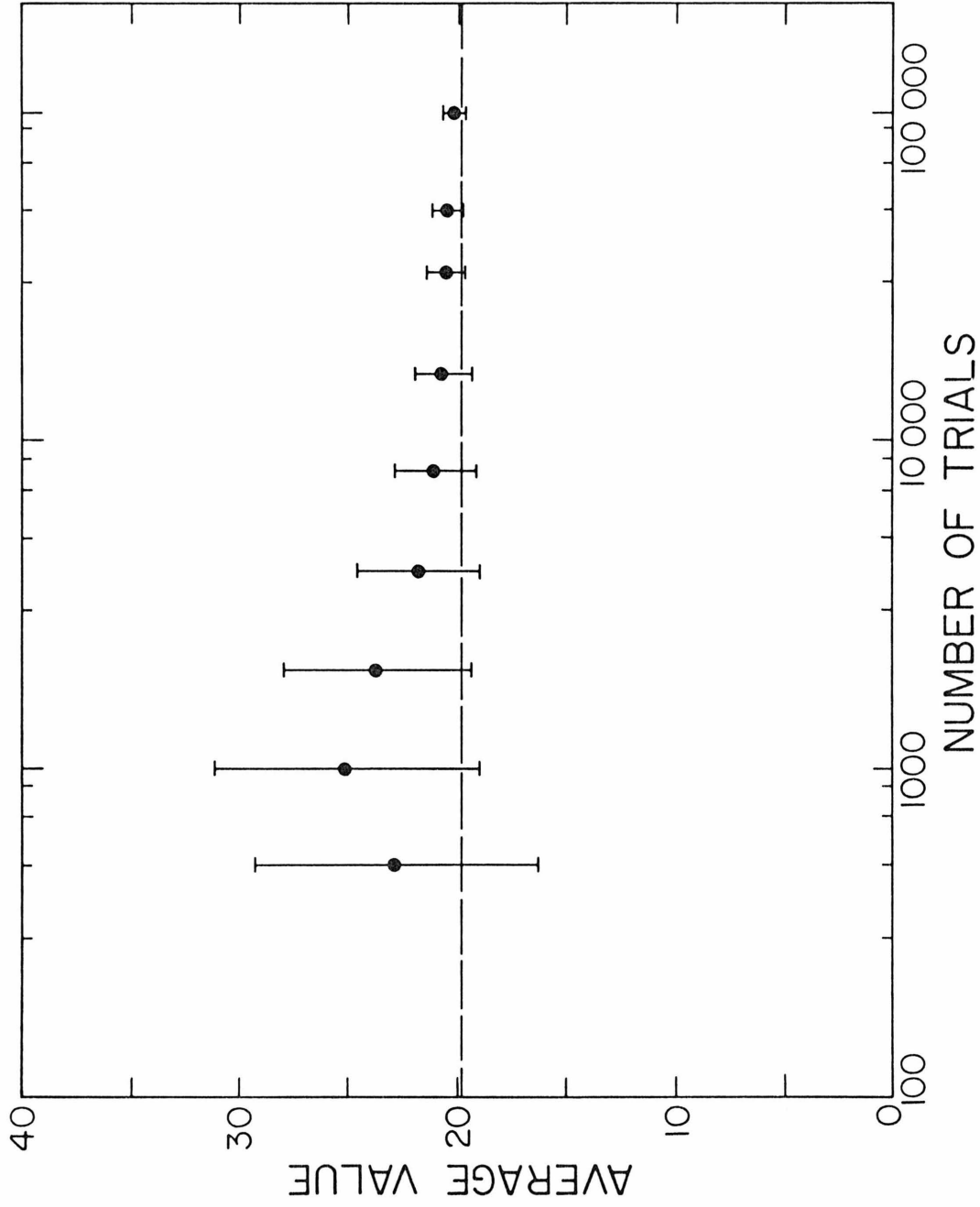B3. J. M. Hammersley and D. C. Handscomb, Monte Carlo Methods (Methuen and Co., Ltd., London , 1964)

Figure B1. Convergence of Monte Carlo Estimate to the Double Volume Integral of $1/r_{12}^2$.
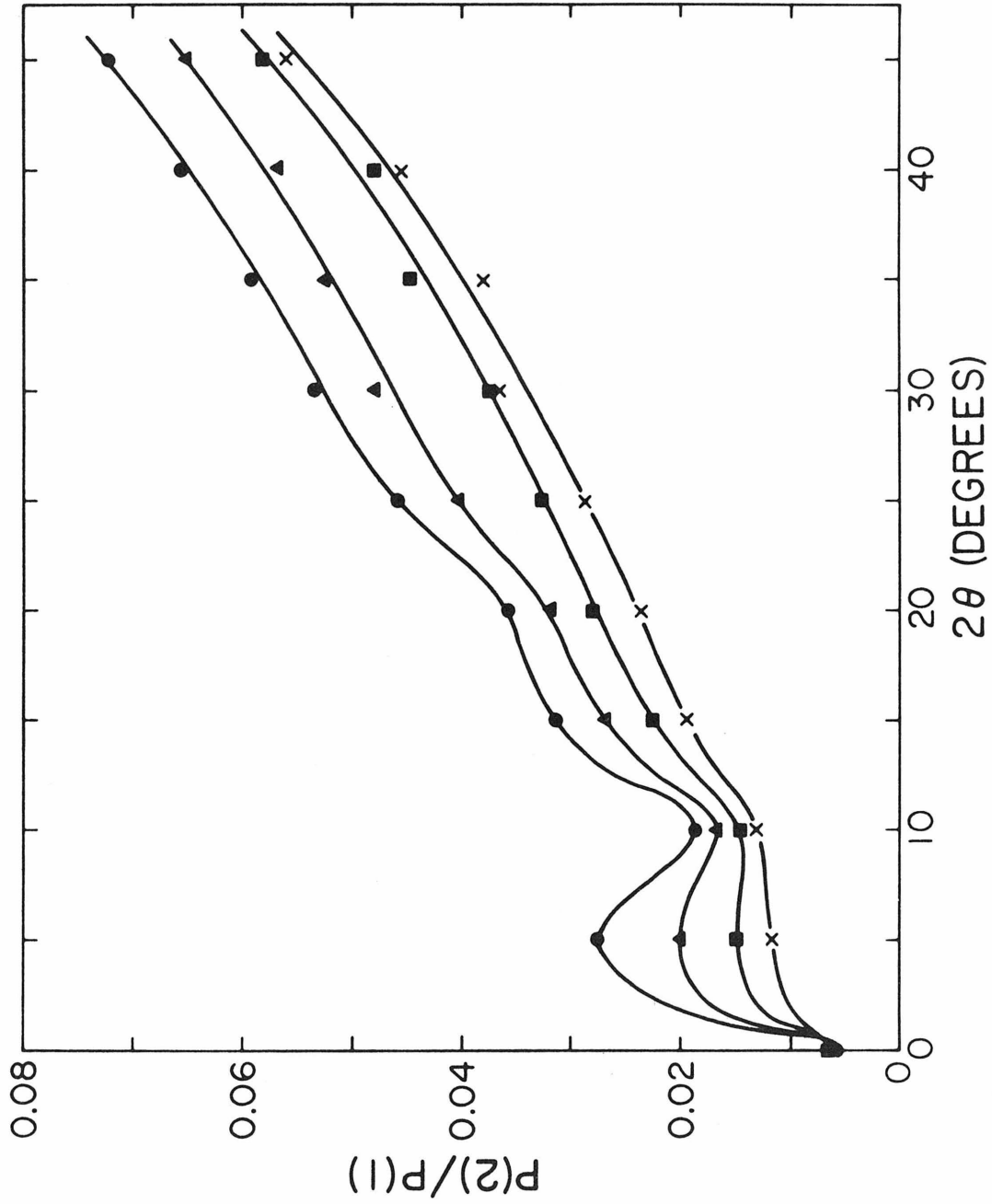● Monte Carlo estimate after N_T trials. Ⱶ 95% confidence limits. --- exact solution.

Figure B2. Ratio of Double Scattering to Single Scattering in the Argon Diffraction. ● n=.3111g/cm³ ; ▲ n=.2087 g/cm³ ; ■ n=.1331 g/cm³ ; ✕ n=.0824 g/cm³.

Table BI

Double Scattering in the Empty Cell

2θ (degrees)	P(2) (counts per second)
0	2.858
5	2.882
10	2.830
15	2.734
20	2.619
25	2.531
30	2.432
35	2.390
40	2.318
45	2.207

Table B II.

Cell-Cell Double Scattering in the Argon Experiments.

2θ (degrees)	P(2) counts per second			
	$.3111g/cm^3$	$.2087g/cm^3$	$.1331g/cm^3$	$.0824g/cm^3$
0	.606	1.015	1.477	1.899
5	.654	1.066	1.528	1.946
10	.674	1.080	1.531	1.934
15	.676	1.070	1.502	1.887
20	.667	1.044	1.457	1.821
25	.659	1.025	1.421	1.770
30	.644	.996	1.375	1.708
35	.640	.986	1.358	1.684
40	.625	.960	1.321	1.636
45	.597	.916	1.258	1.558

Table B III.

Cell-Argon Double Scattering in the Argon Experiments.

2θ (degrees)	P(2) counts per second			
	$.3111g/cm^3$	$.2087g/cm^3$	$.1331g/cm^3$	$.0824g/cm^3$
0	.436	.501	.478	.390
5	.466	.520	.487	.393
10	.503	.549	.507	.404
15	.513	.569	.518	.409
20	.546	.577	.519	.408
25	.581	.604	.538	.420
30	.580	.598	.530	.411
35	.541	.540	.492	.381
40	.518	.532	.469	.363
45	.513	.525	.462	.338

Table B IV.

Argon-Cell Double Scattering in the Argon Experiments.

2θ (degrees)	P(2) counts per second			
	$.3111g/cm^3$	$.2087g/cm^3$	$.1331g/cm^3$	$.0824g/cm^3$
0	.431	.484	.462	.376
5	.448	.505	.481	.392
10	.466	.526	.502	.408
15	.483	.549	.522	.424
20	.484	.551	.521	.422
25	.475	.537	.506	.409
30	.457	.516	.485	.391
35	.435	.489	.460	.371
40	.412	.462	.433	.349
45	.388	.436	.409	.329

Table B V.

Argon-Argon Double Scattering in the Argon Experiments.

2θ (degrees)	P(2) counts per second			
	$.3111 g/cm^3$	$.2087 g/cm^3$	$.1331 g/cm^3$	$.0824 g/cm^3$
0	2.061	1.570	.945	.472
5	1.886	1.405	.838	.416
10	1.642	1.223	.725	.358
15	1.552	1.148	.675	.332
20	1.404	1.027	.602	.295
25	1.364	.991	.577	.282
30	1.265	.916	.533	.260
35	1.120	.809	.470	.229
40	1.040	.749	.433	.211
45	.994	.712	.411	.200

APPENDIX C

ATOMIC SCATTERING FACTORS

$J_{(c)}(2\theta)$, the scattering per atom from a structured assemblage of argon atoms, appears as oscillations about the atomic scattering curve, $f^2(2\theta)$ for argon. In the course of analyzing the diffraction patterns for the first four argon states studied, it was observed that with decreasing density the oscillations in $J_{(c)}$ did not appear to approach f^2 calculated from Hartree-Foch wavefunctions.[C1] It thus appeared to be incorrect to reduce the argon scatter $P_a(2\theta)$ to $i(2\theta)$ (equation (43)) using the Hartree-Foch f^2 values. For this reason it was decided to measure an experimental set of f^2 values for argon.

An argon state at .0824 g/cm^3 (state 4) was chosen as being optimal in that the density is low enough so that differences between f^2 and $J_{(c)}$ are small (i(s) is close to zero) but large enough to have a sufficient ratio of argon scatter to cell scatter. The value of $J_{(c)}$ from the other states was used to make the extrapolation from $J_{(c)}$ at .0824 g/cm^3 to $J_{(c)}$ at .0000 g/cm^3, which is f^2. $J_{(c)}$ was obtained from P_a by assuming the incoherent scatter was that calculated by Cromer and Mann.[C2] Figure C1 shows the results of this experiment in terms of the experimental scattering factor f^o_{exp} and the Hartree-Foch f^o_{HF}. f^2 and f^o are related by the equations

$$f^2 = ff* = (f°+\Delta f'+i\Delta f'')(f°+\Delta f'-i\Delta f'')$$

$$= (f°)^2 + (\Delta f')^2 - (\Delta f'')^2 \qquad (C1)$$

(f* is the complex conjugate of f)

where the values of $\Delta f' = .101$ and $\Delta f'' = .125$ are taken from the calculations of Cromer and Liberman.[C3] These results were listed earlier in Table X. As can be seen in the Figure C1, the experimental $f°$ differs from the Hartree-Foch value by as much as 6% at high s (a difference of about 12% in f^2).

It is not clear whether this is an unreasonably large discrepancy to be attributed to the limitations of the Hartree-Foch one electron wavefunction approximation, which neglects relativistic effects and electron correlation. Previous experimental studies[C4-C8] of the atomic scattering are insufficiently accurate to decide this because of difficulties in obtaining quantitative data at these very low densities of scatterers. The effect of electron correlation on f for lithium atoms has been calculated,[C9] but the extrapolation to argon is uncertain. A comparison of relativistic and non-relativistic Hartree-Foch-Slater wave functions[C1] showed them to be essentially the same for $Z \leq 40$, but, again, it is not clear whether this is the case for the Hartree-Foch wave functions.

Density Variation of f

Note that the use of these atomic scattering factors to reduce the experimental data assumes that the atomic scattering at finite

densities is equal to the scattering from the isolated atom. In the past, this assumption has been made of necessity, and recently it has been shown[C10] to be true in the case of argon for the densities studied here.

References for Appendix C

C1.   D. T. Cromer and J. B. Mann, Los Alamos Scientific Laboratory Report LA-3816, UC-34, Physics, TID-4500(1968) and reference 6 contained therein

C2.   D. T. Cromer and J. B. Mann, J. Chem. Phys. $\underline{47}$, 1892 (1967)

C3.   D. T. Cromer and D. Liberman, J. Chem. Phys. $\underline{53}$, 1891 (1970)

C4.   C. S. Barrett, Phys. Rev. $\underline{32}$, 22 (1928)

C5.   G. Herzog, Helv. Phys. Acta $\underline{6}$, 508 (1932)

C6.   E. O. Wollan, Phys. Rev. $\underline{37}$, 862 (1931)

C7.   E. Laurila, Ann. Acad. Sci. Fennicare Ser. A II $\underline{57}$, 7 (1941)

C8.   D. R. Chipman and L. D. Jennings, Phys. Rev. $\underline{132}$, 728 (1963)

C9.   R. Beneschand and V. H. Smith Jr., J. Chem. Phys. $\underline{53}$, 1466 (1970)

C10.   M. Piliavin, " A Theoretical Investigation of the Effect of Intermolecular Correlations upon Properties of Simple Liquids from X-Ray Diffraction", doctoral thesis, California Institute of Technology, Pasadena, California (1973)
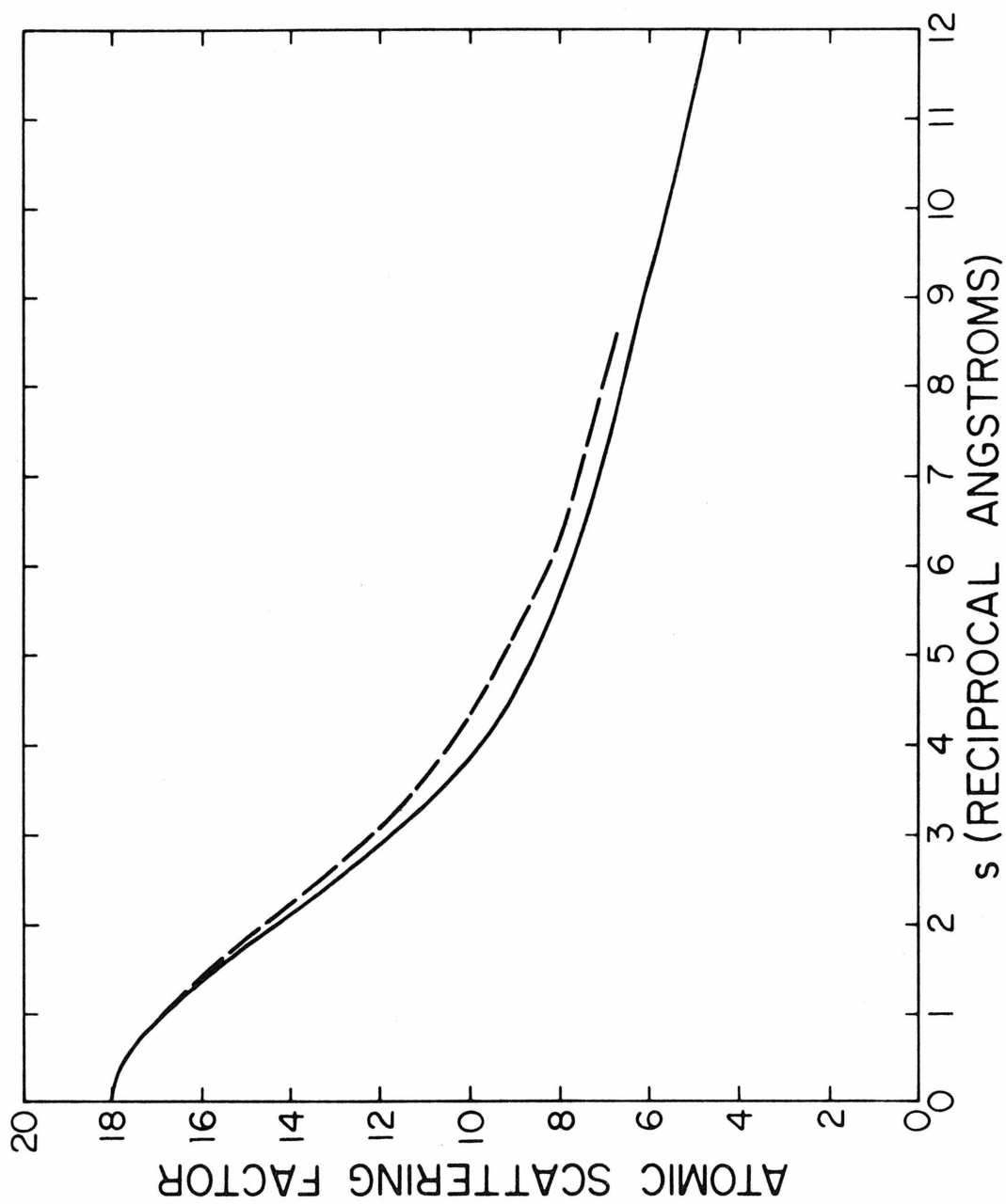
Figure Cl. Experimental and Hartree-Foch Atomic Scattering Factors for Argon.
--- experimental f°, this work. —— f° from Hartree-Foch wave functions, ref. Cl.